January 2016

Deciphering the role of Hsp31 as a multitasking chaperone

Kiran Aslam
Purdue University

PURDUE UNIVERSITY
GRADUATE SCHOOL
Thesis/Dissertation Acceptance

This is to certify that the thesis/dissertation prepared

By Kiran Aslam

Entitled
DECIPHERING THE ROLE OF HSP31 AS A MULTITASKING CHAPERONE

For the degree of Doctor of Philosophy

Is approved by the final examining committee:

Tony R Hazbun
Chair

Jean-Christophe Rochet

Douglas J. LaCount

Ruben C Aguilar

To the best of my knowledge and as understood by the student in the Thesis/Dissertation Agreement, Publication Delay, and Certification Disclaimer (Graduate School Form 32), this thesis/dissertation adheres to the provisions of Purdue University's "Policy of Integrity in Research" and the use of copyright material.

Approved by Major Professor(s): Tony R Hazbun

Approved by: Jean-Christophe Rochet 06/07/16
Head of the Departmental Graduate Program Date

DECIPHERING THE ROLE OF HSP31 AS A MULTITASKING CHAPERONE

Dissertation

Submitted to the Faculty

of

Purdue University

by

Kiran Aslam

In Partial Fulfillment of the

Requirements for the Degree

of

Doctor of Philosophy

August 2016

Purdue University

West Lafayette, Indiana

For my parents;

Aslam and Mukhtiar

And to my wonderful husband Khizar Rouf

ACKNOWLEDGEMENTS

Though only my name appears on the cover of this thesis, earning a doctorate and writing a thesis is certainly not done single-handedly. I owe my gratitude to all those people who have contributed to its production and because of them my experience at Purdue University has been one that I will cherish forever. I would like to reflect on all those people who have supported and inspired me not only in the scientific arena, but also on a personal level throughout this period.

First of all, my deepest gratitude goes to my advisor, Dr. Tony Hazbun. I have been fortunate to have an advisor who trained me how to question thoughts and deliver ideas. He gave me the freedom to explore on my own, and at the same time guided me to recover whenever I faced obstacles. I would like to thank him for his patience in mentoring me as a scientist. Without his guidance, this work would not exist.

I extend my sincere gratitude to Dr. Jean-Christophe Rochet, who has been always there to listen and give advice. I am sincerely grateful to him for the insightful feedback that helped me sort out the technical details of enzymatic assay presented in this thesis. I am also thankful to him for carefully reading and commenting on many revisions of my JBC manuscript. I am indebted to him for his continuous encouragement and guidance that will stay with me for the rest of my life. I am also thankful to Dr. Douglas J. LaCount for reading my reports, providing thought-provoking comments that helped me move

forward in positive direction. I am grateful to him for constructive criticisms at different level of graduate school that have helped me focus on my goals. I also like to thank him and his group members for letting me use their lab's equipment and reagents. Next, I would like to thank Dr. Ruben C Aguilar who is one of the best teachers that I have had in my life. I am grateful to him for teaching me important concepts in cellular biology that help me understand and enrich my ideas.

Next, I would like to acknowledge past and present members of Dr. Hazbun's group, for their friendship, valuable discussion and technical help with scientific projects. I appreciate the efforts of the many undergraduate students who helped me make the media and buffers to run various experiments on time. I am also thankful to the faculty and staff of Medicinal Chemistry and Molecular Pharmacology department for their various form of support during my graduate study.

Most importantly, I would like to express my heart-felt gratitude to my family and friends who have helped me stay sane through these difficult years. I greatly appreciate their love, support and belief in me that has been strength for me. I have to give a special mention to my husband Khizar Rouf who worries about me more than I worry about myself.

Finally, I appreciate the United State Education Foundation in Pakistan and International Institute of Education for providing me Fulbright fellowship that was a huge financial support for me.

TABLE OF CONTENTS

Page

Page

Page

Page

Page

LIST OF ABBREVIATIONS

AD Alzheimer's disease
Ade Adenine
AGE Advanced glycation end products
ALS Amyotrophic Lateral Sclerosis
ANOVA Analysis of variance
ApoA1 Apolipoprotein A1
ApoE Apolipoprotein E
APP Amyloid precursor protein
Arg Arginine
ATG Autophagy related
ATP Adenosine 5'-triphosphate
BBB Blood brain barrier
BSA Bovine serum albumin
BSE Bovine spongiform encephalopathy
CFP Cyan fluorescence protein
CJD Creutzfeldt-Jakob disease
CNS Central nervous system
COMT Catechol-O-methyl transferase
CS Citrate synthase
Cys Cysteine
DHE dihydroethidium
DRPLA dentato-rubral and pallido-luysian atrophy
DsRed Red fluorescence protein from *Discosoma* sp
DTT Dithiothreitol
EDTA Ethylene di-amine tetra acetic acid
EGF Epidermal growth factor
ETC Electron transport chain
FTD Fronto-temporal dementia
Gal Galactose
GC/MS Gas chromatography/Mass spectrometry
GFP Green fluorescence protein
GLO Glyoxalase
Glu Glutamine
GSH Glutathione (reduced form)
GSS Gerstmann-Straussler-Scheinker
HCL Hydrochloric acid
H_2O_2 Hydrogen peroxide
HEPE 4-(2-hydroxyethyl)-1-piperazineethanesulfonic acid
His Histidine
Hr Hour
HSP Heat shock protein
Hz Hertz
iCJD iatrogenic Creutzfeldt-Jakob disease
IPOD Insoluble protein deposits
IPTG Isopropyl β-D-1-thiogalactopyranoside
kDa Kilo dalton
KO Knocked out
LB Luria-Bertani Broth
LBs Lewy bodies
L-dopa L-3,4-dihydroxyphenylalanine
Leu Leucine
Lys Lysine
MAO Monoamine oxidase
$MgCl_2$ Magnesium chloride
MGO Methylglyoxal
Min minute
mM mili molar
MORF Movable open reading frame
MRI Magnetic resonance imaging
MS Mass spectrometry
NaCl Sodium chloride
NAT Nourseothricin N-acetyl-transferase
NDD Neurodegenerative disorder
N-terminal Amino-terminal

NMDA N-methyl-D-aspartate
NMS Non-motor symptoms
OD Optical density
OPR Oligopeptide repeat region
ORF Open reading frame
PBS Phosphate buffered saline
PCR Polymerase chain reaction
PD Parkinson's disease
PEG Poly ethylene glycol
PET Positron emission tomography
PI3K Phospho inositol 3 kinase
PolyQ Poly glutamine
PQC Protein quality control
PrD Prion forming domain
PRNP prion protein
PrP^C Cellular prion protein
PTEN Phosphate and tension homolog
QNR QN rich region
ROS Reactive oxygen species
RPM Revolutions per minute
SBMA Spinal and bulbar muscular atrophy
SCA Spino-cerebellar ataxia
SD Synthetic dextrose
SDD-AGE Semi-Denaturating Detergent Agarose Gel Electrophoresis
SDS-PAGE Sodium dodecyl sulfate polyacrylamide gel electrophoresis
sHSP Small heat shock protein
TCA Tricarboxylic acid
TDP-43 Transactive response DNA-binding protein 43
Trp Tryptophan
UPS Ubiquitin proteasome system
Ura Uracil
USA Ureidosuccinate
vCJD Variant Creutzfeldt-Jakob disease
WT Wild type
YFP Yellow fluorescence protein
YPD Yeast extracts peptone dextrose
α-syn Alpha-synuclein

ABSTRACT

Aslam Kiran. Ph.D., Purdue University, August 2016. Deciphering the Role of Hsp31 as a Multitasking Chaperone Protein Major Professor: Tony Hazbun.

Among different type of protein aggregation, amyloids are biochemically well characterized state of protein aggregation that is commonly associated with a large number of neurodegenerative diseases in mammals and cause heritable traits in *Saccharomyces cerevisiae*. Among many other neurodegenerative diseases linked with amyloids, Parkinson's disease is the second most common disorder that is caused by progressive deterioration of dopaminergic neurons in *substantia nigra*. Cellular stresses such as accumulation of high level of reactive oxygen species, mitochondrial dysfunction and α-syn aggregation lead to toxicity and neuronal cell death in Parkinson's disease patients. Mutations in certain genes are also involved in the development of a familial form of PD including PARK7 that encodes DJ-1. DJ-1 is a member of ThiJ/DJ-1/PfpI protein superfamily that are the quintessential multitasking or moonlighting protein family as evidenced by their involvement in multiple cellular functions including oxidative stress sensing, protein folding, proteasome degradation, mitochondrial complex stabilization, methylglyoxalase and deglycation enzyme activities. The members of the ThiJ/DJ-1/Pfp1 superfamily appear to have evolved to numerous mechanisms to manage cellular stress. The protein superfamily members are present across the evolutionary

spectrum including prokaryotes and the budding yeast, *S. cerevisiae*, that has four paralogs Hsp31, Hsp32, Hsp33, and Hsp34. Hsp31 consists of 237 amino acids with a MW of 25.5 kDa and forms a homodimer in solution. It possesses the Cys-His-Glu catalytic triad common to ThiJ/DJ-1/PfpI superfamily proteins. Previously, we have shown that Hsp31 possesses chaperone properties with protective effects against α-syn toxicity in yeast. Recently, it is shown that Hsp31 has a methylglyoxalase activity that converts the toxic metabolite methylglyoxal into lactate. Here, we confirmed that Hsp31 is a robust methylglyoxalse that is more potent in activity than its human homolog DJ-1. We demonstrated that Hsp31 chaperone activity to protect the cells from α-syn toxicity is not under the influence of its enzymatic activity or autophagy pathway. Moreover, we confirmed that Hsp31 expression is induced by H_2O_2 mediated oxidative stress and further showed an increased expression of Hsp31 under α-syn mediated proteotoxic stress. These results establish that Hsp31 molecular chaperone activity is self-sufficient to protect the cells from stress conditions without requiring its enzymatic activities. Another associated class of amyloid aggregation state includes prions, which are self-replicating, misfolded proteins capable of adopting amyloid aggregates in cells. In yeast, [*PSI*$^+$] prion is the aggregated form of translation termination factor Sup35. Sup35, a translation-termination factor, is one of the original and best-studied prions in yeast. In the present study, we established the role of Hsp31 in preventing Sup35 aggregation both *in vivo* and *in vitro* using fluorescence microscopy, flow cytometry and SDD-AGE respectively. In addition, we provide evidence that Hsp31 act early on in the process of protein aggregation, as we didn't observe any co-localization of Hsp31 with larger Sup35 prion aggregates. Moreover, Hsp31 transiently prevents prion induction with no

significant reduction over a prolonged induction of Sup35 aggregation indicating that Hsp31 acts prior to the formation of larger aggregates. This was further confirmed, as an elevated level of Hsp31 by itself was unable to cure [*PSI*$^{+}$] prion with formerly present large aggregates. We established that Hsp31 inhibit Sup35 [*PSI*$^{+}$] prion formation in collaboration with a well-known disaggregase, Hsp104. Hsp31 inhibits Sup35 aggregates formation and potentiates [*PSI*$^{+}$] prion curing by overexpression of Hsp104. Absence of Hsp31 reduce the rate of [*PSI*$^{+}$] prion curing by Hsp104 without influencing its ability to rescue the cell by thermotolerance. We also showed that Hsp31 physically interact with Hsp104 and together they prevent Sup35 prion toxicity to greater extends than if they were expressed individually in the yeast. These results elucidate a mechanism of Hsp31 on prion modulation that could have implication in many neurodegenerative diseases. Taken together, the results show that Hsp31 is a stress-inducible protein with chaperone and glyoxylase activity that acts on a wide spectrum of misfolded proteins including α-syn and Sup35. These studies set the stage for further mechanistic insight in the biological roles of the Hsp31/DJ-1 chaperone family.

CHAPTER 1. INTRODUCTION

1.1 High-fidelity protein quality control

Biogenesis of protein is carefully monitored by protein quality control (PQC) process to avoid sporadic errors or damage ring during the synthesis or life times of cellular proteins. In order to maintained protein homeostasis, damaged proteins must be corrected or degraded after synthesis (1-5). These two types of defense mechanisms are mediated by a complex network of chaperones, the ubiquitin–proteasome system (UPS) and autophagy mediated-lysosomal proteolysis (2,4,6). Chaperones bind newly synthesized proteins as well as unfolded proteins to assist them in reaching a mature protein conformation at the expense of ATP hydrolysis (2,7,8). Moreover, ubiquitin ligases that are recruited by chaperones, will themselves degrade damaged proteins that are beyond repair (2,6,8,9). In addition, PQC monitors the cell to ensure proper folding of mature proteins that have the tendency to revert into native conformation under oxidative or proteotoxic stress (3,10). Similarly, additional quality control systems will ensure the proper synthesis of other macromolecules such as DNA and RNA (1,3,11,12). The PQC process occurs throughout the cell and is classified according to the location of the misfolded substrate in different cellular compartments (7). Therefore, the PQC system plays a vital role in maintaining the proper folding of proteins and it has significance in

the pathophysiology of diseases associated with protein misfolding and aggregation (13,14).

1.1.1 Consequences of Protein Misfolding

Virtually all aspect of biological life processes is determined by highly diverse enzymatic and the structural characteristics of proteins. On the other hand, protein can be a vulnerable entity for living cells if there is extensive change in their structural conformation (15-18). The alpha helical spiral coils are the most common secondary structure in proteins that must be maintained to their native conformation, in order to be biochemically functional. Although, many functional native proteins contain beta sheets, a protein becomes toxic if it acquires an abnormal conformational transition from alpha helix to beta sheet (19-22). Partially folded or misfolded proteins expose their hydrophobic amino acids and unstructured polypeptide to promote protein aggregation in a concentration dependent manner. Such misfolding or partial folding leads to association of proteins with each other to form protein aggregates that further accumulate together to form larger aggregates (23,24). While, hydrophobic forces driving the formation of smaller aggregates primarily leads to larger amorphous aggregates, it can also guide to the formation of highly structured protofibrils known as amyloids that possess distinct cross β-strands and are thermodynamically stable (16,21,25).

1.1.2 Role of chaperone in protein homeostasis

Amino acid sequences of any protein encoded by DNA, contains all the fundamental information required to fold a protein into a three-dimensional structure, as small proteins can refold *in vitro* from a denatured state without needing other components or energy sources (3). However, research over the past 20 years has revealed that many proteins

particularly large proteins require molecular chaperones to fold effectively and in a timely manner *in vivo* (26,27). Chaperones can be defined as a protein that binds and stabilizes another protein to achieve its functionally active conformation. Chaperones form a complex network of many different classes of structurally unrelated proteins that cooperate together in cells to maintain protein homeostasis (28). Members of these families are often up regulated under conditions of stress in which the concentration of partially folded protein intermediates are increased. They are often known as heat shock proteins (HSPs) or stress proteins and named after their molecular weights such as Hsp40, Hsp60, Hsp70, Hsp90, Hsp100 and small HSPs (27,29-33). They are involved in multiple functions of protein homeostasis including *de novo* protein folding, oligomeric assembly, protein trafficking, refolding of denatured proteins as well as help in proteolytic degradation and disaggregation of larger aggregates (26,33-40). The classes of chaperone, such as Hsp70 and Hsp90 that are involved in the *de novo* folding of protein require ATP hydrolysis and multiple binding and release of co-chaperones. They also cooperate with ATP-independent chaperones, such as small HSPs to facilitate protein disaggregation (33,34,36,37). In the *de novo* folding of proteins, ATP-dependent chaperones usually bind to exposed or accessible hydrophobic amino acids of a non-native protein to transiently prevent aggregation driven by ATP hydrolysis. ATP hydrolysis is facilitated by co-chaperones such as Hsp40, that mediate Hsp70 recruitment to substrate proteins, Hsp40 also interacts with partially folded protein substrate to unfolded peptides. After release of the substrate protein from co-chaperones, Hsp70 rebinds to the peptides until they achieve their functional folded state and therefore prevent them from aggregation (26).

Another role of chaperones in maintaining protein homeostasis is to regulate protein concentration in the cells. During the folding process, chaperones stabilize protein molecules and ultimately increase their concentration to achieve the cells need and similarly, when a particular protein is not in demand chaperones diminish the folding process with the help of regulator proteins to decrease its concentration. Although the primary role of the chaperone machinery is during the initial protein folding process, it is now being accepted that many proteins depend on molecular chaperones assistance to maintain or regain their functionally active conformations throughout their cellular life (26,41).

1.1.2.1 Heat Shock Proteins

Italian geneticist Ferruccio Ritossa first discovered the first evidence of heat shock proteins in 1962. He reported that heat shock treatment of *Drosophila* larvae induces a puff pattern in the polytene chromosomes that was later was identified and associated with the synthesis of heat-shock proteins that are now commonly known as molecular chaperones (42,43). These proteins are highly upregulated under stress conditions such as environmental, metabolic or pathophysiological stress and play a vital role in the survival of cells under such conditions. These proteins are highly conserved across species and generally classified according to their molecular masses into six major families i.e. Hsp100, Hsp90, Hsp70, Hsp60, Hsp40 and small heat shock proteins (sHSPs) (44-46). A list of major HSPs along with their cellular location and brief description of primary functions is outlined in Table 1.1.

Table 1.1 Major heat shock proteins: subcellular location and functions.

Heat-shock protein	Subcellular localization	Known functions
Hsc70	Cytosol/nucleus	Protein folding, clathrin uncoating, peptide binding
Hsc74	Mitochondria	Involved in antigen presentation and radioresistance. Also oncogenic (overexpression of Mot-2 leads to p53 inactivation and cell transformation).
Hsp110	Cytosol/nucleus	Binds to Hsc70 to form high-molecular-weight complex; involved in protein folding, thermotolerance, and embryogenesis
Hsp27	Cytosol	Antiapoptotic, cytoprotection
Hsp40	Cytosol	Repair denatured proteins, together with Hsp70/Hsc70
Hsp60	Mitochondria	Cytoprotection; macrophage activator possibly through Toll-like receptors
Hsp70	Cytosol/nucleus	Cytoprotection and anti-apoptotic, Hsp70-2 implicated in spermatogenesis
Hsp90α	Cytosol	Protein folding, peptide chaperone, cytoprotection, intracellular signaling (e.g., steroid receptor), cell-cycle control and buffering of harmful mutations
Hsp90β	Cytosol	Major cytosol chaperone; protein folding; cytoprotection; intracellular signaling (e.g., steroid receptor); cell-cycle control; and buffering of harmful mutations

1.1.2.2 Small heat shock proteins

The sHSPs are phylogenetically widespread and have been found in almost all organisms ranging from archaebacteria, prokaryotes and eukaryotes. Within cells, they are found in multiple subcellular locations where they bind to wide range of unfolded proteins substrates to prevent their aggregation (44,47-49). Proteins in this family possess 12-43 kDa weights with the ability to form dynamic oligomers. Monomers of many sHSPs are composed of a conserved 80-100 amino acid α-crystallin domain, accompanied with beta-strands responsible for dimerization. The N-terminal domain is responsible for oligomerization, phosphorylation and chaperone activity but it is not a highly conserved domain, while the C-terminal domain is accountable for client protein interaction, nucleotide binding and homodimerization (48). *In vitro* studies revealed that quaternary structures of sHSPs are very stable and can binds to large number of unfolded protein substrates compared to other major chaperones. sHSPs are consider as having 'holdase' activity because of their unusually high tendency to bind unfolded client proteins and to assist subsequent refolding of substrates by ATP-dependent chaperone networks (44,48). Structural and *in vitro* studies have led to a proposed model that under stress conditions, oligomers of sHSPs undergo structural rearrangement and breakdown into monomers to be functionally active. Although the exact mechanism is poorly understood, it is thought that the hydrophobic regions of sHSPs may bind with hydrophobic surfaces of partially misfolded proteins to make larger soluble complexes that inhibit further aggregation of the misfolded proteins (50-52).

The sHSP family displays a functional diversity such as protecting the cells from stressful conditions, involvement in stress tolerance, protein folding, protein degradation, maintaining cytoskeletal integrity, cell cycle, signal transduction, cell differentiation and cell death. Moreover, many members of sHSP family interact with their substrates to display potent anti-apoptotic activity and anti-inflammatory property as well as exhibit cardio and neuroprotection (44,47,53). Therefore, sHSP family members have important implications in a broad range of health and disease conditions. However, many unanswered questions remain regarding the underlying mechanisms of sHsps pleiotropic functions and their promiscuous interactions.

1.2 Neurodegenerative diseases

Several common pathways have been proposed to cause the underlying etiology and pathology of neurodegenerative diseases such as Alzheimer's disease (AD), Parkinson's disease (PD), Fronto-temporal dementia (FTD), Amyotrophic Lateral Sclerosis (ALS), and Prion diseases (54). Multiple factors have been implicated in causing neurodegeneration such as protein misfolding leading to aggregation, mitochondrial dysfunction, free radical formation caused by oxidative stress and environmental exposure of metals and pesticides associated with age (20,22,55,56). Although there is a partial overlap in the general mechanism of these neurodegenerative diseases, each disease has its own distinct molecular mechanism and pathological manifestation including degradation of specific brain regions and deposits of protein aggregates in neurons (55,57). The most common characteristic of this group of diseases is the accumulation and deposition of aggregated or misfolded proteins including α-synuclein (α-syn) in PD, amyloid-β in AD, huntingtin protein in HD and transactive response

DNA-binding protein 43 (TDP-43) in ALS (54,56-61). A list of aggregation associated neurodegenerative diseases are outlined in Table 1.2.

Table 1.2 Aggregation associated neurodegenerative diseases.

Disease	Associated protein/gene	Protein deposits	Most affected regions
Alzheimer's disease	Amyloid beta, APP Tau, ApoE, PSEN1, PSEN2	Extracellular Plaques Intracellular tangles	Cortex, Hippocampus, basal forebrain, brain stem
Parkinson's disease	αSyn, Parkin, DJ-1, UCHL-1, LRRK2	Lewy bodies	Substantia nigra, cortex, locus ceruleus
Huntington's disease	Huntington	Huntington with poly glutamine expansion	Striatum, other basal ganglia, cortex
Prion disease CJD, fatal familial insomnia)	Sporadic, genetic and infectious, PrP^{Sc}, PRNP	Prion amyloid plaques, Spongiform degeneration	Cortex, thalamus, brain stem, cerebellum
Polyglutamine diseases (DRPLA, GSS, SCA1-3, SBMA etc)	PolyQ containing proteins, Genes with CAG repeat expansion	Nuclear and cytoplasmic inclusions	Basal ganglia, brain stem, cerebellum and spinal cord

Table 1.2 continued

Familial amyotrophic lateral sclerosis (ALS)	SOD1	Bunina body tangles	Spinal motor neurons and motor cortex
Tauopathy	Tau	Cytoplasmic inclusions	Cortex, brain stem and other areas

APP, amyloid precursor protein; ApoE, Apolipoprotein; PSEN1/2, Presenilin 1/2; PRNP, prion protein; CJD, Creutzfeldt-Jakob disease; DRPLA, dentato-rubral and pallido-Luysian atrophy; GSS, Gerstmann-Straussler-Scheinker; SBMA, spinal and bulbar muscular atrophy; SCA, spino-cerebellar ataxia.

1.2.1 Mitochondrial dysfunction in neurodegenerative disease

The mitochondria, most often known as powerhouses of the cells, are responsible for most of the energy supply in eukaryotic cells. They play critical roles in regulating cell processes including signaling pathways, calcium balances, reactive oxygen species (ROS) formation, cell cycle regulation, thermogenesis and cell death. The loss of mitochondrial function is associated with increased ROS production and oxidative stress that are responsible for development of numerous neurodegenerative disorders. Mitochondria generate adenosine triphosphate (ATP) during oxidative phosphorylation using metabolic intermediates in tricarboxylic acid (TCA) cycle. Superoxide anion radicals (O^{-2}) that are produced during electron transport chain (ETC) activity are converted into hydrogen peroxide by enzymatic action of superoxide dismutase in the mitochondria. Hydrogen peroxide further detoxifies by the action of glutathione peroxidase into water in the mitochondria. Defects in enzymes involved in the ETC leads to increased production of ROS resulting in a decrease in the mitochondrial membrane potential, energy crisis and finally cell death. In addition to antioxidant activity of mitochondrial enzymes mentioned above, cells also possess glutathione (GSH), Vitamin E, Vitamin C and ubiquinone as antioxidant agents that protect the cell from oxidative stress. An imbalance in the antioxidant homeostasis leads to oxidative stress in cells (62-64). In the CNS, neurons are particularly prone to oxidative stress resulting in accumulation of ROS that potentially leads to the initiation of free radical chain reactions and finally cell death. Many classes of macromolecules ranging from lipids to DNA and proteins are found to be oxidatively damage in neurodegenerative diseases such as PD, AD, HD and ALS (56,65-67). Thus mitochondrial dysfunction and defects in mitochondrial activity parameters including

alteration in mitochondrial dynamics, increase in ROS production and loss of energy leads to neuronal death and are an important contributor in the manifestation of neurodegenerative disorders (66). Therapeutic approaches to target mitochondrial functions could certainly be useful however, using antioxidants, as sole therapy to treat neurodegeneration appears to be not sufficient. In fact, several clinical studies have demonstrated only little success with antioxidants in the treatment of neurodegeneration (68). Targeting mitochondrial proteins to alter abnormal mitochondrial dynamics may provide a potential therapeutic strategy against neurodegenerative diseases (64).

1.2.2 Amyloidogenesis

The term ‘amyloid’ has been used to describe the highly ordered cross beta proteinaceous structures found in various pathological conditions. Amyloids are formed when a soluble and innocuous protein transforms into insoluble protein aggregates that might not be directly invasive but are associated with neuropathology. The tendency of amyloid formation is multifactorial including amino acid composition, protein sequences and concentration, posttranslational modification and environmental factors (16,19). Several studies now clearly show that protein aggregation is a complex process that occurs in several different steps, making different kinds of intermediates and finally turned into larger aggregates that could be either amorphous or amyloids (69). However, there is much to be learned as most of these studies are done *in vitro* and hence may not simulate *in vivo* behavior in human diseases (70). Initiation of the multi-step pathway of protein aggregation begins with modification of protein to an abnormal conformation that may be a covalent modification such as cleavage or phosphorylation of the disease protein. These modifications of proteins facilitate the conversion of monomers into smaller oligomers

that further assemble into protofibrils. Association of these protofibril intermediates can form larger amyloid aggregates that can be visualized under the microscope (71-76). It is hypothesized that intermediate species are more toxic than the precursor protein or final amyloids (73,77,78) (Figure 1.1). Therefore, it would maybe beneficial to inhibit aggregation formation at early stages of the pathway, as it may prevent the formation of toxic oligomeric species.

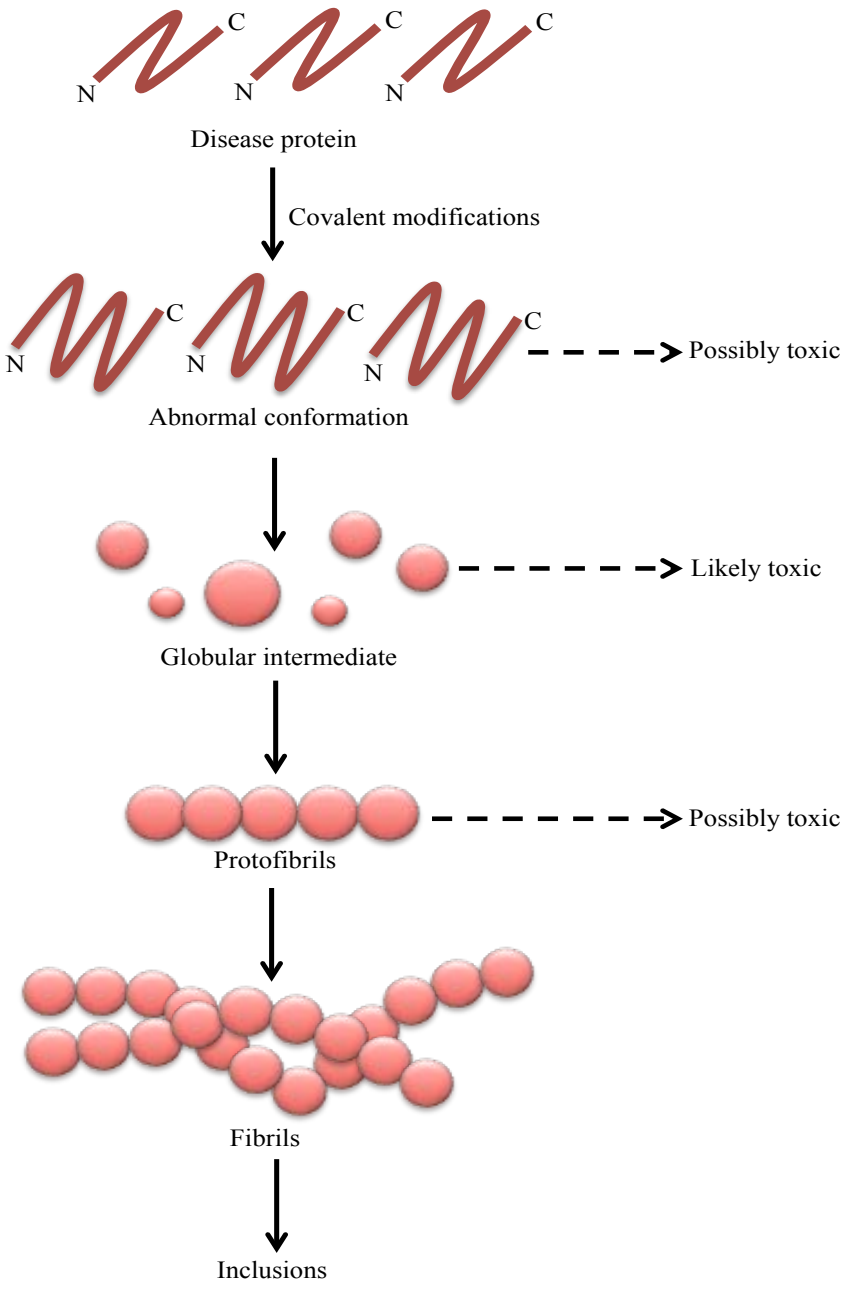

Figure 1.1 Hypothetical pathway in the formation of amyloid.

Amyloidogenesis is considered to be a legitimate pathological reason for neuronal degeneration although the exact mechanism behind this degeneration remains unidentified (14,79). Several models of amyloid-associated toxicity have been proposed.

First, amyloids occupy the extracellular space that damages the normal architecture and function of cells and thus leads to neuronal toxicity. It is also proposed that smaller oligomers formed at initial stages of amyloidogenesis are more toxic to cells as they destabilize cellular membranes (16,74,80,81). These intermediate oligomers assemble into final amyloid fibrils that have been hypothesized as a non-invasive product of the toxic intermediates that might rather be a detoxification mechanism. Another group of studies suggest that generation of ROS by the incorporation of redox metals into amyloids could affect cell viability (74). On the other hand, the larger aggregates could recruit and thus diminish some essential proteins for cell survival (82).

1.3 Parkinson's disease

PD is an idiopathic disease of the nervous system characterized by two neuropathological hallmarks, the preferential loss of dopaminergic neurons in the *substnatia nigra pars compacta* region of the brain and the presence of cytosolic inclusions called Lewy bodies (LBs) in various brain regions (56,58,83). It is a chronic progressive disease that affects the older population but can also occurs in much younger patients and is the second most common neurodegenerative disorder after AD (84,85). Dr. James Parkinson, after whom the disease is named, first recognized PD in the early 1800's. PD affects 10 million people worldwide and it is expected that its prevalence in America will increase dramatically over the next 20 years as the proportion of the population ages (86,87). In developing nations, the life expectancy is rising and cases of such age related neurological disorders is also increasing resulting in a strong impact on the healthcare system and economy due to direct and indirect costs associated with care of PD patients (84,88,89). Therefore, it is critical to understand the molecular mechanisms of PD to

develop better therapeutic strategies, early detection of the disease and identify causative genetic and environmental factors.

1.3.1 Risk factors

Age is the major risk factor for PD with an average age of disease onset of 60 years and risk of diagnosis greatly increases after 85 years of age (90,91). Other risk factors include family history and environmental stress such as exposure to pesticide toxins. Men are more susceptible than women to develop the disease but the causative risk factor is still unclear (92-94). Numerous other risk factors have been associated with PD though the epidemiologic evidence is not robust. These include drinking of well water, excess milk consumption, obesity, living in rural areas with exposure to copper, manganese, lead and hydrocarbon solvents such as industrialized, farming or agricultural work (94-96). On the other hand, cigarette smoking and caffeine intake have been linked with reduced risk of PD (97). Table 1.3 describes the etiology of PD.

Table 1.3 Etiology of Parkinson's disease

Feature	Details
Age of onset	65
Men:women	1.5:1
Idiopathic:hereditary,%	90:10
Frequency/1000persons	
Patients aged 55-65 y	0.3
Patients >85 y	4.4
Percentage prevalence	
Total population	0.3
People >60 y	1
Life expectancy	Varies with the age of the onset and occurrence of dementia
Risk factors	Age, family history, pesticide exposure and head injury
Motor symptoms	Tremor, rigidity, bradykinesia, postural instability, impaired speech and gait
Non motor symptoms	Constipation, autonomic dysfunction, dementia, depression, sleep disorder and psychosis

1.3.2 Genetic factors

Although the majority of PD cases are sporadic, about 5-10% PD cases are familial as they are associated with gene mutation. The number of genes associated with the onset of early or advanced PD have steadily increased over the last 15 years including mutations or amplification in the LRRK2, PARK2, PARK7, PINK1, or SNCA (PARK1) gene and possibly additional unidentified genes (92,94,98). Even though most cases of PD are sporadic, examining the genes associated with PD is valuable as there is evidence to show a strong correlation between sporadic and familial forms of PD. PARK1 encodes α-syn consists of autosomal dominant gene, mutation or multiplication of this can lead to PD (99,100). The α-syn protein is a 140 amino acid protein that exclusively expressed in the CNS. Natively it is present mostly as membrane-bound α-helices in the neurons. (101,102). In the disease form, α-syn mainly presents as an aggregated protein component found in LBs (103). Several α-syn mutants including A53T, A30P, E46K and H50Q have been shown to increase the aggregation formation that leads to form potentially toxic protofibrils. High level of α-syn also sequestered several cytoskeletal proteins, such as tubulin, that prevent the conversion of α-syn into fibrils leading to increase in toxic protofibril species (99,100,104-107).

1.3.3 Diagnosis

Despite extensive research done on the pathophysiology of PD, its diagnosis is still restricted to suboptimal methods for detection and prognosis. There is a critical need for the development of highly sensitive and specific biomarkers as they are lacking currently (108). The PD diagnostic decision in a clinic relies on the presence or manifestations of symptoms associated with the disease such as bradykinesia, rest tremor, rigidity, postural

instability and impaired gait (93,109-111). If patient response to dopaminergic agents such as levodopa and patient history reveals gradual progression of symptoms there is likelihood of accurate diagnosis of PD. However, responsiveness to levodopa has been seen in other parkinsonian syndromes and unrelated dystonias (108,112,113). To confirm PD, presence of Lewy bodies (LBs), protein deposits in *substantia nigra* and loss of neurons is a required diagnostic criteria upon examination of a deceased patient's brain section (110,113). As this approach is a post mortem examination, it has no implications in clinical diagnosis.

There are several biomarkers currently being analyzed that can correlate with PD prognosis with high accuracy and can be used as next generation diagnostic tools (114-117). Among them the major constituent of PD such as oligomeric forms of α-syn and DJ-1 protein level have been analyzed in the blood of PD patients with no success (107,118,119). Several other biomarkers such as uric acid level, iron level in the *substantia nigra* region of brains as well as epidermal growth factor (EGF) and Apolipoprotein A1 (ApoA1) are under investigation (120-123). Currently there is no single biomarker available to predict PD progression with reliability and validity (114,124).

Neurologic imaging tools such as positron emission tomography (PET) scan, magnetic resonance imaging (MRI), ultrasonography and others play small role in diagnosis and are presently not accepted as diagnostic tool for PD (125-127).

1.3.4 Clinical presentation

There are four cardinal components of symptoms associated with PD: motor symptoms, cognitive changes, behavioral/neuropsychiatry symptoms, and autonomic nervous system failures. These can be divided into motor and non-motor symptoms.

1.3.4.1 Motor symptoms

The major motor features of PD are sometime represents by a mnemonic TRAP. It stands for Tremors, Rigidity, Akinesia (or bradykinesia) and Postural instability. According to pathological and neuroimaging studies, onset of motor symptoms occurs only after about 50-70% of neurodegeneration of *substantia nigra* (89,128). Rate of motor symptoms are highly variable among patients. Bradykinesia is the most characteristic clinical manifestation of PD that refers to slowness of movement. Patients often describe bradykinesia as tiredness or weakness and commonly report difficulty from getting up from a chair and opening packages or containers (129). Rigidity of idiopathic PD referred to as 'cogwheel' phenomenon is when patients experience difficulty to initiate a movement. At the beginning, it is unilateral but can move to other sides in the later stages of the disease. Tremors at rest are the most easily recognizable symptom of PD that are always prominent at the distal part in the extremities and occur at frequency between 4 to 6 Hz. At the late stages of PD usually after onset of other clinical features postural instability develops due to loss of postural reflexes. Postural instability along with freezing of gait significantly increases the risk of hip fracture due to sudden fall (130-133).

In addition to classic motor features, other motor symptoms are also observed including dysarthria, masked facial expression (hypomimia), dysphagia, blurred vision, decrease eye blink, dystonia and difficulty turning in bed (93).

1.3.4.2 Non-motor symptoms

Along with the motor symptoms of PD, the non-motor symptoms (NMS) are major cause of disability for PD patients but unfortunately unlike motor symptoms NMS are not well recognized and undertreated (109,134-136). Recognition and treatment of NMS is an important and fundamental aspect to consider in order to delivering a comprehensive healthcare for PD patients. NMS arise with the progression of disease and are diverse including neuropsychiatric symptom, sleep disorder, autonomic symptom, gastrointestinal symptom and sensory symptom (Table 1.4). Sometime treatment of PD leads to development or exacerbation of NMS in PD patients therefore it is important to recognize, monitor and treat these symptoms (135-138).

Table 1.4 Non-motor Symptoms of Parkinson's disease

Neuropsychiatric symptoms	**Sleep disorders**	**Autonomic symptoms**	**Gastrointestinal symptoms**
Depression	Restless legs	Bladder disturbances Urgency Nocturia	Dribbling of saliva
Apathy, anxiety Obsessional behavior	Periodic limb movements	Sweating	Dysphagia/choking
Anhedonia	REM behavior disorder	Orthostatic hypotension (OH)	Reflux
Attention deficit	Excessive daytime somnolence	Sexual dysfunction	Vomiting Nausea
Hallucinations	Vivid dreaming	Erectile impotence	Constipation Fecal incontinence
Delusions Dementia	Non-REM sleep-related movement disorders Insomnia	Hypotestosterone state	Unsatisfactory voiding of bowel

1.3.5 Management of Parkinson's disease

Currently, there are only symptomatic treatments available with no proven neuroprotective agents. For earlier stages of disease after diagnosis, it is important to take time and educate the patient and relative about the condition and its implications. The decision to start the treatment especially at earlier stages of disease when there is little functional deficit is difficult. This decision should be made based on the age of the patient, the consents of the patient, the presence of cognitive impairment, the likelihood of complications associated with treatment and additional health problems (89,139,140). The current gold standard regimen for managing symptoms is precursor of Dopamine i.e. L-3,4- dihydroxyphenylalanine (L-Dopa or levodopa). Levodopa can cross the blood brain barrier (BBB) easily to enter the central nervous system where it converts into dopamine in the presence of an enzyme L-aromatic decarboxylase (133). Although L-Dopa reduced the symptoms of PD and decreased the mortality rate associated with PD, it is responsible for wide range of side effects due to peripheral conversion into dopamine. To avoid these side-affects, dopa decarboxylase inhibitors, Carbidopa and Benserazide are co-administered that cannot cross BBB and only inhibit peripheral dopamine conversion. However, chronic use of L-dopa is associated with induction of dyskinesia that is particularly problematic at later stages of disease with loss of large number of dopaminergic neurons (141).

Another strategy to treat symptoms of PD is the use of dopamine agonists including ergot derivatives such as bromocriptine, pergolide, cabergoline and lisuride; and non-ergot derivatives as ropinirole and pramipexole. Dopamine agonists produced fewer of motor

complication compared with L-dopa but efficacy is much lower when used as mono-therapy (142-144).

One more class of drug, the monoamine oxidase B (MAO-B) inhibitors, Selegiline and Rasagiline, have demonstrated efficacy in PD disease and have potential to use as mono-therapy in both early and advanced disease. An N-methyl-D- aspartate (NMDA) receptor antagonist, amantadine, and anticholinergics such as benztropine have also been proven efficacious in a small sub-population of PD patients (112,139,143,145). After few years of consistent and effective response to L-dopa, the effect of a single L-dopa dose in most patients fluctuates in terms of motor performance leading to wearing-off phenomenon. Several catechol-O-methyl transferase (COMT) inhibitors and amantadine have been used in combination with L-dopa for the treatment of dyskinesias and other motor symptoms (144,146). A surgical procedure called deep brain stimulation has been reserved for patients who are unresponsive to pharmacological treatment and have a high degree of motor fluctuation and dyskinesias (147).

1.3.6 Yeast Model of Parkinson's disease

Saccharomyces cerevisiae is a compatible cell model to understand the molecular mechanisms of several human diseases including PD, for which many α-syn toxicity models have been developed (148,149). This unicellular eukaryote is a well-suited model for studying the disease related phenotypes, for instance, stress response, mitochondrial and vesicular trafficking defects as well as oxidative stress response. In addition, this simple genetic model has been extensively used for large-scale screening of drugs and genes to uncover the underlying mechanism of disease (17,148-157). In this study we used a budding yeast (*Saccharomyces cerevisiae*) model of PD that evaluates α-syn

misfolding, aggregation, and toxicity. In this model, at relatively low concentration of α-syn localizes to membrane and is not toxic to cells. When two gene copies of α-syn are expressed, an increase in the concentration of α-syn forms prominent intracellular cytoplasmic inclusions or foci that are associated with toxicity to the cells. This *Saccharomyces cerevisiae* model throws light on α-syn's role in PD pathogenesis (158). This simple experimental model is very useful to dissect and understand the biochemical mechanisms of many diseases, as there is high mechanistic similarity of many physiological processes with human cells.

1.4 Prion disease

Prions are self-replicating proteins that are responsible for fatal neurodegenerative disorder known as prion diseases or transmissible spongiform encephalopathies affecting multiple mammalian species such as Kuru, bovine spongiform encephalopathy (BSE) and scrapie, in human, cattle and sheep respectively (159-161). They are generally considered a transmissible disease within and between different mammalian species as transfer of brain extracts from affected persons into host species can spread the disease (162-164). Transmission among humans could occur during surgical procedures or pituitary hormone treatment, for example, 450 cases of iatrogenic Creutzfeldt–Jakob disease (iCJD) have been reported during such treatments. Blood donors with undetected subclinical symptoms could be a reason for variant CJD (vCJD) in humans. Cannibalistic rituals in Papua New Guinea were also historically linked with transmission of Kuru (165-173). Normal cellular prion protein (PrP^{C}) is a 253 amino acid long protein encoded by a gene PRNP on chromosome 20 mutations of which is associated to genetic prion disease. The scrapie prion protein (PrP^{Sc}), is a pathological form of prion protein present in the brain

tissue of patients with transmissible spongiform encephalopathy (TSE). PrP^{Sc} differs with normal cellular prion protein (PrP^{C}) by translational modification and is formed by recruiting PrP^{C} conformers, which later perpetuate into larger aggregates that trigger neurotoxic signals (162,163,174-177). These are the characteristics of typical spongiform that are seen in the patient's brain. A list of major prion diseases is provided in the table 1.5.

Table 1.3 List of prion diseases.

Disease	Natural host species	Rout of transmission or disease-induction mechanism
Sporadic CJD	Humans	Unknown
Iatrogenic CJD	Humans	Accidental medical exposure to CJD-contaminated tissues, hormones or blood derivatives
Familial CJD	Humans	Genetic (germline *PRNP* mutations)
Variant CJD	Humans	Genetic (germline *PRNP* mutations)
Kuru	Humans	Ritualistic cannibalism
Fatal familial insomnia	Humans	Genetic (germline *PRNP* mutations)
Sporadic fatal insomnia	Humans	Unknown
Gerstmann–Sträussler–Scheinker syndrome	Humans	Genetic (germline *PRNP* mutations)
Scrapie	Sheep and goat	Horizontal and possibly vertical
Atypical scrapie	Sheep and goat	Unknown

Table 1.5 continued

Chronic wasting disease	Mule deer, white-tailed deer, Rocky Mountain elk and moose	Horizontal and possibly vertical
BSE	Cattle	Ingestion of BSE-contaminated food
Atypical BSE	Cattle	Unknown
Feline spongiform encephalopathy	Zoological and domestic felids	Ingestion of BSE-contaminated food
Transmissible mink encephalopathy	Farmed mink	Ingestion of BSE-contaminated food
Spongiform encephalopathy of zoo animals	Zoological ungulates and bovids	Ingestion of BSE-contaminated food

BSE, bovine spongiform encephalopathy; CJD, Creutzfeldt–Jakob disease; PRNP, gene encoding prion protein; PrPC, cellular prion protein

Adopted from Adriano Aguzzi et. al. (2013) *Nature Reviews Immunology* **13**, 888–902 (178)

Like other neurodegeneration-associated amyloid proteins, PrP^{Sc} protein is rich in β-sheet content and is protease resistant, thus it not easily degraded by cellular enzymes. These protease resistant amyloids of PrP^{Sc} are then deposited in the brain tissue during progression of the disease. Prion aggregation can occur both intracellularly and extracellularly. Specific prion antibodies can detect amyloid plaques caused by prion protein that appear similar to those of AD (162,164,179). On the other hand, how prions destroy the neurons in CNS is still enigmatic. Numerous studies investigating the mechanism of prion aggregate formation and propagation are performed in yeast and many of the findings from these studies are applicable to human prion diseases.

1.4.1 Prions in yeast

Although no homologue of PrP^{C} exists in yeast, many proteins have been discovered that are present in different conformations including normal soluble or amyloid aggregated forms. Different conformations of the same protein are linked with distinct phenotypes in yeast. In yeast, prions act as epigenetic cytoplasmic elements that provide phenotypic diversity in a heritable manner that operates at the level of protein conformation without the need of nucleotide sequences (180-185).

Reed Wickner in 1994 proposed that the previously known yeast non-Mendelian heritable elements [*URE3*] and [PSI^{+}] are prions of Ure2 and Sup35 proteins respectively(186,187). Prion are often linked with a loss of function phenotype in yeast. Sup35 is a translational termination factor that loses its function in a way that translation termination efficiency is compromised in the presence of the prion form of Sup35 (98,188-191). Similarly, the normal function of Ure2 is to regulate nitrogen catabolism, preventing uptake of an intermediate, ureidosuccinate (USA), involved in the uracil

biosynthesis pathway. Thus the [*URE3*] prion form of Ure2, loses its normal function in *ura2* mutant cells and can grow on –Ura media by taking up USA (186,188,192-196). Prion traits are dominant since aggregated forms of a prion can recruit the identical soluble prion protein and convert it into the prion conformation. [PSI^{+}] prion exists in different variants similar to the observation in mammals that are genetically identical showed different characteristics of prion in isolates of disease that can be stably reproduced (164,197). Variation in the ratio of aggregated vs. soluble Sup35 protein is linked with different variants of [PSI^{+}] prion, known as weak or strong forms of the prion. [PSI^{+}] prion variants lead to different degree of loss of function for example, in the presence of *ade1-14* nonsense stop codon, strong variants will cause greater degrees of translational read-through compared with weak variants resulting in accumulation of characteristic red pigments indicating the absence of *ADE1* (198-202).

1.4.2 Structural organization

1.4.2.1 Prion forming domain

Most of the yeast prion proteins contain a region that is required for the formation and propagation of the prion without requiring the remaining portions of the protein (203). Such regions are known as prion-forming domains or PrDs. Sup35 PrD or Sup35N domain is also involved in other cellular functions other than its role in prion formation (204). A middle domain (Sup35M) links PrD to the C-terminal domain. Sup35M domain is composed of highly charged amino acids residues that help to maintain prion aggregation possibly by interaction with HSPs (205). Yeast PrDs are Q and N rich domain, that when artificially recombined to different proteins may confer a prion state.

Sup35 prion forming domain (PrD) can be divided into two segments, the QNR stretch and the OPR element based on the observation that the fragment of PrD required for protein aggregation is shorter than segments needed for efficient propagation of prion (Figure 1.2) (161,180,206,207).

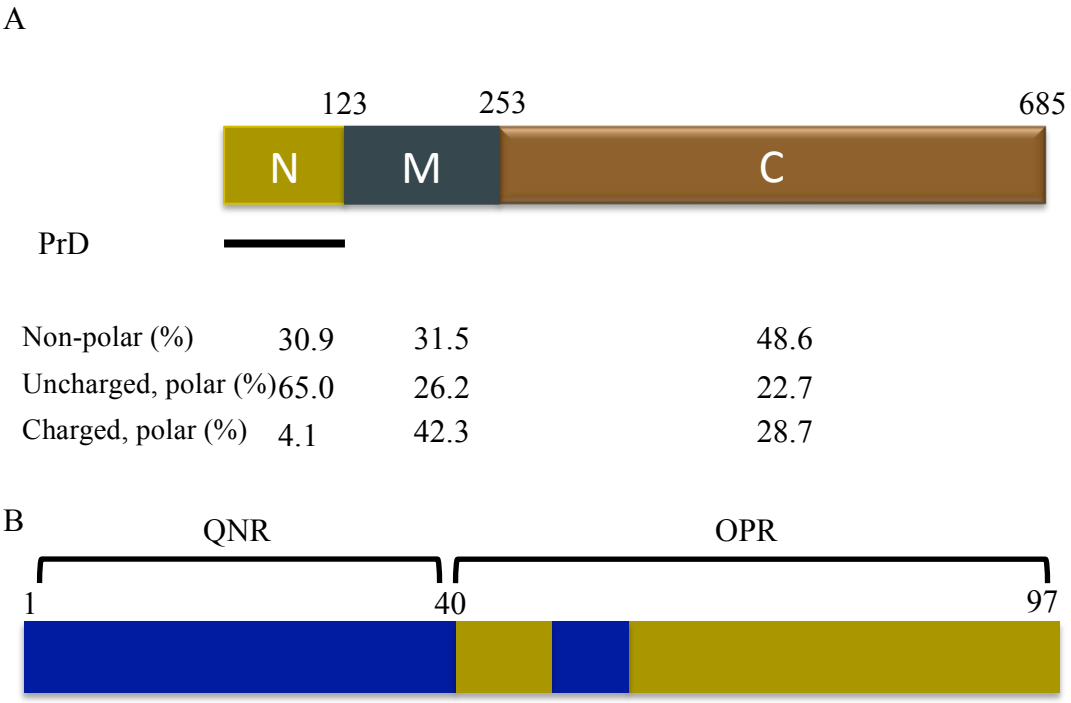

Figure 1.2. Sup35 structural domains organization.

The Sup35 protein is divided into three domains based on the position of Met residues. The first domain N (amino-terminal) Met1 to residue 123, the M (middle) domain between Met 124 and residue 253, and C (craboxy-terminal) region from Met 254 to residue 685. The N-terminal domain is known as the PrD and is enriched in uncharged polar residues that are required for the formation of prions. The C-terminal domain is an essential region that functions as translation termination release factor. The minimal PrD domain consists of 1-97 amino acids that are composed of two distinct regions within it; QN rich region (QNR) and the oligopeptide repeat region (OPR).

1.4.2.2 *De novo* prion formation

The frequency of prion *de novo* appearance is considerably low unless prions or their PrDs are transiently overexpressed resulting in the dramatic increase in the rate of prion formation by up to 3000-fold. Interestingly, overexpression of just the PrD is more efficient than transient overexpression of full-length protein (181,191,201,208). Still elevated levels of PrD as such, is not sufficient for prion formation and requires the presence of another QN rich prion, [*PIN*$^+$] in aggregated state, for *de novo* prion formation (209). [*PIN*$^+$] is a prion form of the Rnq1 protein that was first discovered as a non-Mendelian factor with prion like properties (181,201,208,210-212). The amino acid composition of Rnq1 is similar to the PrD of Sup35 and it is proposed that [*PIN*$^+$] acts as an initial nucleus for *de novo* Sup35 prion aggregation formation. The *de novo* [*PSI*$^+$] prion formation in the presence of [*PIN*$^+$] by transient overexpression of Sup35 or its PrD is a multi-step process initiated by accumulation of misfolded protein in insoluble protein deposits (IPODs) quality control (213,214). Fusing of Sup35 to GFP, allows the visualization of formation of *in vivo* prion behavior, in which the fluorescent signal appears as a ring-like and long filamentous structures at the periphery of cells. These rings later collapse together to form internalized smaller rings that enclose the vacuoles. After cell division the daughter cells appeared with dot-like foci of [*PSI*$^+$] (213).
Aside from the presence of [*PIN*$^+$], several other cellular components have been reported to control *de novo* prion formation and propagation. Most of these components are involved in stress response pathways such as chaperones, ubiquitin-proteasome system, intracellular trafficking networks and members of actin cytoskeleton (215-221).

1.4.3 Effect of heat shock proteins on prion propagation

Although prion proteins require no cofactor to generate and propagate amyloid aggregation *in vitro*, *de novo* prion propagation is modulated by chaperones such as Hsp104, Hsp70, Hsp40 and sHSPs such as Hsp26 and Hsp42 (36,39,53,222-225). Hsp104 is a member of the AAA ATPase chaperone family with homohexameric structure and required for prion propagation *in vivo*. Hsp104 and its bacterial homolog, ClpB, possess potent disaggregase activity against stress damage protein aggregates (226-228). Deletion or overexpression of Hsp104 eliminates [PSI^+] prion, thus an intermediate level of Hsp104 is required for prion propagation (222,223,229,230). It was proposed that Hsp104 generates smaller seeds by promoting fragmentation of larger prion fibers that initiate propagation. It was also hypothesized that elevated Hsp104 cures [PSI^+] prion by monomerization of large aggregates but evidence for this hypothesis are based on the indirect observation that overexpression of Sup35, leading to an increase in aggregate size, partially compromises the curing effect of excess Hsp104 (231). Another model proposes that elevated levels of Hsp104 cures [PSI^+] by dissolution of the prion seeds, the evidence for this model came from observation that Hsp104 overexpression induces a diffuse localization signal for Sup35 tagged with GFP and a large fraction of soluble Sup35 was observed in cell lysate (226,232,233). Recent studies also suggest that dissolution of prion seed might be due to the trimming activity of Hsp104 in which Sup35 dissociates from the seed terminus, hence that reducing its size without generating new seeds. Trimming activity of Hsp104 is still present even when severing activity is inhibited by treatment of guanidine (223). The effects of Hsp104 on prion curing are strongly influenced by other chaperones or co-chaperones including the Hsp70 chaperone

system consisting of Ssa and its co-chaperones, Ydj1 or Sis1 and the Sse proteins (38,40,208,234,235). The Hsp70 co-chaperone system has an essential role at the initial steps of the disaggregation processes possibly by facilitating Hsp104 to recognize and extract single polypeptide from aggregates at later stages (225). Remarkably, different families of Hsp70 i.e. Ssa and Ssb shows contrary effects on [*PSI*$^{+}$] prion. Ssb overexpression enhances curing of [*PSI*$^{+}$] prion by Hsp104 while Ssa protects [*PSI*$^{+}$] from curing by Hsp104. Ssa overexpression and Ssb deletion also increase *de novo* [*PSI*$^{+}$] prion formation. At the molecular level Ssa interacts with Sup35 and overexpression of Ssa increases the polymer size of Sup35 (225,236-239). Altered expression of Hsp40 (Sis1 or Ydj1) by mutation, transient depletion or internal deletion, also influences the dynamics of [*PSI*$^{+}$] prion propagation. Sis1 overexpression promotes [*PSI*$^{+}$] prion curing by Hsp104. It is also proposed that Sis1 is responsible for recruiting Ssa and Hsp104 to prion aggregates. Unlike Sis1, Ydj1 is non-essential and is shown to cure weak variants of [*PSI*$^{+}$] prion, but only when Ssa1 is also co-expressed (225,234). The exact mechanism of action of Hsp70 and Hsp40 family members in prion propagation is still under investigation but it is clear that they collaborate with Hsp104 and play crucial roles in prion propagation. Deletion of co-chaperones of Hsp70/90 such as Sti1 or Cpr7, also inhibit [*PSI*$^{+}$] curing by Hsp104 over-expression (40).

In addition to Hsp104 and its assistant chaperones, sHSPs such as Hsp31, Hsp26 and Hsp42 also play a role in disaggregation of misfolded proteins in yeast (53,240-242). These proteins are highly expressed under moderate stress and during late growth phase for transition to stationary phase. Hsp42 and Hsp26 work synergistically to inhibit prion formation and potentiate dissolution of Sup35 prion aggregates by distinct mechanisms

(53). Furthermore, Hsp26 or Hsp42 collaborate with Hsp70 and or Hsp104 to reduce the SDS-resistant polyglutamine aggregation (243). The diverse effects of chaperones on prion propagation is summarized in table 1.6.

Table 1.6 Effect of chaperones on [*PSI*$^+$] prion curing

Chaperone		**Effect on [*PSI*$^+$]**	
Family	**Protein/Subfamily**	**Excess**	**Inactivation/deletion**
Hsp100	Hsp104	Cures	Cures
Hsp70	Ssa (1-4)	Destabilizes Protects from elevated Hsp104	Destabilizes
	Ssb (1-2)	Destabilizes Helps cure by elevated Hsp104	Protects from elevated Hsp104
Hsp40	Sis1	Helps cure by elevated Hsp104	Antagonizes
	Ydj1	ND	Does not cure
Hsp90	Hsp82	No effect	Protects from elevated Hsp104
SHSPs	Hsp42, Hsp26	Cures	ND
Co-70/90	Sti1	ND	Protects from elevated Hsp104
	Cpr7	ND	Same as above

1.4.4 Prion associated toxicity

The unusual conformations of normal proteins into self-assembly leads to formation of amyloid aggregates that has been implicated in both the acquisition of new traits and in the emergence and progression of disease. In yeast, the presence of [*PSI*$^+$] prion itself is not toxic but overexpression of Sup35 or its PrD in such a strain is lethal (215,221,244). It is proposed that toxicity is caused by recruitment of essential protein(s) including another translational release factor Sup45 (245-247). Also, the combination of [*PSI*$^+$] prion together with tRNA suppressor induces the stress response (248,249). Some variants of [*PSI*$^+$] that are toxic can be rescued by overexpression of Sup35 derivative that lack PrD and cannot be recruited by aggregates (250). Specific mutations in Hsp104 leads to [*PSI*$^+$]-dependent cytotoxicity in yeast cells (251). Some variants of [*PSI*$^+$] prions that are not toxic *per se* may become toxic when combined with other factors such as a polyQ stretch from human Huntingtin protein in [*PIN*$^+$] or [*PSI*$^+$] strains that are otherwise non-toxic (245,252).

1.5 DJ-1/ThiJ/Pfp1 superfamily

The members of DJ-1 superfamily are large number of proteins with conserved three-dimensional structure distributed across eukaryotes and prokaryotes (253-259). Members of the family such as DJ-1, hchA and Hsp31 possess similar primary, secondary and tertiary structures with the difference in the presence of main domains (P and A domains). In addition, they also differ in the formation of homo-dimerization such as DJ-1 monomer interacts through α-helices while Hsp31 dimerization is stabilizes by β-sheets. Another prominent feature of these family members is the presence of a conserved cysteine catalytic triad (Figure 1.3).

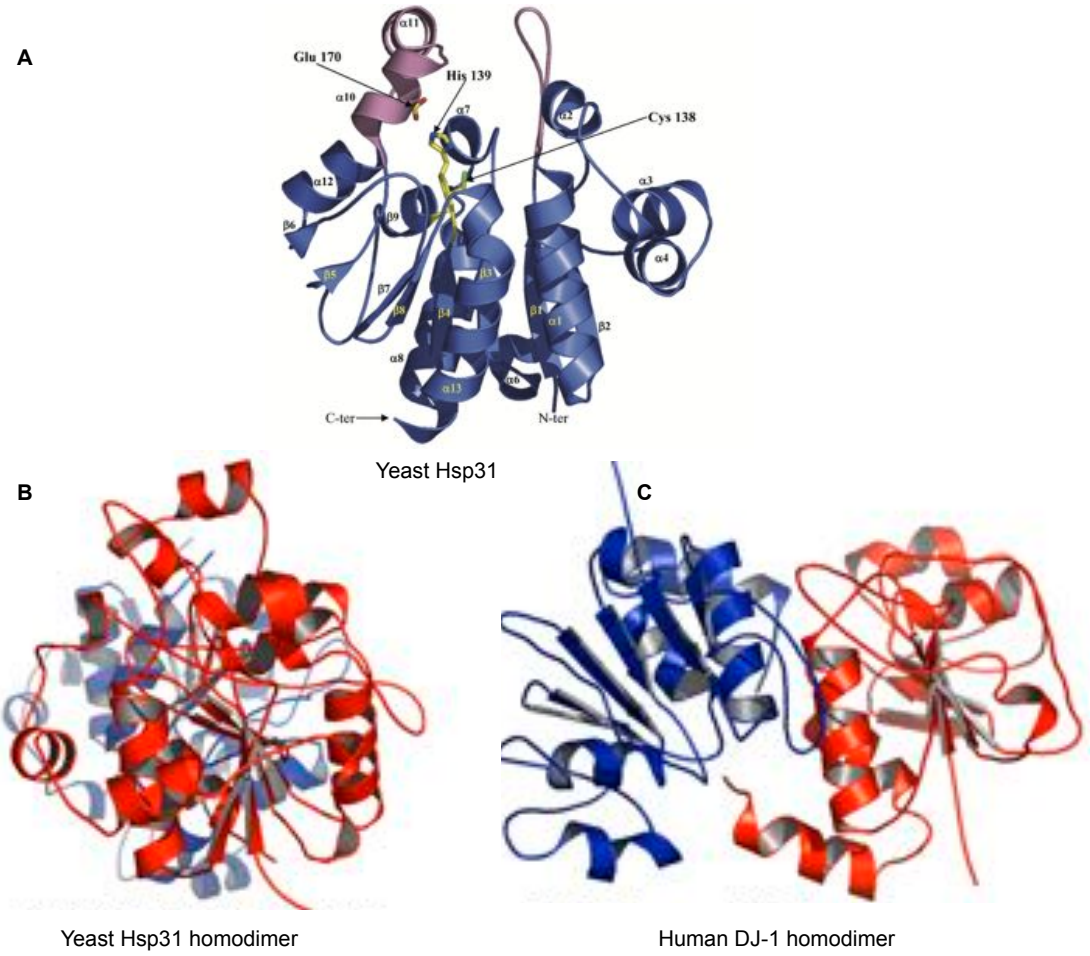

Figure 1.3. Ribbon structure of Hsp31 and dimerization.

(A) Crystal structure of yeast Hsp31 monomer depicting catalytic triad. The core is in color blue and cap is in red. The catalytic triad (Cys138, His139, and Glu170) are shown as sticks in yellow color (Adopted from M Graille et. al. 2004 with permission) **(B)** Ribbon structure of homodimerization of yeast Hsp31. **(C)** Homodimer of human DJ-1 protein. (Adopted from W Ying et. al. (2007) Open access Journal PLoS computational biology.

Despite highly conserved structure, members of this family are diverse in functions including catalases, glyoxalases, proteases, transcriptional regulators and chaperones. However, they are all involved in cellular stress response (158,260-266). Special attention has been drawn to this family because of human member of the family, DJ-1, that has a well-characterized involvement in two major diseases, cancer and PD (267-270). A large number of studies have investigated the cellular function of DJ-1 and its role in modulating disease pathogenesis. Other members of the family include *E.coli* Hsp31, archeal *Pyrococcus horikoshii* proteins (PH1704, YajL and Yhbo) and Hsp31 in the yeast *Saccharomyces cerevisiae* that has three other paralogs (Hsp32-34) (255,258,271-274).

1.5.1 Human DJ-1

Human DJ-1 is a small protein of 189 amino acids that is expressed ubiquitously in several tissues of body including brain and is mainly localized in the cytoplasm but also present in mitochondria and the nucleus. It was first identified as an oncogene that is elevated in several types of cancers such as leukemia, breast cancer, primary lung cancer, prostate cancer, cervical cancer and pancreatic cancer (270,275-279). The oncogenic potential of DJ-1 is thought to be related to its interaction with tumor suppressor phosphate and tension homolog (PTEN) in the PI3K-Akt pathway that regulates cell proliferation and transformation (280). Later studies showed its implication in neurodegenerative disease such as mutations in the gene PARK7 cause early onset of autosomal recessive PD (267,281-285). Mutations in DJ-1 that destabilize homodimerization show the quaternary structure is critical for cellular function. The conserved cysteine residue, C106, is also important to regulate cellular function and

localization of DJ-1. C106 is highly susceptible to oxidation and mutations affect its function, oligomerization and localization(286-289). Interestingly, oxidatively damaged proteins are found in the brains of patients with idiopathic PD, AD and HD. Like other members of the family DJ-1 also function as methylglyoxalase and deglycase of glycated proteins in the cell (290-292). In addition, DJ-1 positively regulates the antioxidant transcription factor, erythroid 2-related factor 2 (Nrf2) (293). The multiple cellular roles of DJ-1 and the different biochemical activity contributions to its overall role are under investigation but compelling evidence indicates that it is a multifunctional chaperone that protects cells from oxidative and associated stress similar to the yeast Hsp31 protein. Interestingly, our understanding of DJ-1 function has been more advanced than the yeast counterpart but new studies including ours are elucidating the function of yeast Hsp31 that will be applicable to DJ-1.

1.5.2 The yeast Hsp31 mini family

The yeast *Saccharomyces cerevisiae* Hsp31 mini-family consists of four paralogs, *HSP31* (*YDR533C*), *HSP32* (*YMR322C*), *HSP33* (*YOR391C*), and *HSP34* (*YPL280W*) (272). Among the four members, *HSP31* is the most divergent and is proposed to have been duplicated during yeast evolution resulting in the paralogous genes. After resolving the crystal structure of yeast Hsp31, the name was given because of structural similarity with *E. coli* Hsp31. Hsp32, Hsp33 and Hsp34 share over 90% sequence homology. While, Hsp31 is only about 70% similar to other members (271,272).

1.6 Role of Hsp31 in cellular stress response

Consistent with the main role of cellular stress response, Hsp31 expression is strongly induced during late phases of growth and required for survival under conditions of

nutrient limitation (294). Hsp31 expression is also induced when yeast cells are treated with H_2O_2 to produce oxidative stress and this up-regulation of Hsp31 is under the control of stress responsive transcription factor, Yap1 (158,295). In addition, Hsp31 possesses robust glutathione independent glyoxalase activity that converts the toxic metabolite, methylglyoxal (MGO), into D-lactate (158,260,261). The catalytic triad Cys-His-Glu of Hsp31 is vital for this enzymatic activity and critical for suppressing the elevated level of ROS by MGO (158,260). An overall view has emerged indicating Hsp31 has important metabolic and regulatory roles in cytoprotective pathways (296).
In addition to the enzyme activity, we also demonstrated that Hsp31 has broad chaperone activity in several classic protein aggregation assays indicating its ability to manage misfolded proteins that initiate proteotoxic stress in the cell. We also demonstrated that the yeast-purified protein was more active in preventing aggregation of several substrate proteins including α-syn (158). The increased activity may be due to the difference in the affinity tags used but may be a result of posttranslational modification(s) that occur in the cell. Several reports have indicated that post-translational modifications or differing levels of oxidation of the cysteine residue can alter activity of DJ-1 (297,298). In addition, we showed that yeast Hsp31 is more active in preventing protein aggregation compared to DJ-1. Interestingly, it has also been observed that Hsp31 rescues α-syn and huntingtin toxicity to a greater extent than DJ-1 *in vivo* using yeast as a model system (106,299). These results raise the intriguing possibility that Hsp31 is constitutively active whereas DJ-1 must undergo an activation event to increase its activity although more studies must be performed to confirm the mechanism for these differences.

Hsp31 inhibits the formation of aggregates of a wide range of proteins including insulin, citrate synthase, α-syn and the Sup35 prion (158). The recombinant soluble α-syn and Sup35 proteins can readily polymerize into amyloidogenic fibrils *in vitro* (300). Hsp31 inhibits protein aggregation formation *in vitro* and foci formation of GFP-tagged proteins *in vivo*. In addition, over-expression of Hsp31 can rescue cells from toxicity associated with overexpression of α-syn. The rescue phenotype could be mediated by several different mechanisms including Hsp31's methylglyoxalase or deglycation activities. However, a Hsp31 mutant deficient in methylglyoxalase activity is still very active in preventing α-syn in vitro aggregation and prevention of toxicity from overexpressed α-syn (158). Another possible rescue mechanism could be the autophagy pathway, particularly because deletion of Hsp31 impairs autophagy under carbon starvation conditions (294). Autophagy does alleviate toxicity from α-syn overexpression because we show a synthetic lethal relationship between α-syn overexpression and deletion of *ATG8*. However, we demonstrated that overexpression of Hsp31 in the *atg8Δ* strain can rescue α-syn-mediated toxicity (158). These data show that despite the multitasking abilities and roles of Hsp31, the chaperone activity appears to have the ability to prevent α-syn toxicity independent of other activities. In support of our finding, another study found the autophagy pathway was not crucial in preventing the Hsp31 chaperone activity against a cytoplasmic aggregation prone protein. The same study also demonstrated that Hsp31 chaperone activity overlaps with the Ubr-dependent degradation pathway but is independent of its function in the oxidative stress response (262). Further exploration of this model would need to utilize mutants that abrogate chaperone function without affecting enzyme activity and other biological functions.

The typical model of protein aggregation proposes that unfolded monomers as an initiating event that progresses to unstable oligomeric intermediates, and finally elongates to larger oligomers. The observed anti-aggregation activity of Hsp31 raises the question of what stage Hsp31 intervenes in the protein aggregation process. On the bases of our *in vitro* studies, Hsp31 likely interacts with early oligomeric intermediates of α-syn and therefore prevents higher oligomer formation. For example, when soluble α-syn was mixed with Hsp31, formation of precipitated SDS-resistant oligomers was markedly reduced. Likewise, the soluble fraction of α-syn, which included SDS-resistant oligomers in the size range of 25-50 KDa, was almost completely abolished in the presence of Hsp31 indicating that Hsp31 likely interacts with the monomeric or early oligomers in preventing the formation of higher order oligomers. We observed similar results with the *in vitro* ThioT assay, in which incubating the Hsp31 with α-syn completely prevented the increase in fluorescence intensity associated with increasing fibril formation again supporting our model that Hsp31 acts at early stages of protein aggregation (158). Of particular interest is that DJ-1 has been shown to interact with monomeric and oligomeric form of α-syn as determined by pull-down assays (106). This same study also showed that DJ-1 interacts with α-syn *in vivo* as well. Along with α-syn aggregation formation, we also demonstrated the inhibitory effect of Hsp31 on the Sup35 prion based on reduction of aggregates observed in cell lysates. These results support the notion that Hsp31 acts at the early stages of oligomerization to prevent further protein oligomerization. Interestingly, we previously showed that the overexpression of Hsp31 reduces the level of Sup35 aggregation but we also show that it is unable to cure prions from a [PSI^+] strain. [PSI^+] strains contain Sup35 prion aggregates that can be cured by

chaperones such as Hsp104, but the lack of curing by Hsp31 suggests that it lacks disaggregase activity and cannot intervene in an established prion cycle. Moreover, our study showed no co-localization of Hsp31 and Sup35 aggregates as observed under fluorescence microscope, rather Hsp31 is occluded from Sup35 prion aggregates, indicating that Hsp31 acts on its substrates prior to the formation of large aggregates. The strong chaperone activity of Hsp31 suggests that it may modulate prion aggregates but might need to cooperate with other chaperones similar to what has been demonstrated with other small HSPs such as Hsp26 and Hsp42 (53).

1.7 Comparison of Hsp31 paralogs

The paralog genes of the Hsp31 mini-family are located at the subtelomeric region of the genome in *Saccharomyces cerevisiae* (272). All the members of Hsp31 family contain the same Cys-His-Glu catalytic triad as present in the *E. coli* ortholog but interestingly no protease activity has been detected so far for Hsp31 or other paralogs. Previously, it was shown that mutation in the catalytic triad largely abolishes glyoxalase activity, but this catalytic triad is not required for chaperone activity of Hsp31 (158). These results indicate that the anti-aggregation activity of Hsp31 is not under the influence of its enzymatic activity rather, it has a direct chaperone activity against misfolded proteins. Intriguingly, all the paralogs of the Hsp31 minifamily possess comparable activity against α-syn aggregation and toxicity when they are overexpressed from the *GAL* promoter (106). Furthermore, the chaperone activity of Hsp31, Hsp32 and Hsp33 against a cytoplasmic aggregation-prone protein is independent of their role in oxidative stress response and the vacuolar degradation pathway (262). However, unlike Hsp31, the other paralogs possess very little methylglyoxalase activity and are unable to protect the cells

from glyoxal toxicity (260). These results again support the notion that anti-aggregation activity of Hsp31 mini-family is independent of its enzymatic activity. In addition, the lack of methylglyoxalase activity in the paralogs is evidence that the paralogs are diverging but additional studies dissecting the roles within this paralog group are needed to further uncover these diverging functions. The Hsp31 protein family is broadly spread across fungal species with varying levels of paralog duplications and additional evidence of divergence including differences in localization in the *Schizosaccharomyces pombe* Hsp31 family members (264). A functional comparison of Hsp31 and its paralogs are summarized in Table 1.7 highlighting the similarities and differences among these proteins.

Table 1.7 Summary of Hsp31 and paralog functions

Function/Attribute	Hsp31	Hsp32	Hsp33	Hsp34
Catalytic triad	Yes	Yes	Yes	Yes
Chromosome Position	Interstitial	Telomeric	Telomeric	Telomeric
Sequence homology	~70%	>90%	>90%	>90%
Chaperone activity	+++	+++	+++	+++
Methylglyoxalase	+++	+/-	+/-	+/-
Deglycase	+++	ND	ND	ND
Role in Autophagy	+	+	+	+
Peak mRNA level	Early SP	DS	Early SP	ND
Stress granule and P body localization	Yes	Yes	ND	ND
Mitochondrial localization	Yes	ND	ND	ND

ND = Not determined
SP = Stationary Phase
DS = Diauxic shif

1.8 Hsp31 role in redox homeostasis

Oxidative stress occurs when intra-cellular ROS overwhelms the anti-oxidative defense system in the cell present during normal aerobic metabolism or by exposure to external radical generating agents. ROS triggers damage to macromolecules in the form of oxidative modifications and misfolding of proteins, associated with the development of diseases and pathological conditions such as PD and prions (62,184,301,302). Hsp31 has an important role in maintenance of redox homeostasis in yeast under oxidative stress generated by MGO or H_2O_2 (260,303). Like many other heat-shock genes *HSP26*, *HSP12*, *HSP82*, and *SSA3*, expression of *HSP31* is strongly induced at diauxic shift when the cells are stressed by nutrient limitation and by accumulation of oxidative metabolites (158,294,303). Others and we also reported an elevated level of Hsp31 under oxidative stress when cells were treated with H_2O_2 (158,303). Similarly, Hsp31 also plays a role in the survival of cells during stationary phase and protects cells from oxidative stress caused by MGO and H_2O_2 accumulation (158,303). In addition, we demonstrated that Hsp31 expression was induced under proteotoxic stress such as overexpression of α-syn (158). In support of the role of Hsp31 in managing this proteotoxic stress, we found that deletion of *HSP31* synergizes with α-syn expression to increasing toxicity. We reported an increase in ROS level in the *hsp31Δ* strain that correlates with increased toxicity by α-syn expression compared to wild type (WT) strain, indicating that the presence of Hsp31 is important in reducing ROS to basal levels. In agreement with our study, overexpression of Hsp31 robustly suppresses both cytosolic and mitochondrial ROS levels instigated by MGO and H_2O_2 and therefore provide cytoprotection (158,260). In addition, Hsp31 localizes to mitochondria and preserves mitochondrial integrity by

redistributing glutathione to the cytoplasm under oxidative stress (260). Another study examined the deglycase activity of Hsp31 and showed that it may efficiently deglycate proteins with glycated Cys, Arg and Lys amino acid residues (265). Taken together, these results suggest that Hsp31 is an integral part of the heat shock protein system and plays a vital role in maintaining cellular homeostasis.

CHAPTER 2. HSP31 IS A STRESS-RESPONSE CHAPERONE THAT INTERVENES IN THE PROTEIN MISFOLDING PROCESS

This chapter contains parts of following publications:

Chia-Jui Tsai*, **Kiran Aslam***, Holli M Drendel, Josephat M Asiago, Kourtney M Goode, Lake N Paul, Jean-Christophe Rochet, Tony R Hazbun Hsp31 is a Stress-Response Chaperone that Intervenes in the Protein Misfolding Process. *The Journal of biological chemistry*, 290(41):24816-34, 2015

Kiran Aslam, Tony Hazbun Hsp31, a member of the DJ-1 superfamily, is a multitasking stress responder with chaperone activity. *Prion* Apr 2016

2.1 Abstract

The *Saccharomyces cerevisiae* Hsp31 is a homodimeric protein that is highly induced under stressful situations and involved in diauxic shift reprogramming. It is a protein with multifunctional roles including functions as a chaperone, methylglyoxalase, deglycase and is involved in the autophagy pathway. Hsp31 is homolog of human DJ-1 that has implications in the pathophysiology of PD. We verified that Hsp31 are highly induced under oxidative stress. Furthermore, we showed its induction under proteotoxic stress condition. We confirmed that Hsp31 is a robust methylglyoxalase that is more potent in activity than its human homolog DJ-1. We demonstrated that Hsp31 chaperone activity to protect the cells from α-syn toxicity is not under the influence of its enzymatic activity or autophagy pathway. We also showed that Hsp31 inhibit Sup35 PrD aggregations as

observed under fluorescence microscopy and flow cytometry. In addition, we provide evidence that Hsp31 act early in the process of protein aggregation because Hsp31 does not co-localize with larger Sup35 prion aggregates. These results establish that Hsp31 molecular chaperone activity is self-sufficient to protect the cells from stress conditions without requiring its enzymatic activities.

2.2 Introduction

Yeast Hsp31 is encoded in the *Saccharomyces cerevisiae* genome and has drawn attention after its structure was solved in 2003 indicating that it has structural similarity with an evolutionarily conserved protein family the DJ-1/PfpI (ThiJ/PfpI) protein family that includes human DJ-1 and *E. coli* Hsp31 proteins (271,272). The DJ-1/PfpI protein family members including human DJ-1 and *E. coli* Hsp31 are moderately characterized for their biological functions and role in pathologies but have many unanswered questions with regards to their multifunctional roles and biochemical activities. Most studies indicate an important role in response to stressed biological processes (303). Mutated forms of DJ-1 are involved in early onset PD and DJ-1 is implicated to function as a chaperone in response to oxidative stress by preventing α-syn fibrillation, a process involved in PD pathogenesis (304). *E. coli* Hsp31 is a stress-inducible molecular chaperone that plays an important role in protein misfolding and helps survival under acidic stress (305). Initial characterization the yeast Hsp31 function showed that deletion of *HSP31* gene sensitized cells to ROS, suggesting a role for Hsp31 in protecting cells against oxidative stress (303). Another study showed that yeast Hsp31 is important in diauxic-shift where its expression is strongly induced and it has a survival role in

stationary phase of growth. In addition, deletion of *HSP31* leads to impaired autophagy under carbon starvation (294).

Furthermore, DJ-1 family proteins including human DJ-1, *E. coli* Hsp31 and yeast Hsp31 have been characterized as methylglyoxalases that detoxify by converting MGO into D-lactate independent of GSH (261,264,290). MGO is a toxic metabolite that is mainly produced as a byproduct of glycolysis. MGO is highly reactive with various amino acids in proteins, nucleic acids and lipids to yield toxic AGE linked to several diseases. Cells mainly catabolize MGO by two major enzymes including glutathione dependent GLO I and GLO II (306,307). DJ-1 and its homologue proteins are characterized as GLO III that do not require GSH as co-factor to convert MGO into D-lactate. Another study examined the deglycase activity of DJ-1 and Hsp31 by showing that they efficiently deglycate proteins with glycated Cys, Arg and Lys amino acid residues (265,292). Investigation of the yeast Hsp31 is an excellent model to delineate and investigate the specific biochemical activities of these proteins.

Previously in our lab, it was shown that Hsp31 protect cells against α-syn toxicity associated with the formation of α-syn foci in a yeast model of PD. It also has been shown that Hsp31 possesses a chaperone-like response against α-syn aggregation as observed by an *in vitro* fibrillization assay as well as insulin and citrate synthase aggregation assays (158). In the present study, we demonstrate that the protective effect of Hsp31 against α-syn toxicity in yeast cells is independent of its methylglyoxalase activity. DJ-1 and Hsp31 possess a conserved catalytic triad Glu-Cys-His, the first two amino acids of this triad are important for GLOIII activity in DJ-1 (290). Here we tested a mutation in Hsp31 C138D for methylglyoxalse activity and its activity against α-syn

toxicity in yeast cells. We also observed the role of Hsp31 in maintaining redox homeostasis by using an α-syn model of toxicity. In addition, we investigated the effect of Hsp31 on Sup35 prion aggregation considering that it is potentially a natural substrate in yeast. Together these findings reinforce the concept that studying the function of Hsp31 in the context of stress conditions in a yeast model provides new insight about its functions and it is likely applicable to higher eukaryotes.

2.3 Results

2.3.1 Hsp31 is an integral part of the yeast cellular stress response

Several studies have shown that environmental stresses, such as oxidative stress and elevated temperature, increased the expression of HSPs. A recent study showed increased Hsp31 expression upon treatment with H_2O_2 and another study demonstrated an increased HSP31 mRNA levels during the diauxic shift growth phase and stationary phase (294,303). However, the Hsp31 protein level was not characterized under these conditions. We integrated a 9myc epitope at the C-terminus of the HSP31 genomic locus to generate a yeast strain that can be used to quantify endogenous protein expression. To assess whether Hsp31 expression increases under stress conditions, we treated cells with H_2O_2 and observed an increased protein expression within an hour of exposure. This was consistent with previous studies in which increased expression of Hsp31 was observed in response to a ROS inducing agent. We also examined the expression profile of Hsp31 under proteotoxic stress by overexpressing α-syn and the results indicated that increased expression of α-syn decreases cell viability, and concomitantly increases the expression of Hsp31 compared to a strain not expressing α-syn. Our data demonstrate that Hsp31

expression is rapidly elevated at the protein level in the event of stress associated with oxidative stress or proteotoxicity (Figure 2.1).

A

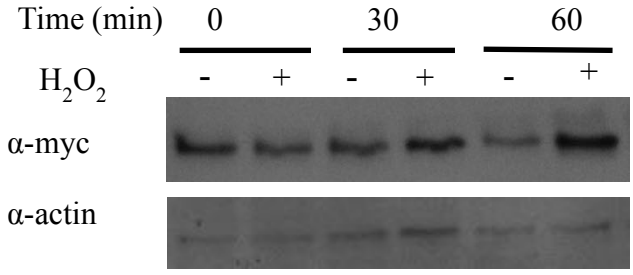
Time (min)
0
30
60
H_2O_2
- + - + - +
α-myc
α-actin

B

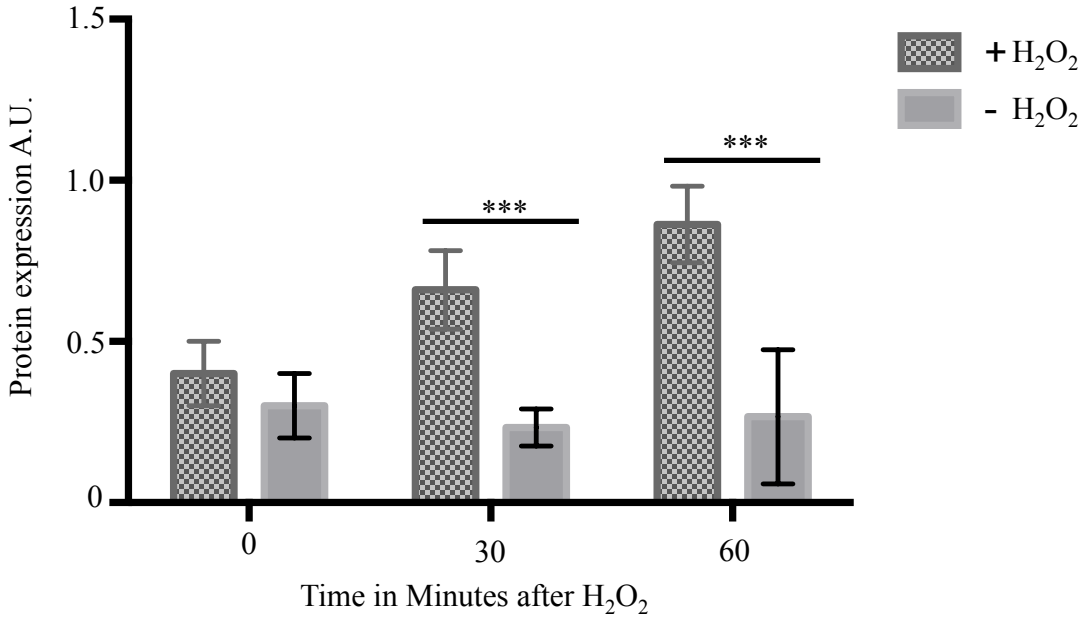
1.5
1.0
0.5
0
Protein expression A.U.
***
***
0
30
60
Time in Minutes after H_2O_2
+ H_2O_2
- H_2O_2

C

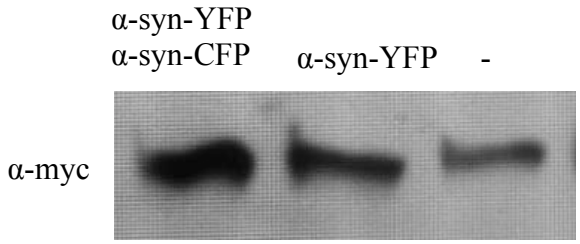

Figure 2.1 Expression of Hsp31 increases under stress.

(A) H_2O_2 treatment increases the expression of Hsp31. The Hsp31- 9myc strain was exposed to 1 mM H_2O_2 treatment for 30 min and 60 min and increased Hsp31 expression was determined by immunoblot. Samples were normalized to OD_{600} for cellular density and β-actin was used as a loading control. This data is representative of three independent experiments. **(B)** Quantification of Hsp31 expression with or without 1 mM H_2O_2 treatment obtained by densitometric analysis and normalized with β-actin western blot. (n=3, ***p< 0.0001 by two way ANOVA test). **(C)** Hsp31-9myc expression increased in the presence of induced expression of *GAL*-α-syn. The immunoblot was probed with anti-myc and anti-β-actin antibodies.

The expression of α-syn has been linked to an increase in the level of ROS in yeast. The *in vivo* suppression of α-syn foci by Hsp31 and increased toxicity of one copy α-syn in the *hsp31Δ* strain prompted us to investigate the level of ROS in these different genetic contexts. We found that wild-type yeast did not have detectable superoxide radicals when treated with dihydroethidium (DHE) using microscopy and a fluorescence level of 0.5 A.U. by flow cytometry. ROS levels were detectable in a fraction of cells in the *hsp31Δ* strain (6 A.U.) indicating that the presence of Hsp31 in the cell can decrease ROS levels of normal cells not expressing α-syn. The remaining strains had increased ROS levels in the following order: α-syn-YFP strain (23 A.U), α-syn-YFP *hsp31Δ* (41 A.U), α-syn-YFP α-syn-CFP (64 A.U) and α-syn-YFP α-syn-CFP *hsp31Δ* (133 A.U). The latter three strains with the most ROS levels exhibit reduced viability when α-syn is expressed and formed increase foci demonstrating a correlation between these phenotypes (Figure 2.2).

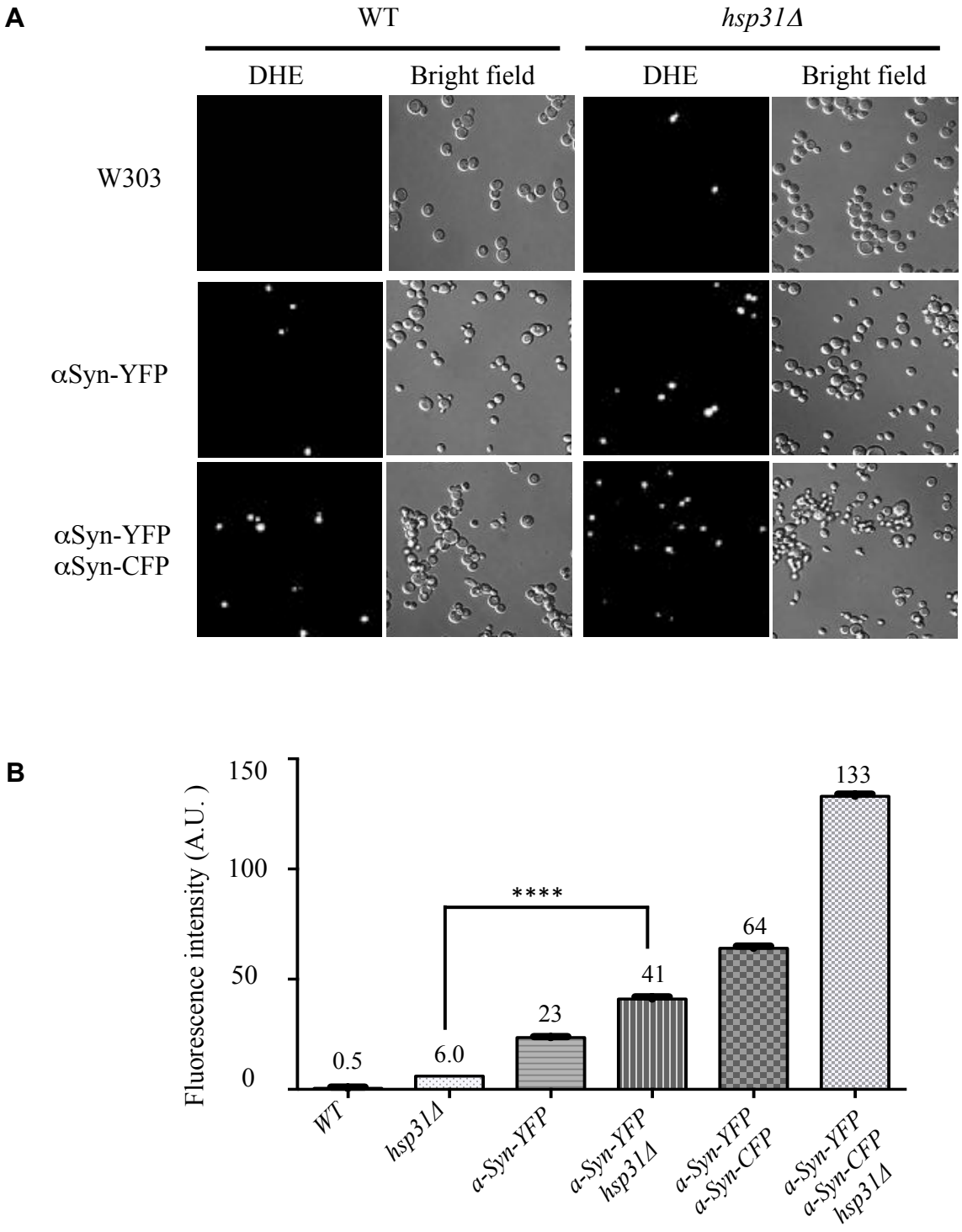
A
WT
hsp31Δ
DHE
Bright field
DHE
Bright field
W303
αSyn-YFP
αSyn-YFP
αSyn-CFP
B
Fluorescence intensity (A.U.)
150
100
50
0
****
0.5
6.0
23
41
64
133
WT
hsp31Δ
α-Syn-YFP
α-Syn-YFP hsp31Δ
α-Syn-YFP α-Syn-CFP
α-Syn-YFP α-Syn-CFP hsp31Δ

Figure 2.2. Hsp31 decreases the ROS generated by α-syn.

(A) Superoxide ions increase when HSP31 is deleted and when α-syn is expressed. *In vivo* presence of superoxide ions is detected by treatment with DHE and visualization by fluorescence microscopy. Representative fields of view are presented. **(B)** Quantification of superoxide ion increase in *hsp31Δ* and *GAL*-α-syn expressing strains. Flow cytometry was performed on three biological replicates. n=3 **** $P \leq 0.0001$ based on the one-way ANOVA with multiple comparison t-test. Error bars = 1 SD.

2.3.2 Hsp31 methylglyoxalase activity is not required for rescue of α-syn-mediated toxicity

Recent studies have shown that DJ-1 and Hsp31 are methylglyoxalases that convert MGO into D-lactate in a single step independent of GSH. Hsp31, like other members of the DJ-1 superfamily, possesses the conserved Glu-Cys-His catalytic triad. The first two residues of this triad are critical for MGO activity of DJ-1 as well as Hsp31 in *S. pombe* (260,261). We determined the methylglyoxalase activity for recombinant Hsp31 (purified from *E. coli* with the GST tag removed on the C-terminus) and a catalytic triad mutant, Hsp31 C138D, using a commercially available D-lactate assay kit. As expected, Hsp31 could convert MGO into D-lactate with a calculated specific activity of 28.4 μmol/min/mg enzyme (using a saturating substrate concentration of MGO at 6 mM). These enzymatic parameters indicate a more efficient enzyme activity than the previously reported Hsp31 specific activity of 10.5 D-lactate μmol/min/mg. Interestingly, the Hsp31 purified directly from a yeast expression system, the *GAL* promoter induced movable ORF tag system (MORF), had increased enzymatic activity compared to Hsp31 purified from recombinant *E. coli*. We also showed that Hsp31 is a more potent methylglyoxalase compared to DJ-1, this observation is consistent with several other studies (260,261). Enzymatic parameters were calculated by measuring the time dependent production of D-lactate with varying substrate concentrations and fitting to a Michaelis-Menten kinetics model resulting in a Vmax of 0.0356 μmoles D-lactic acid/min (Standard error=0.0016) and Km was 247.4 μM (standard error=31.5). Specific activity for the mutant could not be determined because low levels of D-lactate were produced despite using five times the amount of protein (detection limit of 0.4 μmol/min/mg). The reaction products of these

assays were examined by GC-MS and a peak identical to the lactic acid standard (6.09 min elution time) was identified, confirming the production of lactic acid by Hsp31. Lactic acid was undetectable by GC-MS analysis in the Hsp31 C138D sample (Figure 2.3).

A

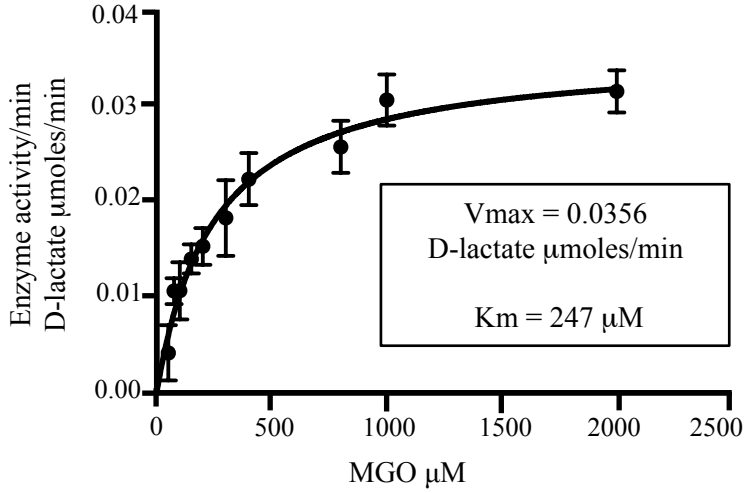
0.04
0.03
0.02
0.01
0.00
Enzyme activity/min
D-lactate µmoles/min
Vmax = 0.0356
D-lactate µmoles/min
Km = 247 µM
0
500
1000
1500
2000
2500
MGO µM

B

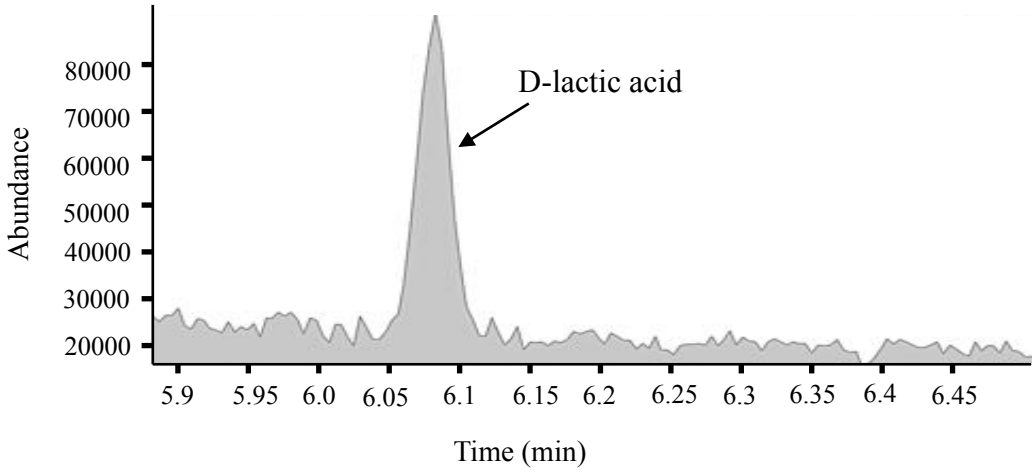
Abundance
80000
70000
60000
50000
40000
30000
20000
D-lactic acid
5.9
5.95
6.0
6.05
6.1
6.15
6.2
6.25
6.3
6.35
6.4
6.45
Time (min)

C

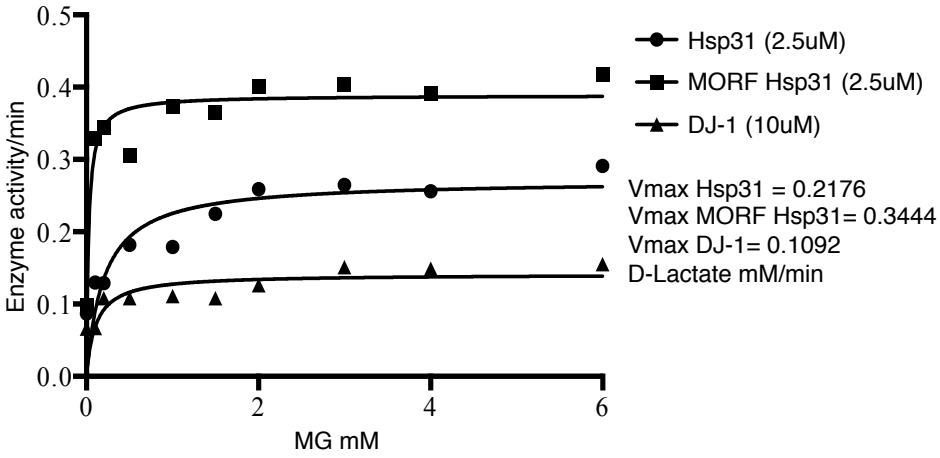

Figure 2.3. Hsp31 is a methylglyoxalase that produces D-lactic acid.

(A) The plot of substrate concentration versus rate of D-lactate production by Hsp31 is depicted and the michaelis-menten best fit model is represented by the solid line and was the Vmax and Km were determined based on this model. Mean values of triplicate experiments are plotted. Error bar = 1 SD. **(B)** GC-MS trace demonstrates a peak (6.09 min) consistent with the production of D-lactic acid by Hsp31 in the enzymatic reaction. **(C)** The hyperbolic plot of substrate concentration versus rate of D-lactate production by Hsp31 (circles), MORF Hsp31 (squares) and DJ-1 (triangles) are shown and the solid line represents the Michaelis-Menten best-fit model. The Vmax parameters were determined based on this model.

We next determined if methylglyoxalase activity is required for rescue of α-syn toxicity. One copy of α-syn-YFP decreases fitness in the *hsp31Δ* strain but *GPD* driven expression of Hsp31 rescues that toxicity. The expression of *GPD* driven Hsp31 C138D restored the α-syn expressing strain to full viability comparable to expression of the wild-type Hsp31. The lack of enzyme activity for this mutant and ability to rescue α-syn toxicity indicated that the *in vivo* mechanism of rescue is not dependent on methylglyoxalase activity (Figure 2.4).

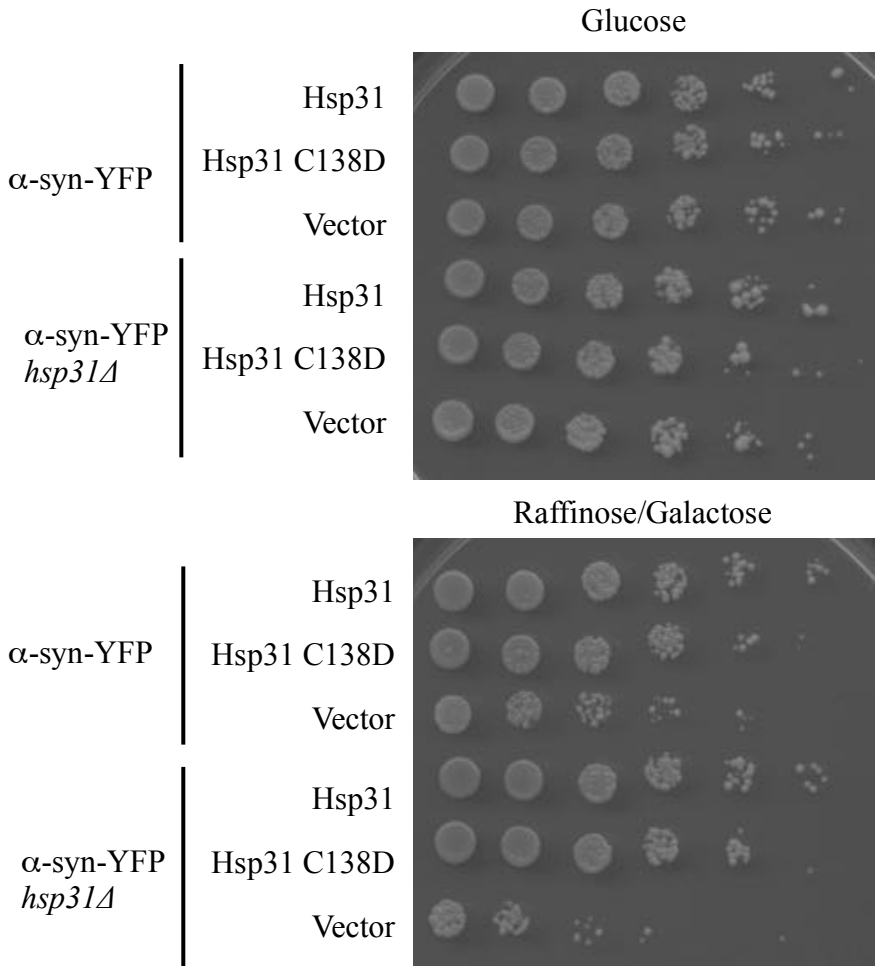

Figure 2.4. The enzyme activity of Hsp31 is not necessary for rescuing α-syn toxicity. Overexpression of *pGPD* HSP31 or the C138D mutant rescues toxicity from α-syn expressing strains**.**

MGO is a toxic metabolite produced during glycolysis that reacts with proteins to yield toxic AGE and has been associated with increased α-syn cross-linking and formation of intracellular foci formation in neuroblastoma cells (261,264,290,306-308). We examined if increased levels of MGO could increase the α-syn foci or toxicity by treating cells with exogenous MGO and found no increased foci formation in wild-type yeast indicating that foci formation is likely not influenced by MGO. In addition, the *hsp31Δ* strain also did not have increased foci suggesting that lack of Hsp31 is not sufficient to increase foci formation due to MGO treatment. We determined that MGO was toxic to wild-type yeast at 10 and 20 mM MGO and viability in the *hsp31Δ* strains was similar to WT suggesting that Hsp31 is not sufficient for detoxification. The concomitant expression of α-syn (one or two copies) and treatment with MGO did not have differential effects on viability (Figure 2.5). Consistent with these results is that cell lysates of the *hsp31Δ* strain had equivalent levels of overall methylglyoxalase activity as wild-type because other yeast methylgloxalase enzymes, Glo1 and Glo2, are present in yeast and have been shown to detoxify MGO.

A

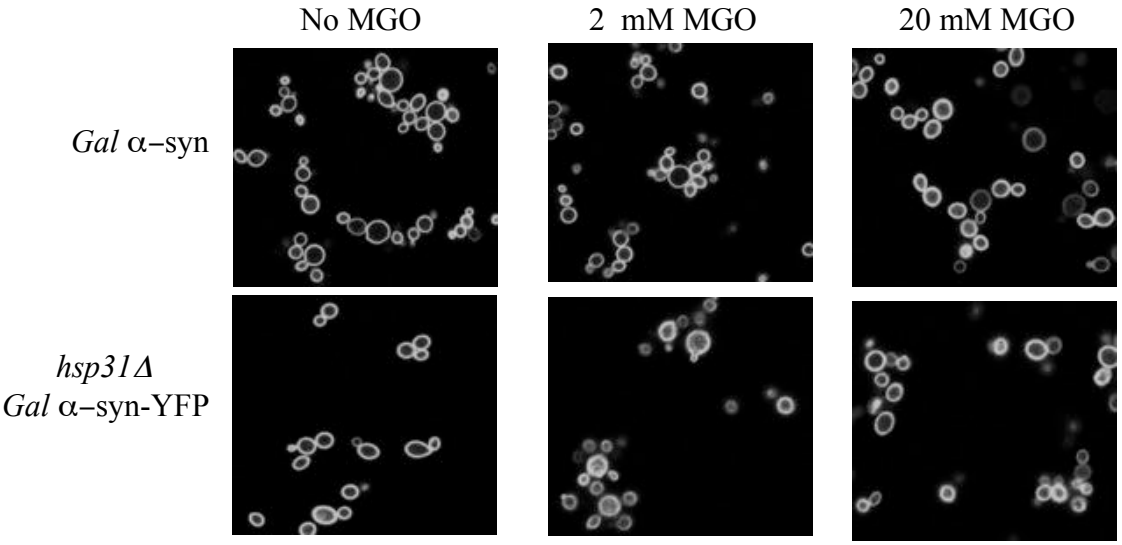
No MGO
2 mM MGO
20 mM MGO
Gal α–syn
hsp31Δ
Gal α–syn-YFP

B

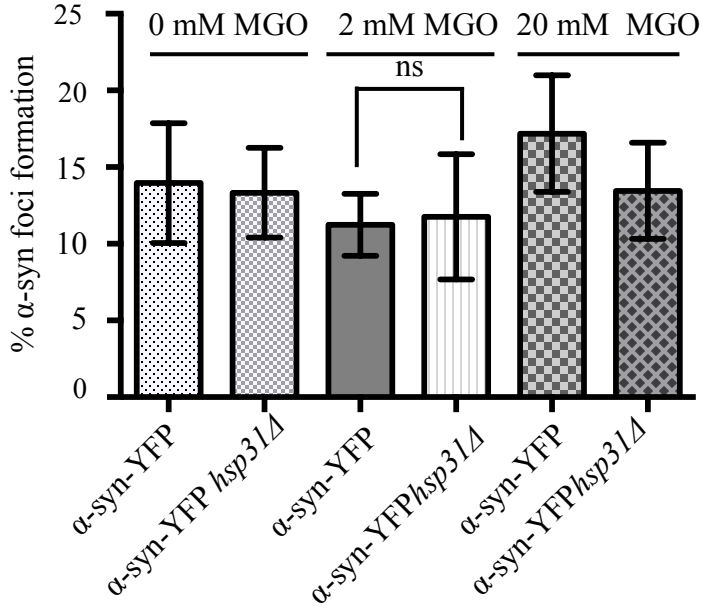
0 mM MGO
2 mM MGO
20 mM MGO
ns
% α-syn foci formation
25
20
15
10
5
0
α-syn-YFP
α-syn-YFP hsp31Δ
α-syn-YFP
α-syn-YFPhsp31Δ
α-syn-YFP
α-syn-YFPhsp31Δ

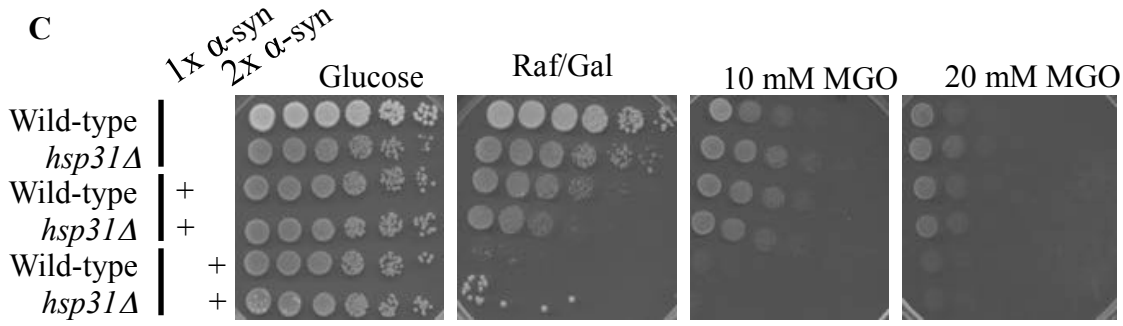

Figure 2.5 MGO does not increase α-syn foci or toxicity.

(A) Representative fluorescence microscopy images of α-syn expressing cells treated with 2 mM and 20 mM MGO. **(B)** The level of α-syn foci does not increase with MGO treatment. Percentage of cells with α-syn foci formation was quantified for the two strains (α-syn-YFP and α-syn-YFP/*hsp31Δ*) in the presence of 2 mM and 20 mM MGO. Cells in three or more fields of view were counted and the mean values plotted (Error bar = 1 SD) ns= one-way ANOVA with multiple comparison t test indicates no significant difference. **(C)** MGO treatment does not differentially increase toxicity of α-syn expressing strains compared to non-expressing counterparts. Strains were serially diluted on agar plates containing 10 mM and 20 mM MGO.

2.3.3 D-lactate supplementation suppresses the steady state level of α-syn

Since, Hsp31 is a methylglyoxalase that converts MGO into D-lactate we further investigated the possibility that deletion of *HSP31* causes the toxicity in α-syn expressing strains due to compromise in the glutathione-independent methylglyoxalase activity of Hsp31. We explored if the lack of enzyme activity leads to a build up toxic cellular MGO or if the altered phenotype of the strain results from the lack in enzymatic product i.e. D-lactate. More recently, it was shown that supplementing the cell with D-lactate restores the mitochondrial membrane potential in DJ-1 deficient (RNAi-treated) HeLa cells (291). We tested if external lactate supplementation could cure the α-syn toxicity similar to Hsp31. First, we performed dilution growth assays on media containing lactic acid to observe any rescue effect in α-syn expressing cells. Surprisingly, there was improved growth of cells even in the presence of low levels of 0.2% lactic acid compared to cells grown without lactic acid supplementation. In parallel to the dilution growth assay, we performed microscopy on cells grown in liquid media containing lactic acid along with galactose to induce α-syn expression and observed these cells under microscope. Cells that were grown in media containing lactic acid showed reduced expression of α-syn compared to non-treated cells. We further confirmed the reduced expression level of α-syn protein in cells treated with lactic acid through western blot analysis using α-syn specific antibody. These results showed that although supplementation with lactic acid reduces α-syn toxicity the mechanism is due to a decreased expression of α-syn, which has been demonstrated to be concentration dependent (1 copy of p*GAL*-α-syn is not as toxic as 2 copies of p*GAL*-α-syn). It is not clear how lactate supplementation affected the steady state level of α-syn. Further studies would be needed to determine if transcription

of α-syn was reduced or if post-translational regulation events affected the overall level of α-syn (Figure 2.6).

A

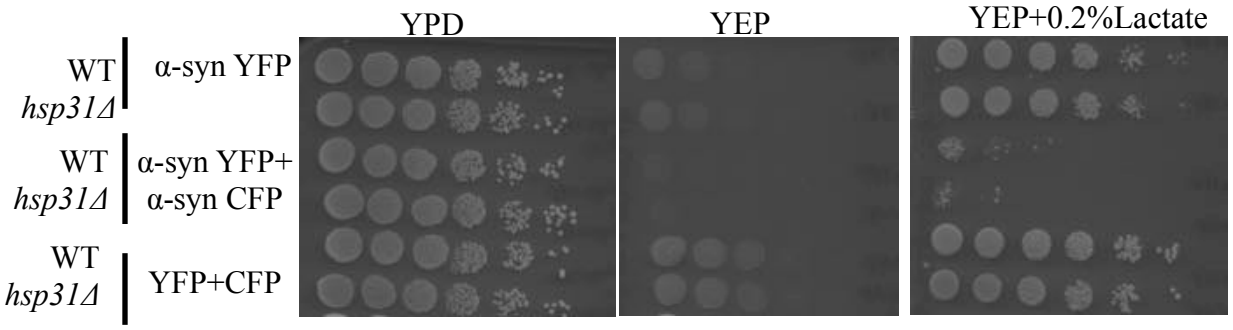
YPD
YEP
YEP+0.2%Lactate
WT
hsp31Δ
α-syn YFP
WT
hsp31Δ
α-syn YFP+
α-syn CFP
WT
hsp31Δ
YFP+CFP

B

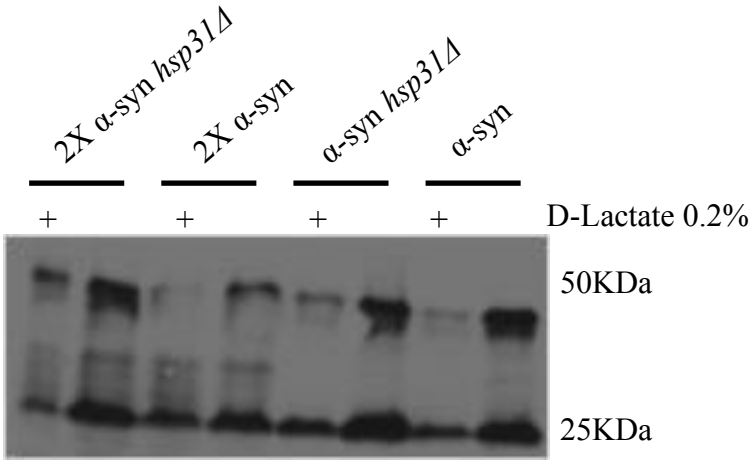
2X α-syn hsp31Δ
2X α-syn
α-syn hsp31Δ
α-syn
+
+
+
+
D-Lactate 0.2%
50KDa
25KDa

C

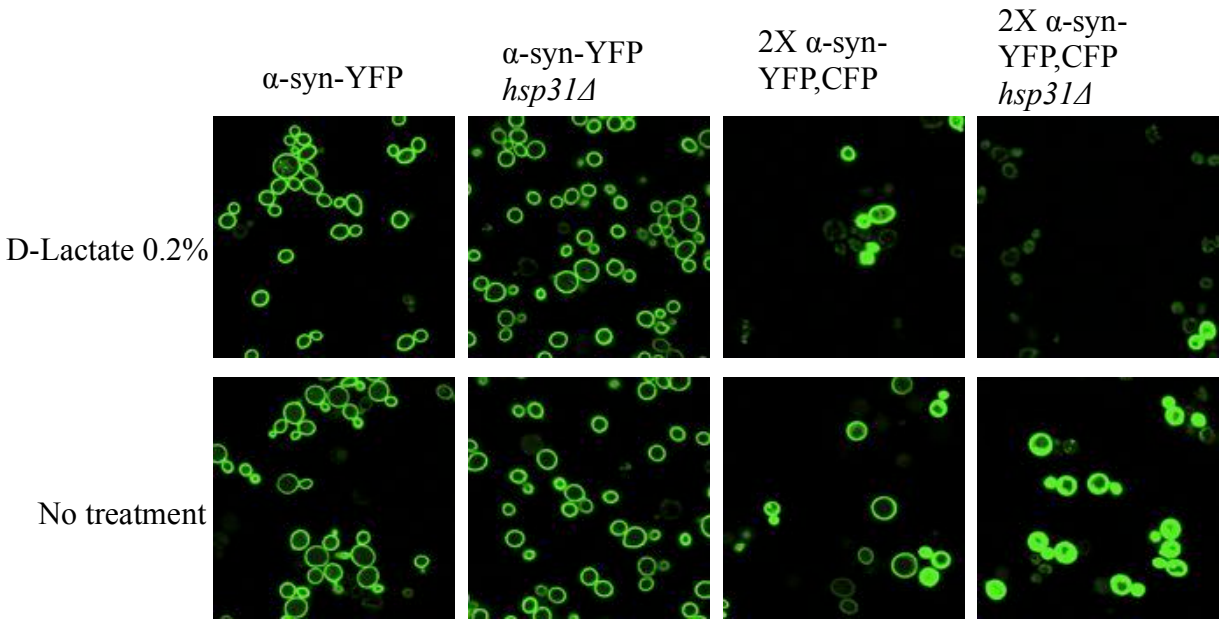

Figure 2.6 Effect of D-lactate on α-syn toxicity.

(A) Effect of D-Lactate on α-syn toxicity as analyzed by dilution growth assay. Fivefold serial dilution of indicated yeast strain was spotted onto plates. Cells were grown for 3 days at 30 °C. **(B)** α-syn expression was induced for 24hrs in the presence and absence of D-Lactate. Cell lysate were subjected to 10%SDS-PAGE and probe with α-syn specific antibody. **(C)** Fluorescence microscopy of yeast cells expressing α-syn -YFP. Cells were supplemented with 0.2% D-lactate for 12hrs with α-syn expression turned on. Cells that were treated with D-lactate showed a suppressed α-syn expression (upper panel).

2.3.4 Hsp31 prevents formation of large prion aggregates

The demonstration that Hsp31 possesses chaperone activity in a variety of anti-aggregation assays prompted us to investigate if Hsp31 could also modulate the oligomeric state of yeast prion proteins, such as the Sup35 prion. The aggregation state of prions in living cells can be monitored by fusion of fluorescent protein tags to Sup35 PrD, so we overexpressed Hsp31 to determine if it modulated the aggregation of Sup35 PrD. Consistent with previous findings, cells overexpressing PrD in the presence of endogenous Sup35 showed characteristic ribbon- like or punctate aggregates, which are localized around the vacuoles or/and adjacent to plasma membranes. The cells co-expressing pAG415-*GPD*-HSP31-DsRed and pAG424-*GAL*-PrD- Sup35-EYFP had approximately 3 fold less Sup35 fluorescent aggregates compared with cells harboring pAG424-*GAL*-PrD-Sup35-EYFP plus vector control, indicating that Hsp31 can inhibit the formation of microscopically visible Sup35 prion aggregates (figure 2.7A-B). The intrinsic fluorescence of Sup35-EYFP appears to increase upon aggregation, which allowed us to utilize flow cytometry as an alternative method to quantitatively measure and show decreased Sup35 aggregation. This phenomenon has not been exploited widely but was noted in at least one previous study investigating the aggregation of a Huntington-GFP fusion protein (309). Cell cultures co-expressing Sup35 and Hsp31 used in the microscopy experiments were prepared for flow cytometry and analyzed for EYFP fluorescence intensity. The flow cytometry results were similar to the microscopy results because Hsp31 expressing cells consistently exhibited lower median Sup35-EYFP fluorescence intensity when compared with cells containing Sup35-EYFP expression plasmid and empty vector. Individual traces depicting the number of counting events for

each yeast strain also showed the decrease in cellular fluorescence intensity when Hsp31 is expressed (Figure 2.7).

A

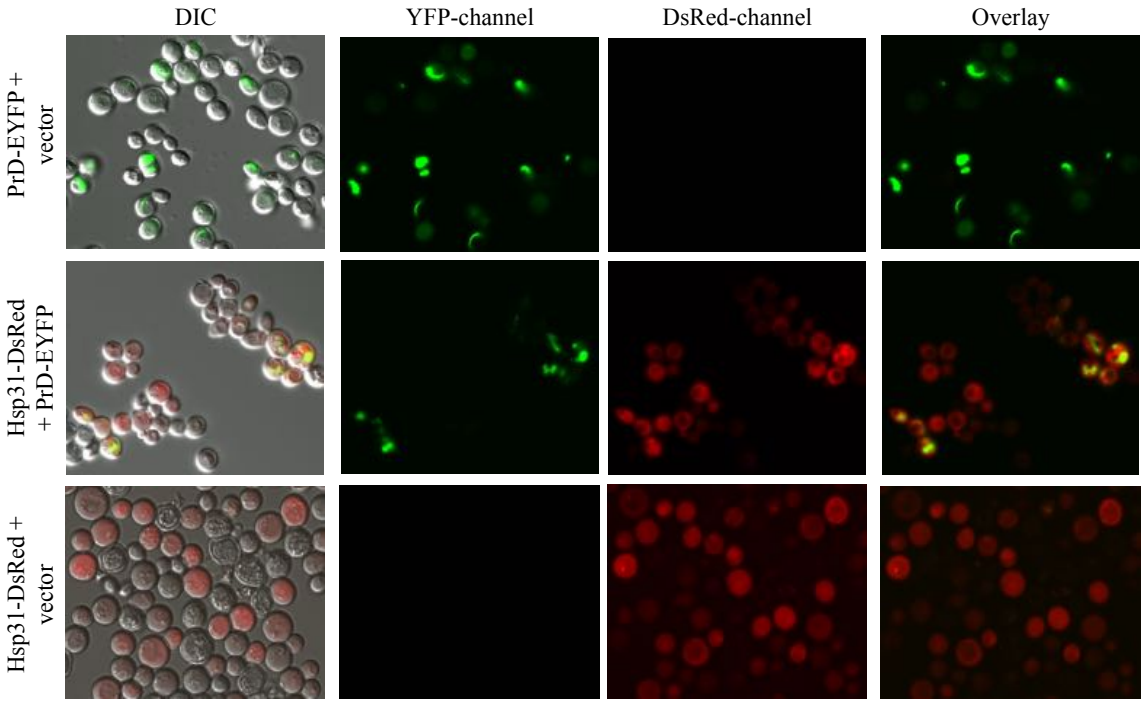
DIC
YFP-channel
DsRed-channel
Overlay
PrD-EYFP + vector
Hsp31-DsRed + PrD-EYFP
Hsp31-DsRed + vector

B

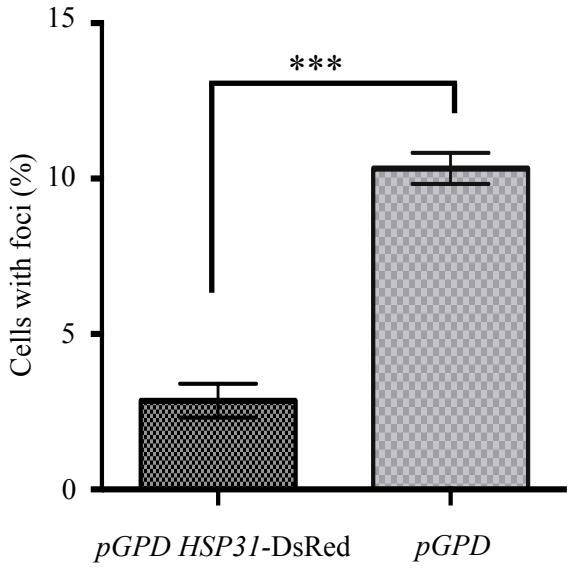
15
10
5
0
***
Cells with foci (%)
pGPD HSP31-DsRed
pGPD

C

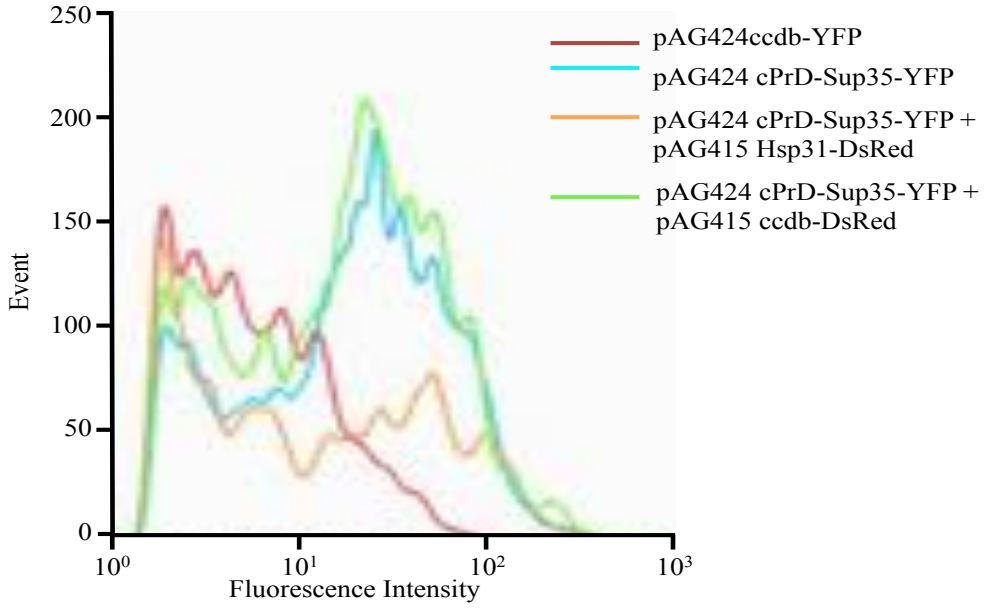

D

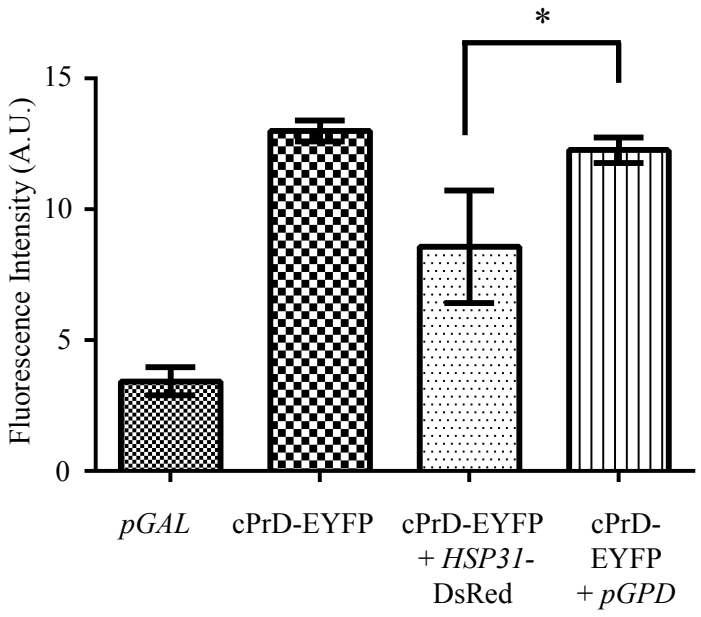

Figure 2.7. Fluorescence microscopy demonstrating Hsp31 suppression of Sup35 aggregation

(A) PrD-Sup35 produced ribbon-like and punctate aggregates that are decreased when Hsp31 is overexpressed. PrD-Sup35-EYFP was overexpressed for 48 h at 30° C in control W303 cells or W303 cells expressing elevated levels of Hsp31. Hsp31 was diffuse in the cytoplasm and decreased the presence of Sup35 aggregates. The diffuse cytoplasmic localization of Hsp31 did not appear to be altered as a result of Sup35 expression. **(B)** Quantitation of cells with one or more Sup35-EYFP foci. A smaller proportion of cells with Sup35 aggregates were evident in Hsp31 overexpressing cells compared to vector control (p*GPD*). Values represent mean ±SEM (n = 3). (*** two-tailed Student's t-test; $p \leq 0.001$). **(C)** Tracing of fluorescence obtained by flow cytometry **(D)** Quantitation of Sup35-EYFP fluorescence suppression by Hsp31 using flow cytometry. Hsp31 overexpression lowers the median fluorescence intensity (FI – arbitrary units) of Sup35 compared to empty vector control. (* two-tailed Student's t-test; $p \leq 0.05$) (±SEM error bars; n = 3 biological replicates).

Expression of Hsp31 with the *GPD* promoter was diffuse and cytoplasmic, and varied in intensity in individual cells across the total cell population. The cytoplasmic localization profile of Hsp31 was not altered when PrD-Sup35 was expressed. Interestingly, we observed overlapping localization in cells with Sup35 aggregates and relatively high levels of Hsp31 but the proteins do not appear to mutually co-localize. In some cells it was evident that the DsRed signal was decreased in the area where there was a Sup35 aggregate suggesting that Hsp31 is not incorporated in aggregates. The aggregate appears to occlude Hsp31 and the diffuse overlapping signal observed in some cells is consistent with the presence of Hsp31 throughout the cytoplasm surrounding the aggregate (Figure 2.8).

A

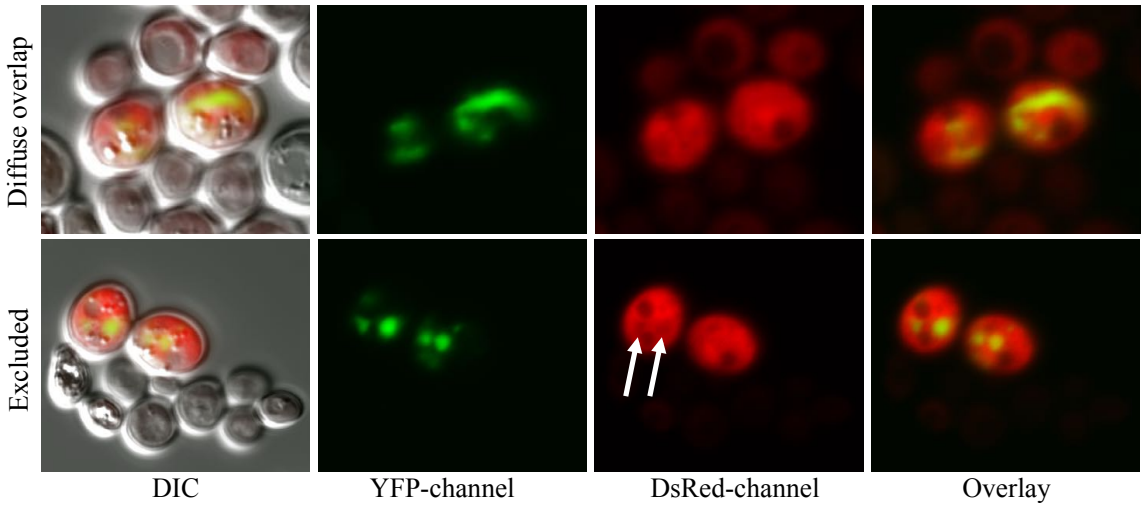

Figure 2.8 Hsp31 and Sup35 are not mutually co-localized.

Most cells with high levels of expression of Hsp31 and Sup35 exhibited diffuse cytoplasmic localization for Hsp31 that overlapped with Sup35 (Top panel). Occlusion of Hsp31 from the Sup35 aggregate was also observed as evidenced by the decreased DsRed signal at aggregate sites (white arrows – bottom panel).

We also confirmed that Hsp31 overexpression reduces the formation of *in vivo* aggregates based on assessing cell lysates by SDD-AGE. We found that SDS-resistant Sup35 aggregates were greatly reduced when Hsp31 was over-expressed. The positive control, Hsp104, completely eliminated detectable Sup35 aggregates. These results are consistent with the ability of Hsp31 to inhibit the formation of large protein aggregates. We also ascertained if other chaperones are induced upon overexpression of Hsp31. We demonstrated Hsp70 and Hsp104 expression are not altered and hence elevated expression of these chaperones is not responsible for the observed suppression of prion aggregates (Figure 2.9). This is in agreement with our in vitro aggregation studies establishing that purified and recombinant Hsp31 protein is solely sufficient to prevent protein aggregation although we cannot exclude the possibility that Hsp31 could collaborate with other chaperones to prevent prion aggregation in the cell.

A

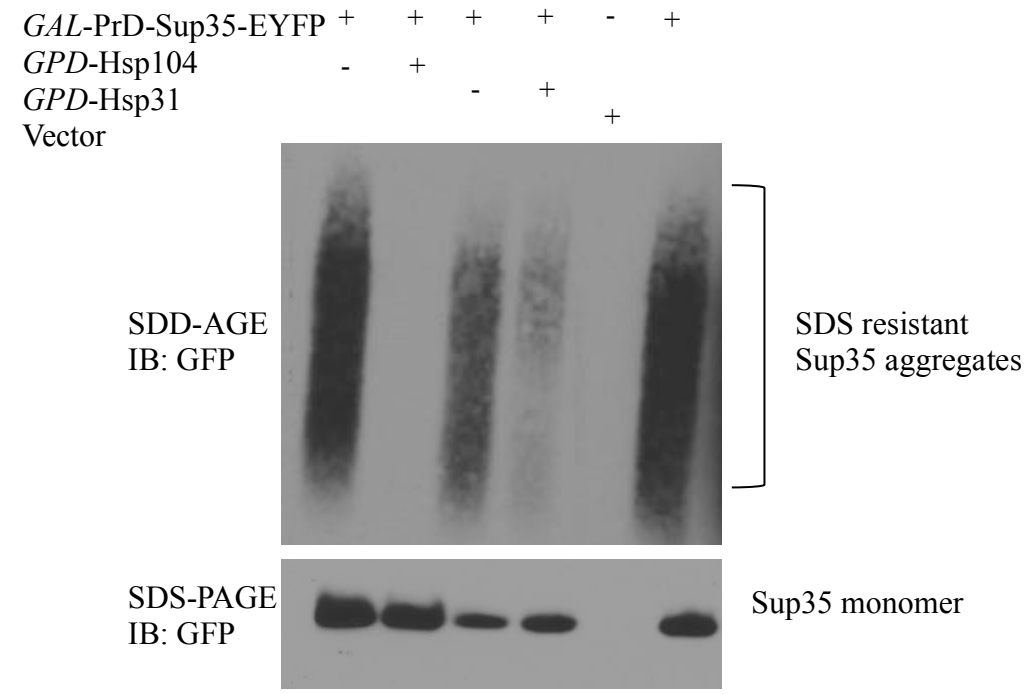

B

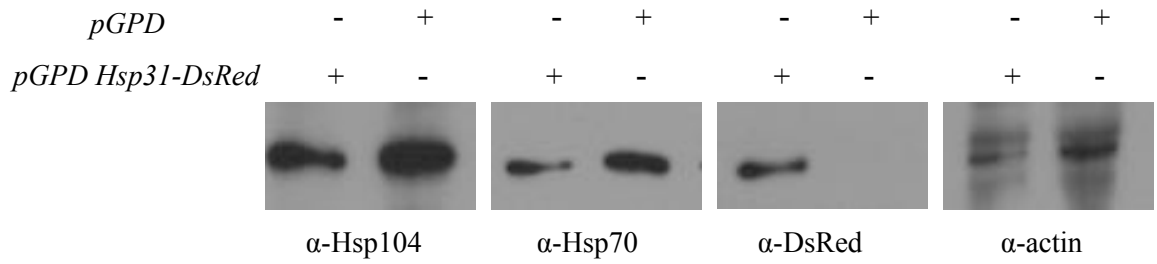

Figure 2.9. Hsp31 suppresses SDS resistant Sup35 aggregates

(A) Cellular lysates were subjected to SDD-AGE and SDS-PAGE. Overexpression of Sup35-PrD-EYFP initiated the formation of Sup35 aggregates which were detected with anti-GFP antibody **(B)** Hsp31 overexpression does not alter the expression levels of Hsp104 and Hsp70. Immunoblots were probed with anti-Hsp104, anti-Hsp70, anti-DsRed and anti-actin antibodies.

2.3.5 Hsp31 rescue of α-syn -mediated toxicity is independent of the autophagy pathway

In several recent studies, autophagy has been identified as one of the main mechanisms to clear and recycle misfolded proteins and aggregates in the cytosol (310,311). In addition to the ubiquitin proteasome system, autophagy is a major cellular function involved in clearance of misfolded and aggregated proteins including α-syn aggregates (310). Deletion of autophagy genes such as *ATG5* or *ATG7* leads to neurodegenerative disease in mice (312,313). In yeast, deletion of *ATG1* gene that is required for induction of autophagy reduced the clearance of α-syn aggregates (314). Deletion of *HSP31* was also demonstrated to impair autophagy under carbon starvation conditions (152). These studies raise the question that Hsp31 could be promoting autophagy of aggregated protein. In order to exclude the possibility that the Hsp31 rescue effect on α-syn toxicity depends on autophagy, we deleted the *ATG8* gene in the α-syn strains and assessed the synthetic lethal effects of α-syn expression in these strains. As expected, expression of α-syn in the *atg8*Δ strain resulted in decreased viability compared to the wild-type strain. The *atg8*Δ *hsp31*Δ strain had similar viability to the *atg8*Δ strain when α-syn is expressed. These results confirm that autophagy is a protective mechanism against α-syn toxicity. The lack of synthetic lethal defect between *ATG8* and *HSP31* with and without α-syn expression is consistent with genes that are in the same pathway and hence do not buffer each other (Figure 2.9).

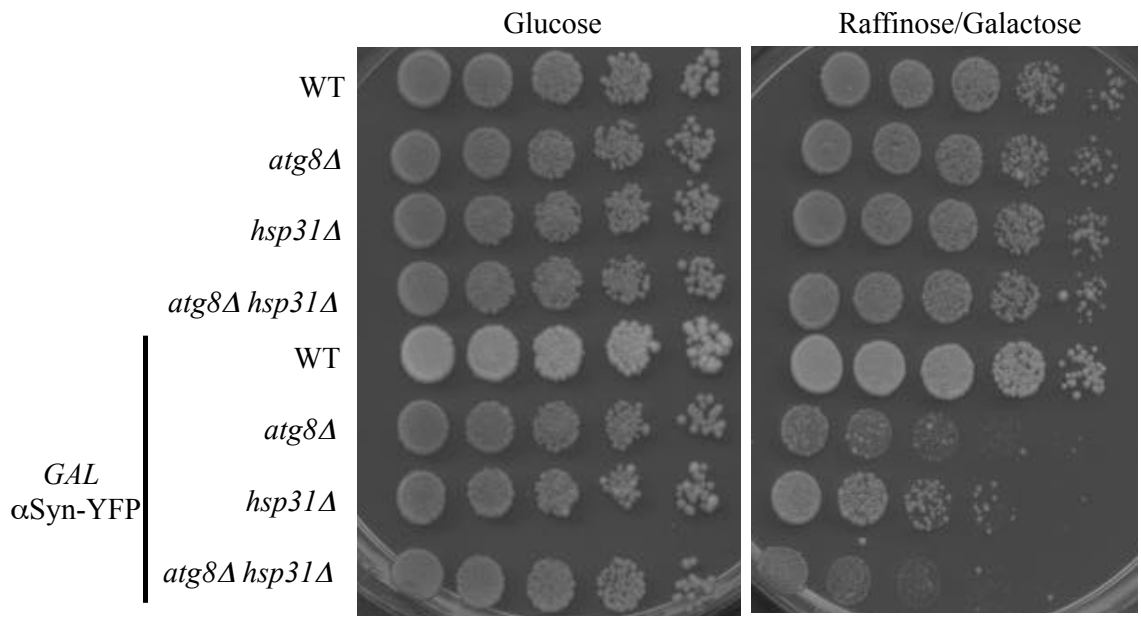

Figure 2.10 The autophagy pathway prevents α-syn toxicity but is not required for Hsp31 mediated rescue.

Yeast strains serially diluted on YEP agar plates (Glucose or Raffinose/Galactose) demonstrating the toxicity of *GAL*-α-syn in the *atg8Δ*, *hsp31Δ* and *atg8Δ hsp31Δ* strains.

Expression of Hsp31 and the C138D mutant in the autophagy strains, *atg8*Δ α-syn or *atg8*Δ *hsp31*Δ α-syn, increased viability in rich YEP media compared to vector controls. We found that the rescue effect in synthetic media was not easily observed because expression of α-syn was not toxic in the *atg8*Δ strain background but it was toxic in *hsp31*Δ indicating media conditions are an important factor in this complex relationship. These results demonstrate that Hsp31 can rescue α-syn toxicity in autophagy deficient cells (Figure 2.10).

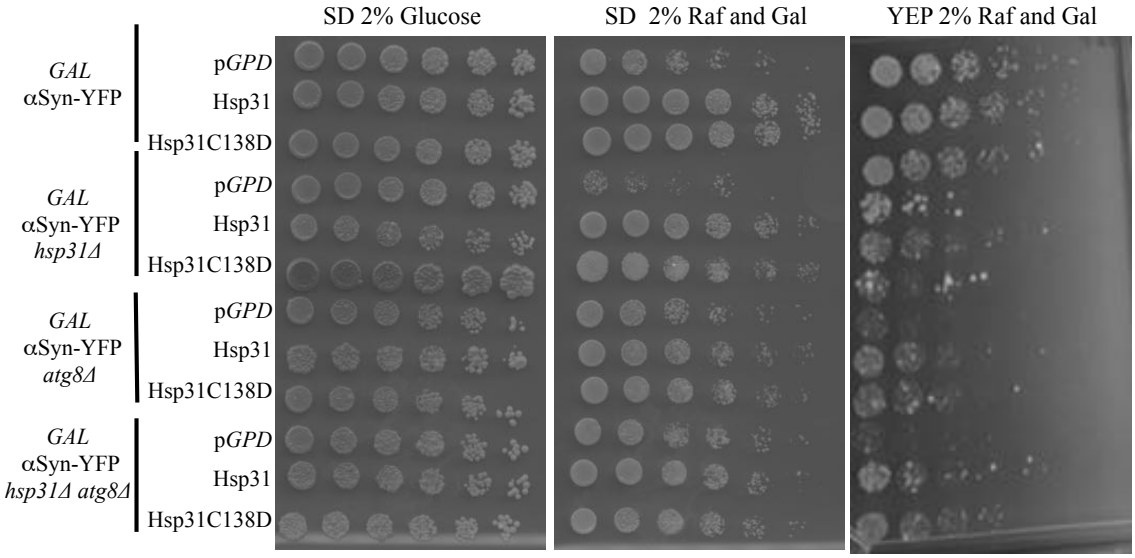

Figure 2.11 Effect of Hsp31 overexpression on *atg8Δ* strains

Overexpression of Hsp31 using pAG415-*GPD*-HSP31-DsRed or the C138D mutant partially rescued toxicity of α-syn expression on YEP media for the *atg8Δ*, *hsp31Δ* and *atg8Δ hsp31Δ* strains (right panel). Rescue by Hsp31 overexpression could not be assessed in synthetic media for strains with the *atg8Δ* genotype because *GAL*-α-syn expression not toxic in these strains (middle panel). Rescue of *GAL*-α-syn expression in the *hsp31Δ* strain was toxic and rescued by Hsp31 overexpression in synthetic and YEP media.

2.4 Methods

2.4.1 Yeast cell growth conditions

Yeast media were prepared according to Amberg D C. et al. (315). Liquid yeast extract/peptone dextrose (YPD) medium contained Bacto yeast extract (1%, Fisher Scientific), Bacto peptone (2% Fisher Scientific) and glucose (2% Fisher Scientific). Synthetic dextrose (SD) minimum liquid medium was made of 0.17% Difco yeast nitrogen base (without amino acids), 2% glucose, and supplemented with necessary amino acids for auxotrophic strains needed at concentrations described previously (315). Solid medium plates were made with the same components of liquid medium plus 2% agar (Fisher Scientific). To express galactose-inducible proteins, 2% raffinose (Affymetrix, Cleveland OH) and 2% galactose (Affymetrix, Cleveland OH) were used to replace glucose. Fractions of culture were obtained at designated times to monitor the cell fitness and protein levels by OD_{600} and immunoblotting, respectively.

2.4.2 Spotting assay / Dilution growth assays

All the yeast strains were grown at 30 °C in 2% glucose minimal media overnight. Strains were diluted to OD_{600} of 0.2 and grown in minimal media switching the carbon source with 2% raffinose for overnight. Cultures were normalized to OD_{600} of 0.8 and 5X serial dilutions were spotted onto the respected dropout plate containing 2% glucose or Yeast strains construction galactose. Plates were grown at 30 °C for 2-3 days before taking pictures.

2.4.3 Yeast strains construction

Yeast strains used in this study are listed in Table 2.1. The *hsp31*Δ and *atg8*Δ deletions were generated in W303-1A or in a strain expressing one or two copies α-syn fused to

fluorescent proteins (CFP and YFP) using the primers listed in Table 2.2. The nourseothricin N- acetyl-transferase (NAT) gene flanked by Hsp31 homology regions was obtained by PCR with 70 nucleotide long forward primer and reverse primer. The primers consisted of 20 nucleotides for amplifying the NAT gene from pFA6a-natNT2 (Euroscarf), and 50 nucleotides immediately preceding the Hsp31 or Atg8 start codon or after the stop codon. The amplified product was integrated into W303 α-syn expressing strains at ChrIV:1502160 to 1501447 as described previously. For double knockout *hsp31*Δ *atg8*Δ strain KanMX4 resistance cassette was used to delete Hsp31 and than NATMX4 resistance cassette for deletion of *ATG8*.

Table 2.1 List of strains used in this study

Strain	Genotype	Source or reference
BY4741	*MATa his3, leu2, met15, ura3, ARL1, GCS1, ARL3, ARF3, YPT6, IMH1, SYS1, GAS1*	Invitrogen
W303-1A	*MATa can1-100 his3-11, 15 leu2-3, 112 trp1-1 ura3-1 ade2-1*	R. Rothstein
W303-*hsp31Δ*	*W303-1A hsp31Δ*::NATMx	This study
W303-*HSP31-9myc*	*W303-1A HSP31-9myc::*KanMX	This study
W303-1x α-syn	W303 *GAL*-α-syn-YFP at *URA3* or *TRP1* loci	J-C. Rochet(316,317)
W303-2x α-syn	*W303 GAL-* α-syn-YFP at *URA3 GAL-* α-syn-CFP at *TRP1* loci	J-C. Rochet
W303-1x α-syn *HSP31-9myc*	W303 *GAL-* α-syn-YFP at *URA3* or *TRP1* loci *HSP31-9myc::*KanMX	This study
W303-2x α-syn *HSP31-9myc*	*W303 GAL-* α-syn-YFP at *URA3 GAL-* α-syn-CFP at *TRP1* loci *HSP31-9myc::*KanMX	This Study
W303-*hsp31Δ*	*W303-1A atg8Δ*:: NATMx	This study
W303-*hsp31Δ*	*W303-1A atg8Δ*:: NATMx *hsp31Δ*:: KanMx	This study

Table.2.2 List of plasmids used in this study

Plasmids	Type of plasmid	Source or reference
pGEX6P-1 Hsp31	*E. coli*	This study
pAG415-*GPD*-Hsp31-dsRed	Yeast, CEN	This study
pAG415-*GPD*-ccdB-dsRed	Yeast, CEN	Alberti et al.(318)
pAG-425-*GAL*-PrD-Sup35-EYFP	Yeast, 2 μ	Alberti et al.(318)
p2HG	Yeast	Rochet's lab
p2HG-Hsp104	Yeast	Rochet's lab
BG1805 HSP31-MORF	Yeast, 2 μ	Gelperin,D.M.,et al.(319)

Table 2.3. List of primers used in this study.

Primer name	Primer sequence (5'→ 3')
***HSP31*_NAT_F**	AAGTACTTCCCACTGGCTAATTACACAGATAAAACTCA AACAAATTTATAATGACATGGAGGCCCAGAATACCC
***HSP31*_NAT_R**	CTTACATCTATATAGTAGTACAAAGGAAATTCTAATTA TCAACCTTTGGCTCACAGTATAGCGACCAGCATTCAC
Hsp31_9myc_F	TCTGCGCACTCCACTGCCGTAAGATCCATCGACGCTTT AAAAAACCGTACGCTGCAGGTCGAC
Hsp31_9myc_R	TCCTTACATCTATATAGTAGTACAAAGGAAATTCTAAT TATCAACCTTTGGCTCAATCGATGAATTCGAGCTCG
***HSP31*-9myc tag diagnostic-F**	ACAGAGAATTAACGTTACTC A TTCC
***HSP31*-9myc tag diagnostic-R**	ATATTTGGATATTGGGGAAACAC AT
Atg8-NAT_F	AGTTGAGAAAATCATAATAAAATAATTACTAGAGACA TGACATGGAGGCCCAGAATACCC
Atg8-NAT_R	CGATTTTAGATGTTAACGCTTCATTTCTTTTCATATAAA AGACTACAGTATAGCGACCAGCATTCAC
***ATG8* diagnostic-F**	GGGAACCATTAAAGGTTGAG GAGG
***ATG8* diagnostic-R**	GTAAACATTCTTATACTGGAACA

2.4.4 *HSP31* 9myc tagging

We endogenously tagged *HSP31* with 9myc epitope using a PCR- based integration. The pYM20 plasmid was used as template and appropriate primer set to obtain PCR product with *HSP31* genomic flanking sequence and the PCR product was transformed into W303 and W303 α-syn-CFP + α-syn-YFP strains. The transformants were selected on media containing hygromycin B (300mg/L) and correct integration was verified by PCR using primers spanning the integration junctions and by DNA sequence analysis. DNA manipulation - The plasmids used in this study are listed in Table 2.2. Hsp31 was shuttled into pAG415- *GPD*-ccdB-DsRed (Addgene Cambridge MA (318) from pDONR221 with LR clonase (Invitrogen, Grand Island, NY) to produce pAG415-*GPD*- HSP31-DsRed. Both DJ-1 and Hsp31 were cloned into BamHI/XhoI sites of pGEX 6p-1. pESC-Leu myc-*HSP31* was constructed by cloning at the XhoI/NheI sites. The *HSP31* gene was amplified from yeast genomic DNA. The Hsp31 C138D mutant was prepared by PCR amplification using pAG415-*GPD*-Hsp31-DsRed as template and set of primers listed in Table 2.3 Each successfully mutated insert was sequenced to confirm the mutation.

2.4.5 Antibodies and immunoblotting

To determine protein expression yeast cells were collected by centrifuging at 5000 rpm and pellets were resuspended in extraction buffer (50mM Tris-HCl pH 7.5, 1mM EDTA, 4mM MgCl2; 5mM DTT). Glass beads (Sigma, St. Louis, MO) were added into the mixture, which was vortex 5 times for 10 s each, plus 1 min intervals on ice. Clear crude protein lysate was obtained by spinning down the cell debris at 1000 xg at 4 °C for 10 min. The SDS- PAGE loading dye (4 % SDS, 40 % glycerol, 0.02% bromophenol blue, Tris-Cl, pH6.8) was added to supernatant and samples were boiled, followed by SDS-

PAGE and immunoblotting with antibodies. Monoclonal anti-myc and anti-β-actin antibody were purchased from Sigma-Aldrich (St. Louis, MO). Monoclonal anti-α-syn was obtained from BD biosciences (San Jose, CA). The following antibodies were also used to detect expression of Hsp104 (Abcam; ab69549), Hsp70 (Stressgen; SPA-82); DsRed (Santa Cruz Biotechnology; Sc-33353) and GFP (Roche; anti- GFP).

2.4.6 Protein purification

BY4741 harboring yeast Hsp31 expression plasmid from the yeast moveable ORF collection (Thermo Fisher Scientific Open Biosystems, Huntsville, AL) was used to express and purify the protein. We did not see any evidence of co-purifying proteins on SDS-PAGE gels and observed similar high activity from protein purified under high salt conditions, which minimizes contaminant co-purifying proteins. Human DJ-1 was encoded in pGEX 6p-1 (GE Healthcare Life Sciences), hchA was encoded in pNT-hchA, and α-syn was expressed from the pT7 plasmid. The protein expression and purification was described previously. Briefly, constructs were transformed into BL21 (DE3) cells. The transformants were grown to an OD_{600} of 0.4 – 0.6 in LB medium supplemented with 100 μg/ml ampicillin at 37 °C, and Isopropyl β-D-1- thiogalactopyranoside (IPTG) (1mM as final concentration) was added to induce protein expression. After 3 h of induction at 37 °C, cells were harvested by centrifugation at 2,000xg, and re-suspended in lysis buffer (25 mM KPi pH 7.0, 200mM KCl) containing protease inhibitor cocktail set IV (Calbiochem, Billerica, MA). Crude protein was prepared by sonicating cells and clarifying the lysate by centrifugation at 10,000xg for 10 min. GST tagged DJ-1 was immobilized by Glutathione agarose resin (Thermo scientific) and DJ-1 was eluted by cleaving from the GST tag with PreScission Protease (GE Healthcare Life Sciences,

Pittsburgh, PA) (2 units of protease for every 100 µg of tagged DJ-1) leaving a linker amino acid sequence: (NPAFLYKVVDVSRHHHGRIFYPYDVPDYAG LEVLFQ) The protein was approximately 95% pure based on band intensity coomassie blue staining with SDS- PAGE.

2.4.7 Dilution growth assays

Plasmids pAG415-*GPD*- ccdB-DsRed and pAG415-*GPD*-HSP31-DsRed were transformed into W303 α-syn expressing strains with or without genomic copy of the HSP31 gene knocked out using the PEG/lithium acetate transformation method. Single colonies of transformants were grown in SD-Leu overnight, the cells were washed, normalized and grown in synthetic complete without leucine (SC-Leu) + raffinose (2%) to switch the carbon source. After incubating in the raffinose medium over night, the cell number was normalized, and spotted on SD-Leu (suppressed expression) plate and SC-Leu with 2% raffinose and 2% galactose (induced expression) with five-fold serial dilutions. The plates were incubated at 30 °C for 3 days.

2.4.8 Fluorescence imaging analysis α-syn localization

pESC-Leu myc-Hsp31 and control empty vector were transformed into 2 copies of α-syn expressing strain. Transformants were inoculated and grown as described in the growth dilution assay. The α-syn expression was induced by growing the cells in synthetic minimum medium with 2% raffinose and galactose for 8 h. The live cells were visualized using Nikon TE2000-U inverted fluorescence microscope with Nikon Plan apochromat 60X (NA 1.4) oil immersion objective and YFP filters plus 300X magnification. In order to differentiate the localization of protein, approximately 50 individual cells were randomly counted in multiple regions of interest for each set of experiment. The ratio of

membrane to cytoplasmic localization of α-syn fluorescent fusion protein was presented as the mean from three independent sets of experiments.

2.4.9 MGO addition and microscopy

α-syn expressing strains with or without the Hsp31 gene deleted were grown in YPD media and transferred into media containing 2% galactose and MGO (0.5mM-2mM) for 6 h and 12 h. Cells were washed and subjected to confocal microscopy to observe α-syn foci formation. The presence of MGO inhibited the growth of cells for the initial 12 h and resulted in equal growth rate between strains regardless of the Hsp31 gene deletion. Strains could not be grown in the presence of high concentrations of MGO (20mM) so α-syn was induced for 10 h and then MGO was added and incubated for another 2 h before confocal microscopy analysis.

2.4.10 Assessment of intracellular ROS

Cells were harvested after induction of α-syn expression for 12 h and 5 × 106 of cells were prepared to stain with dihydroethidium (DHE). Cells were suspended in 250 µl of 2.5 µg/ml DHE in PBS, and incubated in the dark for 10 min. Cells were washed in the PBS and were subjected to fluorescence microscopy (excitation at 485 nm and emission at 520 nm) and flow cytometry with FL-2 channel. FlowJo software was used to calculate median fluorescence intensity.

2.4.11 Prion expression experiments

W303 WT strain was co-transformed with pAG424-*GAL*- PrD-Sup35-EYFP and pAG415-*GPD*-HSP31-DsRed. Single transformations were also performed using the same constructs and their corresponding control vector. Cells were grown at 30°C in appropriate medium overnight (SD-Trp for pAG424, SD-Leu for pAG415 and SD-Trp-

Leu for co-transformants) and protein expression was induced for 24 h in SC 2% Raffinose and 2% Galactose containing medium at 30 °C. After induction, cells were subjected to fluorescence microscopy using a Nikon A1 confocal microscope with a Nikon Plan apochromat 60X (NA 1.4) oil immersion objective to acquire fluorescence and DIC images and were analyzed using Image J. The identical cultures used in microscopy were used to prepare samples for flow cytometry, cells were washed and re-suspended in PBS at a density of ~$10x10^6$ cells/ml. Cells were filtered and analyzed for EYFP fluorescence intensity using a flow cytometer with the FL-1 channel. A total of 10,000 events were acquired for each sample and data was analyzed using FlowJo software to calculate median fluorescence intensity after three biological replicates.

2.4.12 Glutathione-independent glyoxalase biochemical Assay

Purified recombinant Hsp31 and Hsp31 C138D with GST tag removed were used to assay methylglyoxalase activities. The reaction was initiated by adding specified concentration of proteins (1 μM Hsp31 and 5 μM Hsp31C138D) in reaction buffer (100 mM HEPES, pH 7.5, 50 mM KCl, 2 mM DTT) to 6 mM initial concentration of MGO (Sigma, 40% solution), followed by incubation at 30 °C. The assay was performed, by removing 50μl aliquots of the reaction at fixed time points (15, 30, 45, and 120 s) after addition of protein. The amount of D-lactic acid produced by Hsp31 as a result of MGO consumption was measured. The initial rate obtained was divided by amount of protein in the reaction mixture to calculate the specific activity. Samples were also subjected to Gas Chromatography-Mass Spectroscopy analysis (Agilent 5975C MSD) to identify the presence of D-lactic acid. Samples were derivatized with N, O-bis (trimethylsilyl) trifluoroacetamide) and trimethylchlorosilane and heated to 50 °C for 10 min and run in

the electron impact mode with scanning from 42-400 atomic mass units. A lactic acid standard displayed a peak at 6.09 min identical to the peak detected in the Hsp31-treated sample whereas Hsp31C138D did not display this peak. The spectral scan was visualized and displayed using the OpenChrom software (320). To obtain the enzymatic parameters, the reaction was initiated as described above by adding 1 μM Hsp31 or 5 μM Hsp31C138D protein into reaction buffer and reactions were stopped after 1 min by heating at 85 °C for 30 s. A range of MGO substrate from 50 μM to 2 mM and the EnzyFluo D-Lactate Assay kit (Bioassay System) was used to determine the amount of D-lactic acid produced in each reaction. Each rate was determined in triplicate and mean values were plotted to obtain enzymatic parameters (Vmax and Km) by fitting to michaelis-menten model using Graphpad prism.

2.4.13 Semi-denaturing detergent-agarose gel electrophoresis (SDD-AGE)

W303 cells harboring pAG424-*GAL*-cPrDSup35-EYFP and pAG415-*GPD*-HSP31-DsRed plasmids were used and aggregates produced by inducing for 24 h in SC 2% raffinose + 2% galactose media. Prion aggregates were analyzed using SDD-AGE (321). Briefly, to prepare lysates, cells were harvested by centrifugation at 3,000'g for 2'min and re- suspended in spheroplast solution (1.2 M D-sorbitol, 0.5 mM MgCl2, 20 mM Tris (pH 7.5), 50 mM β-mercaptoethanol and 0.5 mg/ml Zymolyase and incubated at 30 °C for 30 min with shaking. After spheroplast formation the samples were centrifuged at 800 rpm for 5 min at room temperature and supernatant was removed. The pelleted spheroplasts were resuspended into 100 μL lysis buffer (100 mM Tris 7.5, 50 mM NaCl, 10 mM β-mercaptoethanol and protease inhibitor and vortexed at high speed for 2 min. The lysates were collected and mixed with 4 x sample buffer (2 x TAE; 20 % glycerol; 4 % SDS;

0.01% bromophenol blue). The samples were incubated at room temperature for 15 min and loaded onto a 1.8 % agarose gel containing 1 x TAE and 0.1 % SDS and run at 50 V, followed by transfer onto nitrocellulose membrane using capillary transfer method. The nitrocellulose membrane was subjected to western blot analysis using anti-GFP antibody (Roche). A strain harboring p2HG-Hsp104 plasmid was included as a positive control.

2.5 Discussion

DJ-1/ThiJ/PfpI superfamily members composed of structurally similar proteins that are present in prokaryotes and eukaryotes. Often these proteins are associated with stress response. However, structural and biochemical studies have proven that they are diverse in functions with the ability to perform multiple activities that include chaperone, protease, methylglyoxalase, deglycase and role in autophagy. In this study we aimed to delineate the functions of Hsp31 by using yeast as a model. Recently, we established that Hsp31 is a potent chaperone that can inhibit the aggregate formation of large number of proteins such as insulin, citrate synthase as well as prevent α-syn fibrillization *in vitro* and α-syn toxicity *in vivo*. Because Hsp31 is a multifunctional protein, we sought to identify the interaction between different functional pathways of Hsp31 and define its role in protecting against cellular stress. We also obtained insight into the role of Hsp31 in Sup35 prion aggregations.

2.5.1 Role of Hsp31 in redox homeostasis

Previous studies showed the protective effect of Hsp31 under oxidative and proteotoxic stress in that overexpression of Hsp31 protect yeast cell viability under these conditions

(260,303). In the past, our lab has shown that Hsp31 protects cells from α-syn mediated toxicity. These observations led us to explore the expression profile of Hsp31 in response to oxidative and proteotoxic stress. A genomically tagged strain shows an increase in Hsp31 expression under both oxidative and proteotoxic stress (Figure 2.1). Previous studies have shown that an increased level of Hsp31 at the diauxic shift and during stationary phase of growth cycle. These phases in the growth cycle are associated with stress due to accumulation of toxic metabolites and lack of nutrients (322). An elevated level of Hsp31 at later phases of growth indicates that it could possibly be due to the stress associated with these phases. *HSP31* expression is also induced when yeast cells are treated with H_2O_2 to produce oxidative stress and this up-regulation of *HSP31* in response to ROS has been reported to be under the control of stress responsive transcription factor Yap1, as removal of Yap1 binding site (-363 and -353 bp relative to the ATG) from *HSP31* promoter has shown to reduce Hsp31 expression under oxidative stress (303). However, we observed that this shortened promoter also eliminates another stress response element (STRE, a CCCCT site at -379 to -383 from the ATG) in addition to the Yap1 binding site. STREs are the binding site for Msn2/4, and several other stress-related yeast genes have been documented to be transcriptionally activated by these transcription factors, including genes up-regulated after the diauxic shift in stationary phase cells (303).

Finally, we also reported an increase in ROS levels upon *HSP31* deletion that correlates with increased toxicity by α-syn expression compared to WT strains, as level of superoxide was higher when we overexpressed α-syn indicating that the presence of

Hsp31 is important in reducing ROS to basal levels. A previous study has shown that α-syn expression is associated with caspase-mediated ROS generation (323) (Figure 2.2). In agreement with our study, overexpression of *HSP31* robustly suppresses both cytosolic and mitochondrial ROS levels instigated by MGO and H_2O_2 and therefore provide cytoprotection. In addition, Hsp31 localizes to mitochondria and preserves mitochondrial integrity by redistributing glutathione to the cytoplasm under oxidative stress (260). Another study examined the deglycase activity of Hsp31 and showed that it may efficiently deglycate proteins with glycated Cys, Arg and Lys amino acid residues (265). Taken together, these results suggest that Hsp31 is an integral part of the heat shock protein system and plays a vital role in maintaining cellular homeostasis. These results establish that Hsp31 has a role in response to ROS and its expression is induced in response to several types of stress.

2.5.2 Hsp31 chaperone activity is independent of its methylglyoxalase activity

Recently in our lab we demonstrated the robust chaperone activity of Hsp31 that can rescue the α-syn toxicity *in vivo*. A question was raised that the *in vivo* rescue effects could have been mediated by the Hsp31 methylglyoxalase activity or interaction with other biological pathways such as the metabolic or autophagy pathway. First we confirmed that Hsp31 does have methylglyoxalase activity and demonstrated that mutation of the catalytic triad residue, C138D, results in greatly reduced methylglyoxalase activity (Figure 2.3). However, this mutation did not inactivate the chaperone activity in terms of rescuing the cells from α-syn-mediated toxicity when expressed under *GPD-HSP31* C138D system (Figure 2.4). Furthermore, we showed that

that exogenous MGO did not differentially affect viability suggesting that Hsp31 does not rescue by reducing accumulation of this toxic metabolite in α-syn expressing cells (Figure 2.5). Another study also reported that mutation in the catalytic triad largely abolishes glyoxalase activity but this catalytic triad is not required for chaperone activity of Hsp31 (260). These results indicate that the anti-aggregation activity of Hsp31 is not under the influence of its known enzymatic activity rather; it has a direct chaperone activity against misfolded proteins. Intriguingly, all the paralogs of the Hsp31 minifamily possess comparable activity against α-syn aggregation and toxicity when they are overexpressed from the *GAL* promoter (106). However, unlike Hsp31, the other paralogs possess very little methylglyoxalase activity and are unable to protect the cells from glyoxal toxicity (260). Furthermore, the chaperone activity of Hsp31, Hsp32 and Hsp33 against a cytoplasmic aggregation-prone protein is independent of their role in oxidative stress response and the vacuolar degradation pathway (262). These results again support the notion that anti-aggregation activity of Hsp31 mini-family is independent of its enzymatic activity.

2.5.3 Autophagy pathway is not essential for chaperone activity of Hsp31

We also demonstrated the autophagy pathway is an important mediator in the α-syn toxicity because deletion of ATG8 resulted in synthetic lethal interaction with α-syn expression (Figure 2.10). This is consistent with *atg1Δ* or *atg7Δ* strains having synthetic lethal interactions with α-syn expression and having defects in clearing α-syn foci (324). However, we show that *hsp31Δ atg8Δ* strain does not have increased α-syn- mediated toxicity when compared to *atg8Δ*, consistent with these genes occurring within the same

synthetic lethal pathway. A recent result indicates that *hsp31Δ* strains are defective in autophagy (301) so the additional deletion of an autophagy gene should not increase toxicity. Interestingly, overexpression of Hsp31 in these autophagy deficient strains can rescue cells from α-syn toxicity indicating that autophagy pathway is not essential for chaperone rescue (Figure 2.11). Autophagy may be beneficial for controlling α-syn toxicity but it appears that chaperone activity of Hsp31 is also important.

2.5.4 Hsp31 inhibits Sup35 prion aggregation

Several orthologous experiments suggest that Hsp31 intervenes early in the misfolding process and prevents the formation of larger oligomeric species. Previously, we showed that the addition of Hsp31 to α-syn monomers in a fibrillization assay resulted in a baseline level of ThioT fluorescence signal indicating that the formation of larger oligomeric species was prevented. Analysis of the SDS-resistant oligomeric species by SDS-PAGE demonstrated that the presence of Hsp31 prevented the formation of higher order oligomeric α-syn species. Here, our studies demonstrate the ability of Hsp31 to prevent prion aggregation *in vivo* and *in vitro*. Our results indicate that Hsp31 inhibits prion assembly before the formation of visible subcellular YFP-tagged PrD aggregates and those detected by SDD-AGE (Figure 2.7, Figure 2.9). Furthermore, the Sup35 aggregates occlude Hsp31, indicating that the anti-aggregation activity of Hsp31 commences prior to the formation of the visible aggregate and probably does not act to remove or disassemble any preformed aggregates (Figure 2.8). This is in contrast to large chaperones, Hsp104, Ssa1/2, Sis1 and Sse1, which mutually co-localize with prion aggregates (325). A previous study has demonstrated that small HSPs can inhibit

formation of Sup35 aggregates and found that Hsp26 and Hsp42 inhibit rare transient oligomers at distinctly different steps in the prion formation process (53). Further studies are done to determine Hsp31 role in inhibiting prion aggregation. These results are listed in Chapter 3. Overall, we demonstrate that Hsp31 can inhibit oligomerization or aggregation of α-syn and Sup35 by intervening early in the process.

2.5.5 Yeast purified MORF-Hsp31 is more potent than recombinant Hsp31 or DJ-1

Intriguingly, Hsp31 purified directly from a yeast expression system, the *GAL* promoter induced movable ORF tag system (MORF) (319), had increased enzymatic activity compared to Hsp31 purified from recombinant *E. coli* (Figure 2.3). We also demonstrated that the yeast-purified protein was more active in preventing aggregation of several substrate proteins including α-syn. The increased activity may be due to the difference in the affinity tags used or fusion tag orientation, that has been previously observed for *E coli* Hsp31 (256,271) but, it may be a result of posttranslational modification(s) that occur in the cell. Several reports have indicated that post-translational modifications or differing levels of oxidation of the cysteine residue can alter activity of DJ-1 (297,326). We also show that Hsp31 is a more potent methylglyoxalase compared to DJ-1 consistent with several other studies (Figure 2.3) (260,261). In addition, we have shown that yeast Hsp31 is more active in preventing protein aggregation compared to DJ-1. Interestingly, it has also been observed that Hsp31 rescues α-syn and Huntingtin's toxicity to a greater extent than DJ-1 *in vivo* (106,299). These results raise the intriguing possibility that Hsp31 is constitutively active whereas DJ-1 must undergo an activation event to increase its activity.

2.6 Conclusion and future directions

Recent studies have demonstrated the facility of yeast to investigate pathogenic mechanisms underlying α-syn toxicity including the identification of novel biological pathways that impinge on α-syn biology and small molecule modulators of α-syn toxicity (314,327). In addition, the action of Hsp31 on α-syn may provide insight into the mode of toxicity of α-syn because recent evidence suggests that the α-syn toxic species is smaller than the visible aggregate (314).

Our results together with other recent findings demonstrate the multitasking ability of Hsp31, which is particularly important during stressful situations. It functions as a stress response chaperone, glutathione independent methylglyoxalase, has a role in the autophagy pathway and acts as a deglycase. Other possible functions have been observed for this superfamily including a report of RNA binding for DJ-1 and protease activity for other family members (328-330). These multiple functions can modulate the protein misfolding and stress pathways at various points in the cellular network but our results also highlight that Hsp31 has the ability to inhibit protein aggregation distinct of its enzymatic activity (Figure 2.12). We believe that Hsp31 acts at the initial phases of protein misfolding process and prevents the formation of larger aggregates but does not possess disaggregase activity.

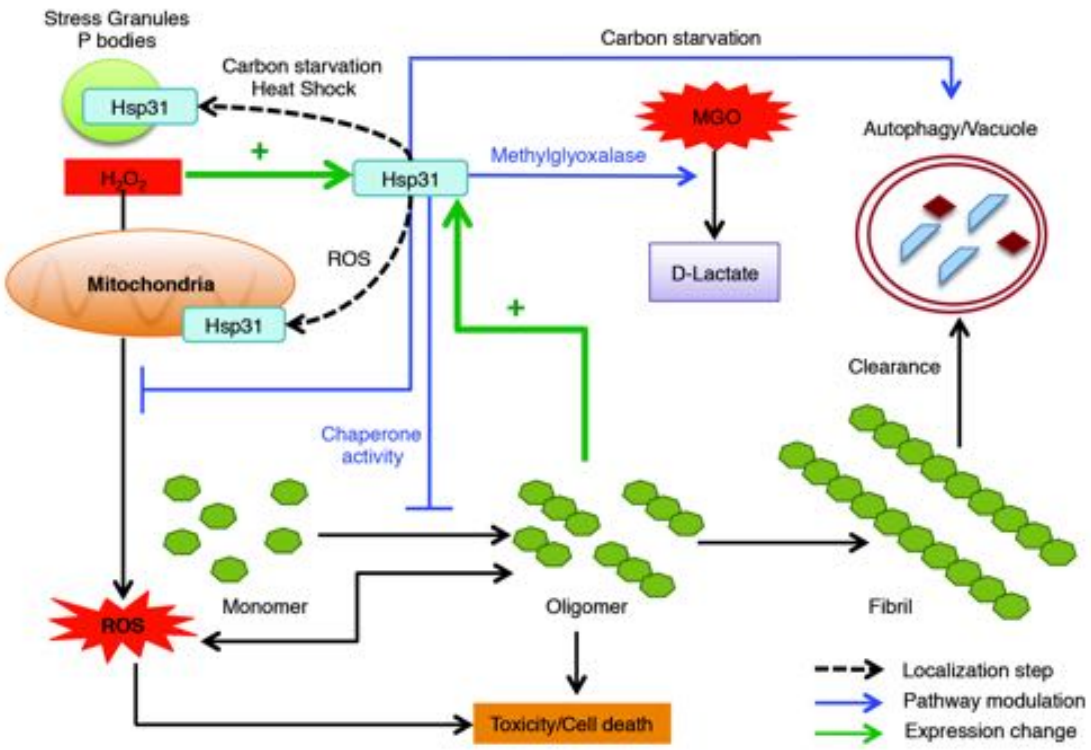

Figure 2.12 The homeostatic functions of Hsp31 associated with protecting cells from stress.

Hsp31 is a methylglyoxalase that converts MGO into D-lactate independent of glutathione. Proteotoxic stress induced the expression of Hsp31, which exerts a protective function against toxic effect of oligomers in yeast cells. Oxidative stress induces the expression of Hsp31, re-localizes it to mitochondria resulting in reduced levels of ROS. Response to other stresses leads to Hsp31 localization to P bodies and stress granules. *HSP31* deletion under carbon starvation compromises the autophagy pathway, which is a pathway used to clear oligomerized or aggregated proteins. Despite the role of Hsp31 in autophagy, it has a protective effect against α-syn oligomerization independent of its role in autophagy because of its inhibitory effect early in the oligomerization process.

We have established a framework that extends the yeast model for investigating mechanisms of α-syn toxicity in the context of the DJ-1/ThiJ/PfpI superfamily in yeast. Extension of this work will assist elucidating the chaperone-like mechanisms of Hsp31, and a comparison with DJ-1 may provide evolutionary insights into the activities of the DJ-1/PfpI/ThiJ superfamily family. Our model may also be used to further delineate the nature of oligomeric species in the pathogenesis of PD and possibly what species of α-syn should be targeted therapeutically.

Given the apparent functional diversity of Hsp31 revealed so far, it is likely that there might be other chaperone dependent and independent functions of this protein that may exist. Many HSPs work in collaboration with other chaperone in order to be fully active. The exploration and identification of protein-protein interaction partners of Hsp31 would provide insight on mechanism and roles of Hsp31. There is s dearth of protein-protein interaction information for Hsp31 although it was reported to interact with other chaperones according to a large-scale proteomic study (28). Deletion of *HSP31* down-regulates the Ssa3, a Hsp70 paralog, mRNA level at stationary phase suggesting a correlation between Hsp31 and Hsp70 activity (114). Human homolog DJ-1 is known to interact with many chaperones including Hsp70 and mitochondrial Hsp70 indicating that translocation of DJ-1 to mitochondria depends on these chaperones (304). A distinct possibility is that relocation of Hsp31 to mitochondria, P bodies or stress granules under oxidative stress is dependent on interactions with other chaperones. Our data support that Hsp31 acts at early stages of protein aggregation do not delineate the stage of intervention and therefore further investigation is needed. Hsp31 may interact with

unfolded monomers to sequester them from progressing to oligomers or alternatively, it might become active only after smaller oligomers are formed.

CHAPTER 3. THE SMALL HEAT SHOCK PROTEIN HSP31 COOPERATES WITH HSP104 TO MODULATE THE SUP35 PRION

3.1 Abstract

The yeast homolog of DJ-1, Hsp31, is a multifunctional protein that is involved in several cellular pathways including detoxification of the toxic metabolite MGO and as a protein deglycase. Prior studies ascribed Hsp31 as a molecular chaperone that can inhibit α-syn aggregation *in vitro* and alleviate its toxicity *in vivo*. It was also shown that Hsp31 inhibits Sup35 aggregate formation in yeast. However, it is unknown if Hsp31 can modulate [*PSI*$^+$] phenotype and Sup35 prionogenesis. Other small heat shock proteins (sHSPs), Hsp26 and Hsp42 are known to be a part of a synergistic proteostasis network that inhibits Sup35 prion formation and promotes its disaggregation. Here, we establish that Hsp31 inhibits Sup35 [*PSI*$^+$] prion formation in collaboration with a well-known disaggregase, Hsp104. Hsp31 transiently prevents prion induction but does not suppress induction upon prolonged expression of Sup35 indicating that Hsp31 can be overcome by larger aggregates. In addition, elevated levels of Hsp31 do not cure [*PSI*$^+$] strains indicating that Hsp31 cannot intervene in a pre-existing prion oligomerization cycle. However, Hsp31 can modulate prion status in cooperation with Hsp104 because it inhibits Sup35 aggregate formation and potentiates [*PSI*$^+$] prion curing upon overexpression of Hsp104. The absence of Hsp31 reduces [*PSI*$^+$] prion curing by Hsp104 without influencing its ability to rescue cellular thermotolerance. Hsp31 did not synergize

with Hsp42 to modulate the [*PSI*$^{+}$] phenotype suggesting that both proteins act on similar stages of the prion cycle. We also showed that Hsp31 physically interacts with Hsp104 and together they prevent Sup35 prion toxicity to greater extent than if they were expressed individually. These results elucidate a mechanism for Hsp31 on prion modulation that suggest it acts at a distinct step early in the Sup35 aggregation process that is different from Hsp104. This is the first demonstration of the modulation of [*PSI*$^{+}$] status by the chaperone action of Hsp31. The delineation of Hsp31's role in the chaperone cycle has implications for understanding the role of the DJ-1 superfamily in controlling misfolded proteins in neurodegenerative disease.

3.2 Introduction

Amyloids are highly ordered cross β-sheet protein polymers that are associated with a broad range of neurodegenerative diseases including PD, AD, HD and Prion diseases (16,331). Growth of amyloids occurs by the nucleated polymerization of soluble proteins of a particular sequence (69,332). Many proteins can polymerize to form amyloid when provided an appropriate environment *in vitro*, indicating this as inherent characteristic of polypeptides. Indeed, many recent studies have shown the existence of beneficial amyloids that are important for survival of a host organism (185). Furthermore, the highly rigid structure of self-propagating amyloids provides a possible tool in designing a unique nanomaterial (333). Therefore, it is important to study the process of amyloid formation as well as its modulation.

The budding yeast *Saccharomyces cerevisiae* provides a useful model to understand the formation, modulation and disaggregation of amyloids including prions (182). One of the most extensively studied yeast prions is the translation termination factor Sup35, which

has the normal function of releasing polypeptide chains from the ribosome upon encountering a stop codon. The prion form of Sup35 involves a self-perpetuating conformational change that results in stop codon suppression and translational read-through (180). This termination defect can be visualized easily *in vivo* by nonsense suppression of a designed premature stop codon in a gene that affects colony color, thus providing a convenient phenotypic assay to monitor [*PSI*$^+$] prion (180).

The propagation of [*PSI*$^+$] prion in yeast is rigorously controlled by molecular chaperone machinery including, Hsp104, Hsp70, Hsp40 and their co-chaperones (40,232,334). Hsp104 is a member of AAA+ ATPase superfamily and its expression is induced under stress to facilitate refolding and dissociation of protein aggregates (228,335). A moderate level of Hsp104 is required for [*PSI*$^+$] prion propagation as overproduction or deletion of Hsp104 cures the [*PSI*$^+$] prion in yeast (45,222). Since Hsp104 disaggregates the misfolded protein after heat shock, it is postulated that Hsp104 generates “propagons” by fragmenting the prion polymers that are available for further polymerization and therefore maintain the prion propagation (182). Another model proposes that elevated levels of Hsp104 cure [*PSI*$^+$] prion by dissolution of the prion seeds. The evidence for this model came from the observation of the diffuse expression of Sup35 tagged with GFP when Hsp104 was overexpressed in [*PSI*$^+$] cells, (229) and a large fraction of soluble Sup35 was observed in the cell lysate of [*PSI*$^+$] with excess of Hsp104 expression (187). Recent studies also suggests that dissolution of prion seed might be due to trimming activity of Hsp104 in which Sup35 dissociates from the end of the prion seed thus reduces its size without generating new seeds (223,233). Trimming activity of Hsp104 is still present even when severing activity is inhibited by treatment with

guanidine (233). Hsp104 collaborates with Hsp70 and Hsp40 families in dissolution of heat-damaged proteins as well as prion propagation (38,39,225,227,336,337). Interestingly, different Hsp70 homologues have opposing effects on [*PSI*$^{+}$] in which the Ssa proteins antagonize while the Ssb proteins potentiate [*PSI*$^{+}$] curing by elevated levels of Hsp104 (40,224,238). Deletion of co-chaperones of Hsp70/90, such as Sti1 or Cpr7, also inhibit [*PSI*$^{+}$] curing by Hsp104 overexpression (40).

In addition to Hsp104 and its assistant chaperones, sHSPs such as Hsp31, Hsp26 and Hsp42 also play a role in disaggregation of misfolded proteins in yeast (53,240,242,243,262,299,338). These proteins are highly expressed under moderate stress and during late growth phase for transition to stationary phase (262,294). Hsp42 and Hsp26 work synergistically to inhibit prion formation and potentiate dissolution of Sup35 prion aggregates by distinct mechanisms (53). Furthermore, Hsp26 or Hsp42 collaborate with Hsp70 and or Hsp104 to reduce the SDS-resistant polyglutamine aggregation (234,243). Hsp31 inhibits the formation of α-syn aggregates *in vitro* and toxicity *in vivo* (106,158). It was also demonstrated that Hsp31 inhibits Sup35 aggregation formation in yeast (158) However, it is unknown whether Hsp31 interferes with [*PSI*$^{+}$] prion induction and propagation and if like other sHSPs it can coordinate with Hsp104.

In the present study, we aimed to explore the role of Hsp31 in prion propagation and induction using [*PSI*$^{+}$] prion model. We investigated the ability of Hsp31 to inhibit Sup35 prion aggregation and induction by overexpression of the prion-forming domain (PrD) in [*psi*$^{-}$] strain. In this study we have delineated the collaboration between Hsp31 and Hsp104 on [*PSI*$^{+}$] prion curing and prion associated toxicity. These results are the

first evidence that Hsp31 acts as a chaperone protein that coordinates with Hsp104 to rescue cells from prion toxicity.

3.3 Results

3.3.1 Hsp31 antagonizes the Sup35 aggregation formation in [*psi⁻ PIN⁺*] strain background.

We previously reported that Hsp31 has chaperone activity against Sup35 aggregates when tested in the wild-type (WT) W303 yeast strain. In this study, we validated the ability of Hsp31 to inhibit Sup35 fibril formation in the [*psi⁻ PIN⁺*] strain background. [*PIN⁺*], an epigenetic element, is required to induce [*PSI⁺*] formation spontaneously or by overexpression of Sup35 or its PrD (181). The presence of [*PIN⁺*] is necessary at early stages of prion formation but is not needed for maintenance and propagation of [*PSI⁺*] (182). We overexpressed Hsp31-DsRed under the *GPD* promoter concomitantly with PrD-Sup35-EYFP under *GAL* expression in a [*psi⁻ PIN⁺*] strain. When examined by confocal microscopy, PrD-Sup35 fluorescent foci were greatly reduced in cells co-expressing pAG415-*GPD-HSP31*-DsRed and pAG424-*GAL*-PrD- Sup35-EYFP as compared to empty vector control (Figure 3.1 A-B). We further confirmed reduced foci formation by measuring fluorescence intensity using flow cytometry and obtained similar results as fluorescence microscopy (Figure 3.1C). We have previously observed and established that Sup35 aggregates are associated with increased fluorescence and can be quantified using flow cytometry (158). Finally, we performed semi-denaturing detergent agarose electrophoresis (SDD-AGE) to determine the level of SDS-resistant aggregate forms. Consistent with the previous results, elevated Hsp31 greatly reduced the level of Sup35 aggregates as measured by SDD-AGE but did not greatly reduce the overall

steady-state level of Sup35 in SDS-PAGE (Figure 3.1D). These results show that Hsp31 can prevent *de novo* [*PSI*$^{+}$] aggregate formation in the presence of the [*PIN*$^{+}$] genetic element.

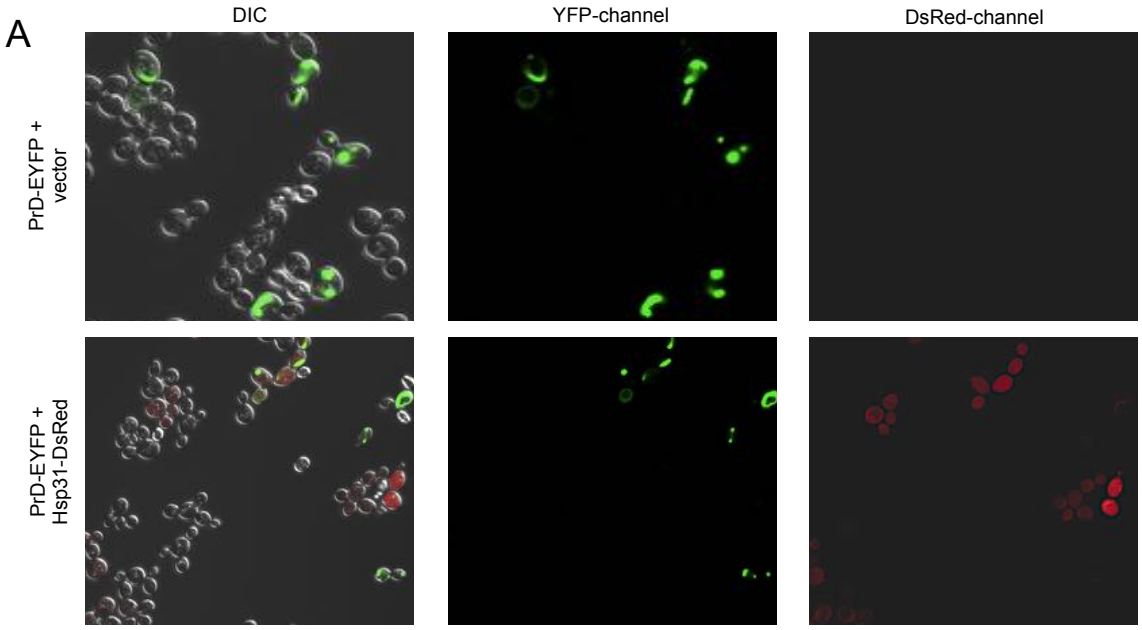
A
DIC
YFP-channel
DsRed-channel
PrD-EYFP + vector
PrD-EYFP + Hsp31-DsRed

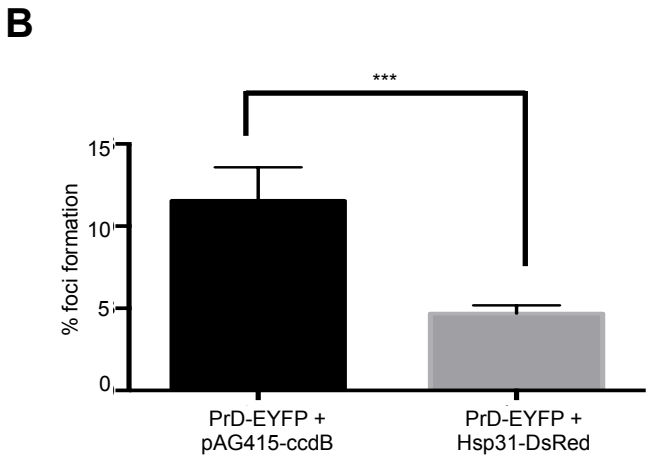
B
***
% foci formation
15
10
5
0
PrD-EYFP + pAG415-ccdB
PrD-EYFP + Hsp31-DsRed

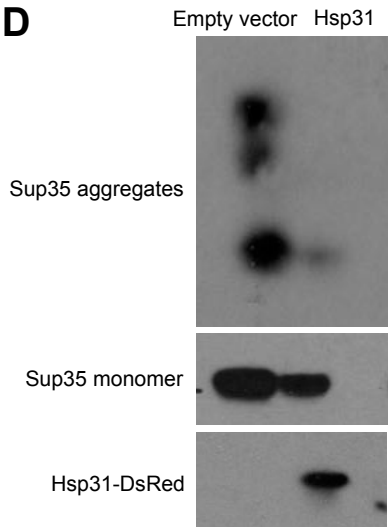
D
Empty vector
Hsp31
Sup35 aggregates
Sup35 monomer
Hsp31-DsRed

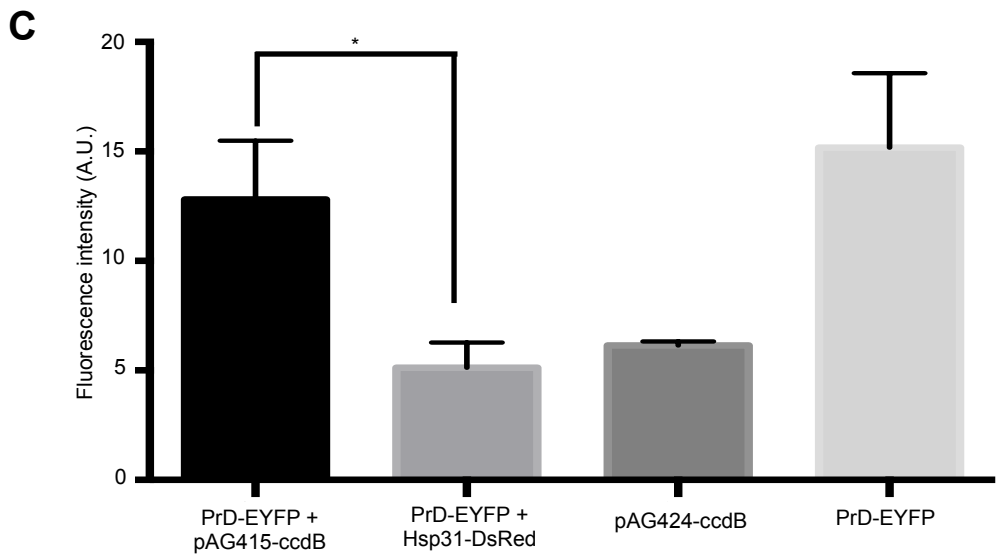

Figure 3.1. Hsp31 overexpression decreases the level of PrD-Sup35 aggregates.

(A) *GAL*-driven PrD-Sup35-EYFP was overexpressed for 24 h at 30 °C in [*psi*$^-$ *PIN*$^+$] cells with or without overexpression of DsRed tagged Hsp31. PrD-Sup35-EYFP aggregates appeared as ribbon-like vacuolar peripheral rings. Hsp31 remains cytoplasmically diffuse in these cells. Elevated levels of Hsp31 decreased the presence of Sup35 aggregates in individual cells. **(B)** Quantitation of the number of cells with one or more Sup35-EYFP foci. The average of at least three independent experiments was plotted; error bars represent mean ±SEM. (*** unpaired Student's t-test; $p \leq 0.001$). **(C)** Quantitation of the level of Sup35-EYFP fluorescence aggregates using flow cytometry. Aggregates are associated with higher fluorescence. Elevated levels of Hsp31 lowered the median fluorescence intensity (FI – arbitrary units) of Sup35-EYFP compared to empty vector control. Values represent mean ±SEM of three independent biological replicates (* unpaired Student's t-test; $p \leq 0.01$). **(D)** Cellular lysate of cells describe in A and B was analyzed by semi-denaturing agarose electrophoresis and SDS-PAGE. Overexpression of Hsp31 suppresses the level of SDS-resistant Sup35 aggregates as detected with anti-GFP antibody. Lower panel shows the expression of Hsp31 detected by anti-DsRed antibody.

3.3.2 Hsp31 transiently inhibits Sup35 prion induction *in vivo*

The ability of Hsp31 to inhibit Sup35 aggregation in the [*psi*$^-$ *PIN*$^+$] background led us to investigate its ability to inhibit [*PSI*$^+$] induction. Spontaneous *de novo* [*PSI*$^+$] induction frequency is extremely low unless Sup35 or its PrD is overexpressed (180,189). This system is widely used to investigate the process of prion induction in yeast. To determine whether Hsp31 can inhibit prion induction we used a [*psi*$^-$ *PIN*$^+$] strain that forms red color colonies on ¼ YPD plates with limited adenine. This strain forms white colonies in the presence of [*PSI*$^+$] because soluble Sup35 is depleted by aggregate formation resulting in suppression of a premature stop codon and restoration of adenine prototrophy. We observed that overexpression of Hsp31 antagonized [*PSI*$^+$] prion induction triggered by overexpression of Sup35 PrD for 6 h (Figure 3.2A-B). However, when Sup35 PrD was expressed for 12 or 24 h, the [*PSI*$^+$] prion induction rate between empty vector and Hsp31 was statistically similar (Figure 3.2C). These findings suggested that Hsp31 antagonizes prion induction transiently but can be overcome by excess production of PrD or cannot intervene when cells have established a full and more mature prion cycle. These results are consistent with our previous proposal that Hsp31 intervenes early in the protein misfolding processes (158,339).

A

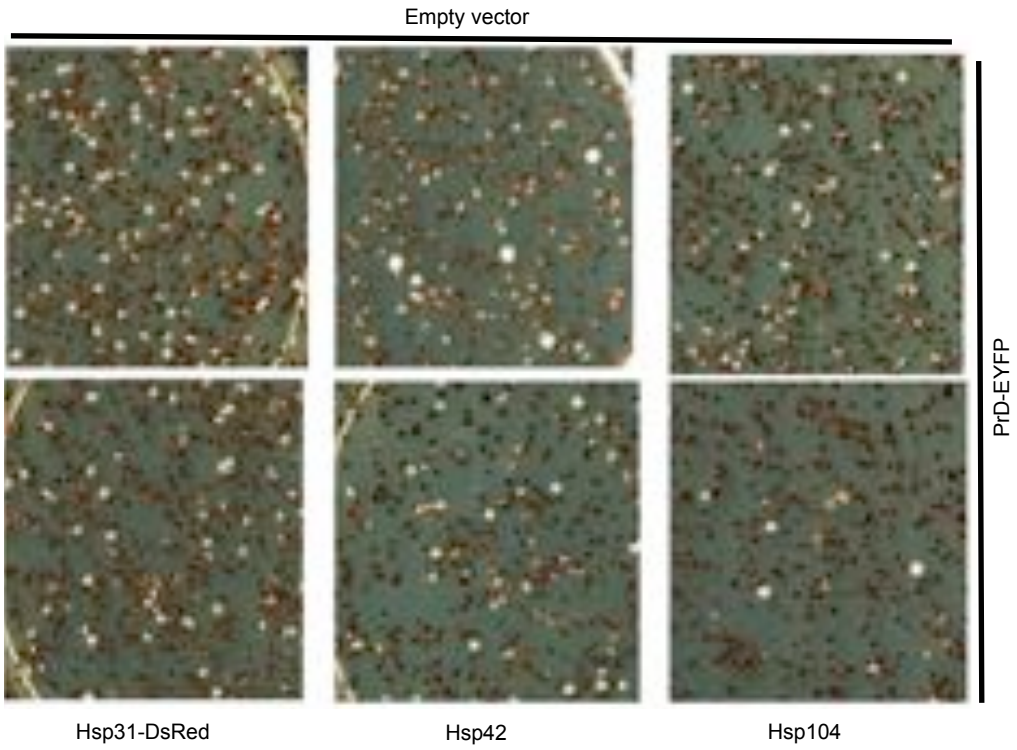
Empty vector
PrD-EYFP
Hsp31-DsRed
Hsp42
Hsp104

B

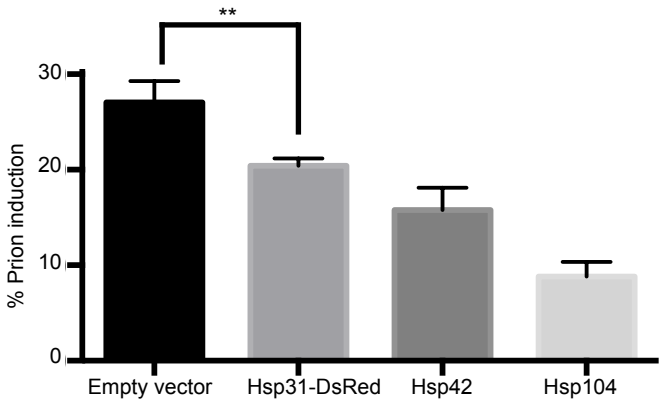
**
% Prion induction
30
20
10
0
Empty vector
Hsp31-DsRed
Hsp42
Hsp104

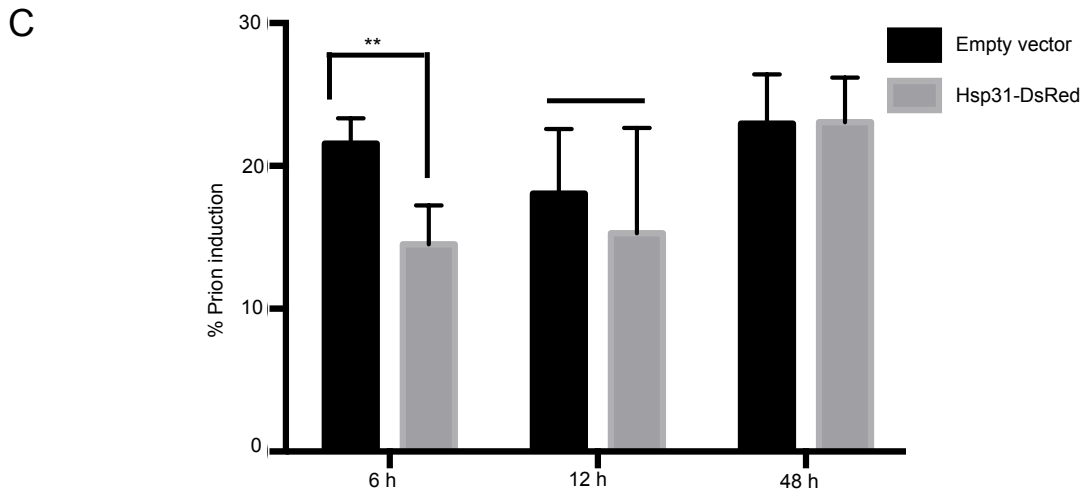

Figure 3.2. Hsp31 transiently inhibits Sup35 prion induction.

(A) To induce prion formation, a *GAL*-driven vector expressing PrD-Sup35-EYFP was expressed in the [*psi*$^{-}$ *PIN*$^{+}$] strain containing the ade1-14 nonsense mutation. Constitutive expression of Hsp31 was driven by the *GPD* promoter and [*PSI*$^{+}$] formation was scored by quantifying white color colonies on ¼ YPD plates. Plates were grown for 2-3 days at 30 °C and incubated at 4 °C for increased color development. Plasmids expressing Hsp42 and Hsp104 were added as positive controls. **(B)** PrD-Sup35-EYFP was expressed for 6 h to transiently induce prion formation. Hsp31 overexpression decreased the prion induction rate. Error bars represent ±SEM (** unpaired Student's t-test; p≤0.001, n=3). **(C)** Time course of prion formation by pAG424-*GAL*-PrD-Sup35-EYFP with varied expression times in the presence of *GPD*-Hsp31. Error bars represent mean ±SEM (** unpaired Student's t-test; p≤0.001, n=3) ns= not significant. All experiments in this figure were biological replicates.

3.3.3 [*PSI*$^+$] prion state is not affected by Hsp31 overexpression or deletion

Transient overexpression of sHSPs such as Hsp26 and Hsp42 cure the [*PSI*$^+$] prion, converting white colonies of [*PSI*$^+$] into red colonies of [*psi*$^-$] on ¼ YPD plates with limited adenine (53). First, we tested if overexpression of Hsp31 can cure the [*PSI*$^+$] prion. Despite the fact that Hsp31 can prevent *de novo* prion aggregate formation *in vivo* as detected by SDD-AGE (Figure 3.1), overexpression of Hsp31 is not sufficient to cure the [*PSI*$^+$] prion phenotype (Figure 3.3A). In addition, Hsp42 was used as a control and was able to cure [*PSI*$^+$] as previously reported (53). However, we found that Hsp26 overexpression using the identical plasmid vector from Duennwald et al. (53) could not cure [*PSI*$^+$] in this strain and under these experimental conditions. Our results are more consistent with Wickner and colleagues (340) who reported lack of prion curing by Hsp26 for both [Ure3-1] and [*PSI*$^+$] phenotypes, which could be explained by differences in strain genotypes and experimental conditions (340). We tested different plasmid systems to express Hsp31 including the *GPD* and *GAL* promoters and none of them were able to modulate the [*PSI*$^+$] prion phenotype (data not shown). Next, we determined if deletion of *HSP31* influences the [*PSI*$^+$] prion status. We constructed a [*PSI*$^+$ *PIN*$^+$] *hsp31Δ* strain carrying the reporter nonsense allele *ade1-14*, so that the Sup35 read-through caused by [*PSI*$^+$] presence could be detected by development of white colonies. The phenotype of the [*PSI*$^+$] prion was similar in the *hsp31Δ* strain compared to WT with no change in colony color (Figure 3.3B), suggesting that Hsp31 cannot intervene in an established prion cycle.

3.3.4 Hsp31 deletion impairs [*PSI*$^+$] prion curing by Hsp104 overexpression

A moderate level of Hsp104 is required for maintenance of [*PSI*$^+$]; either deletion or overexpression of Hsp104 cures the [*PSI*$^+$] prion. Numerous chaperones such as Hsp70, Hsp40 and Hsp90 along with its co-chaperones Sti1 and Cpr7 are known to modulate prion curing by Hsp104 (39,40). To determine if Hsp31 altered Hsp104-mediated [*PSI*$^+$] prion curing, we transformed WT [*PSI*$^+$] or *hsp31Δ* [*PSI*$^+$] cells with p426-*GPD*-Hsp104 (low level of overexpression), pAG425-*GAL*-Hsp104-DsRed (medium overexpression) or p2HG-Hsp104 (high overexpression *GPD*) plasmids (Figure 3.3C-E). The varied overexpression level of Hsp104 under these different plasmid systems was confirmed by western blotting (Figure 3.3F). The rate of [*PSI*$^+$] prion curing was correlated to the level of Hsp104 expression in WT [*PSI*$^+$] cells. The rate of [*PSI*$^+$] prion curing was significantly reduced in *hsp31Δ* [*PSI*$^+$] under the lowest overexpression condition of *GPD*-Hsp104 (2% compared to 7% in WT) (Figure 3.3C). Under high overexpression of Hsp104, a 100% curing rate was observed in the presence of *HSP31* but the *hsp31Δ* strain never achieved 100% curing rates and clearly white colonies were observed at 3% frequency (Figure 3.3D). Induction of the *GAL*-Hsp104-DsRed construct for varied time points from 2 h to 72 h also showed consistently less efficient prion curing by the *hsp31Δ* strain (Figure 3.3E). The decreased prion curing in the *hsp31Δ* [*PSI*$^+$] strain background was not due to decreased Hsp104 expression because we observed a similar expression level compared to WT (Figure 3.5B). These results demonstrate the presence of Hsp31 is required for optimal prion curing efficiency at varied Hsp104 expression conditions.

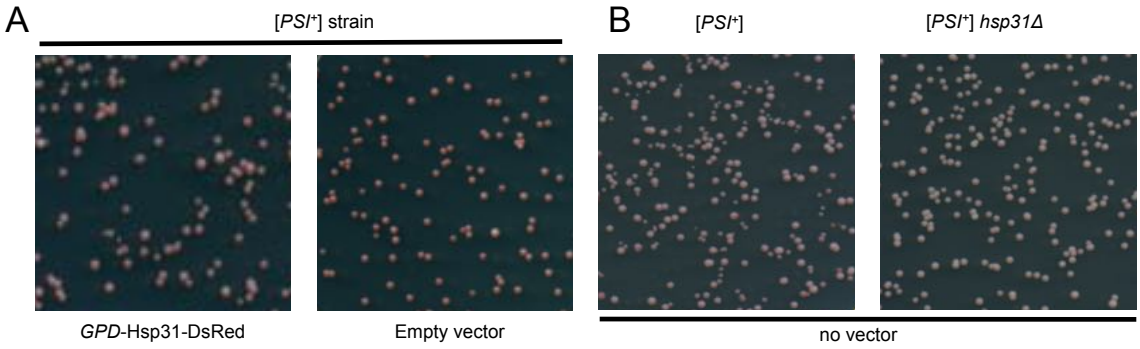
A
[PSI+] strain
GPD-Hsp31-DsRed
Empty vector
B
[PSI+]
[PSI+] hsp31Δ
no vector

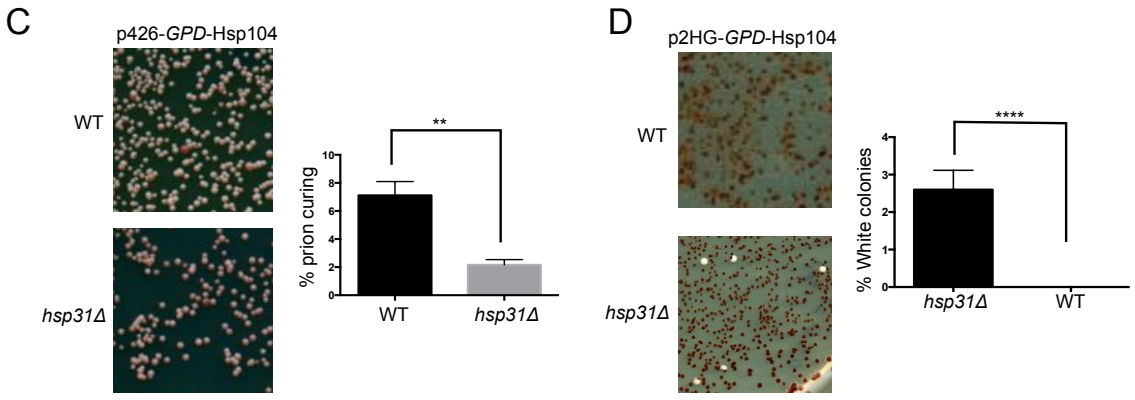
C
p426-GPD-Hsp104
WT
hsp31Δ
% prion curing
**
WT
hsp31Δ
D
p2HG-GPD-Hsp104
WT
hsp31Δ
% White colonies
****
hsp31Δ
WT

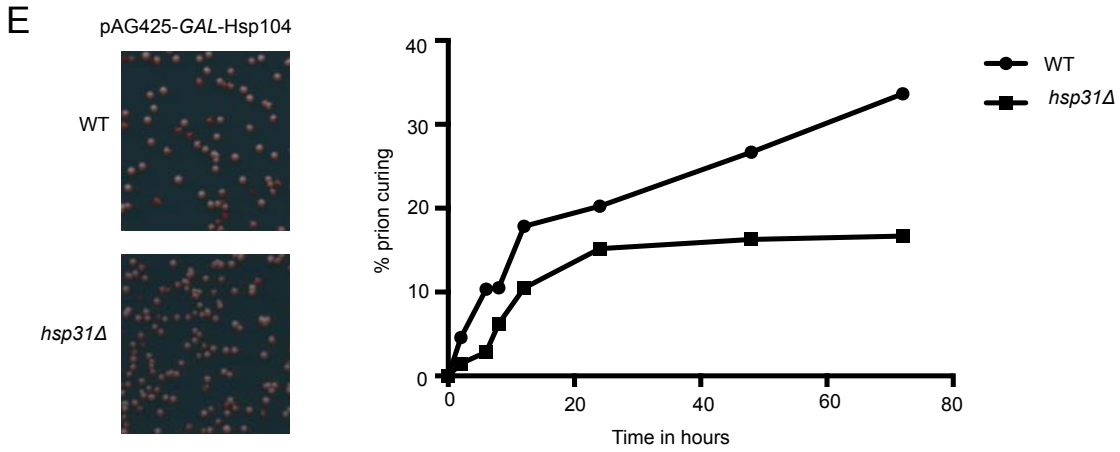
E
pAG425-GAL-Hsp104
WT
hsp31Δ
% prion curing
Time in hours
WT
hsp31Δ

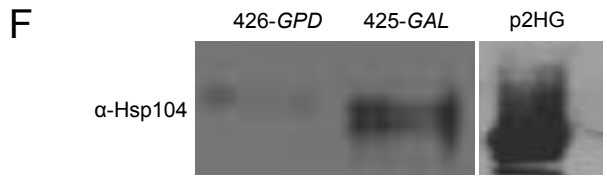

Figure 3.3. Hsp31 is required for optimal Hsp104-induced curing of the [PSI+] phenotype

(A) To determine the effect of Hsp31 on [*PSI*$^{+}$] prion curing, the WT and *hsp31Δ* [*PSI*$^{+}$] strains harboring the *GPD*-Hsp31 expression vector (pAG415-*GPD*-Hsp31-DsRed) or the empty vector (pAG415-*GPD*-ccdB-DsRed) were grown for 12 h at 30 °C before plating on ¼ YPD plates. **(B)** The WT and *hsp31Δ* [*PSI*$^{+}$] strains with no vector were also grown and treated in the same way. Plates were grown for 2-3 days at 30 °C and transferred at 4 °C for increased color development. No difference in colony color was observed in these strains. **(C)** Low-level overexpression of Hsp104 was used to induce prion curing in [*PSI*$^{+}$] *hsp31Δ* and WT strains. Cells were grown in liquid media for 12 h at 30 °C before plating on ¼ YPD plates. Significantly less prion curing was observed in the [*PSI*$^{+}$] *hsp31Δ* strain (**unpaired Student's t-test; $p \leq 0.001$, n=3). **(D)** High-level overexpression of Hsp104 was used to induce prion curing in [*PSI*$^{+}$] *hsp31Δ* and WT strains. A 100% curing rate was observed in WT strain. In the [*PSI*$^{+}$] *hsp31Δ* strain, 100% curing was never achieved. White color colonies were plotted for the WT and [*PSI*$^{+}$] *hsp31Δ* strain (****unpaired Student's t-test; $p \leq 0.0001$, n=3 biological replicates). **(E)** Hsp104 expression under the *GAL* promoter for 2 to 72 h in WT and [*PSI*$^{+}$] *hsp31Δ* strain. At each indicated time point, cells were plated on ¼ YPD plates. Percentage of prion curing was calculated at each point for both WT and [*PSI*$^{+}$] *hsp31Δ* strain. The plotted graph is one representation of three independent biological repeats. (unpaired Student's t-test; $p \leq 0.001$ at 24, 48 and 72 h; n=3). **(F)** Western blot demonstrating the relative expression levels of Hsp104.

3.3.5 Hsp31 collaborates with Hsp104 to cure [*PSI*$^+$] prion

The decreased efficiency in Hsp104 curing [*PSI*$^+$] in the absence of Hsp31 lead us to further explore the relationship between these two chaperones. Small HSPs Hsp26 and Hsp42 are known to collaborate with Hsp104 in rescuing the polyglutamine toxicity and solubilization of amyloid aggregates (243). We aimed to test the effect of expressing Hsp31 and Hsp104 together in curing of the [*PSI*$^+$] prion. Expression of Hsp104 (p426-*GPD*-Hsp104) in the [*PSI*$^+$] strain resulted in a curing rate of 3 % that is lower than the rate in Figure 3.3 because the co-existence of two different constructs decreases plasmid copy numbers and affects expression levels. Co-expression of Hsp31 and Hsp104 increased the rate of prion curing to 6 % compared to the respective controls (Figure 3.4A-B). We also tested the collaboration between Hsp104 and Hsp31 in the *hsp31Δ* strain and detected that co-expression of Hsp104 with Hsp31 was able to cure the [*PSI*$^+$] prion to a greater extent than individual chaperone expression (Figure 3.4C-D). These results corroborate the inefficient curing in *hsp31Δ* and establish that Hsp31 is required for optimal Hsp104 activity.

Previously, it was shown that sHSP, Hsp42, collaborates with Hsp26 to prevent [*PSI*$^+$] prionogenesis by distinct and synergistic mechanisms with Hsp104 (53), hence we tested the interaction between Hsp42 and Hsp31 on [*PSI*$^+$] prion curing. Elevated levels of Hsp42 driven by the *GPD* promoter was sufficient to increase curing of [*PSI*$^+$] in this strain transformed with a single plasmid (5.4% compared to 1.4%). Introduction of a second empty vector plasmid decreased the curing rate of the *GPD-HSP42* construct to background levels. We also co-expressed Hsp31 and Hsp42 in the [*PSI*$^+$] strain and did not detect any increased curing rate, in contrast to Hsp31 co-expression with Hsp104

(Figure 3.4E-F). This lack of synergy between these proteins implies that Hsp42 and Hsp31 act at a similar stage of the prion cycle.

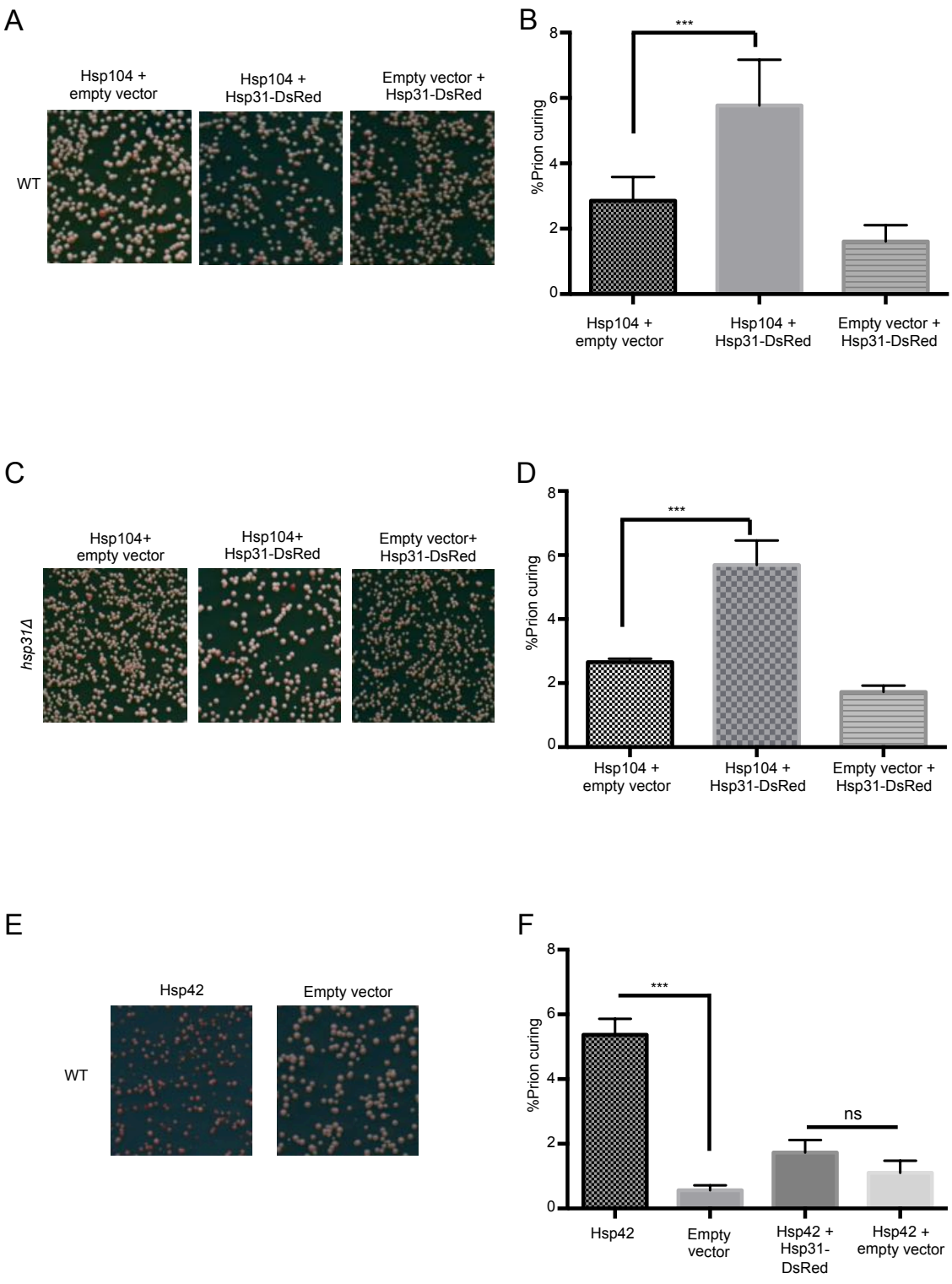
A
Hsp104 + empty vector
Hsp104 + Hsp31-DsRed
Empty vector + Hsp31-DsRed
WT
B
%Prion curing
***
Hsp104 + empty vector
Hsp104 + Hsp31-DsRed
Empty vector + Hsp31-DsRed
C
Hsp104+ empty vector
Hsp104+ Hsp31-DsRed
Empty vector+ Hsp31-DsRed
hsp31Δ
D
%Prion curing
***
Hsp104 + empty vector
Hsp104 + Hsp31-DsRed
Empty vector + Hsp31-DsRed
E
Hsp42
Empty vector
WT
F
%Prion curing
***
ns
Hsp42
Empty vector
Hsp42 + Hsp31-DsRed
Hsp42 + empty vector

Figure 3.4. Expression of Hsp31 in combination with Hsp104 increases the rate of prion curing.

(A) Hsp31 and p426-*GPD*-Hsp104 were co-transformed in the [*PSI*$^{+}$] strain. Empty vectors served as controls. **(B)** Quantification of the experiments in panel A. Prion curing rate was increased from about 2.5% to 6% when Hsp31 was co-expressed with Hsp104 compared to the control strain (*unpaired Student's t-test; $p \leq 0.001$, n=3). **(C)** [*PSI*$^{+}$] *hsp31Δ* strain harboring plasmids for Hsp104 and Hsp31. **(D)** Quantification of experiments describe in panel C. The combination of Hsp104 and Hsp31 increased the rate of prion curing in [*PSI*$^{+}$] *hsp31Δ* strain consistent with WT strain in A-B. (** One-way ANOVA; $p \leq 0.001$, n=3). **(E)** Image of p426-*GPD*-Hsp42 transformed cells demonstrating curing compared to empty vector. **(F)** Hsp31 and p426-*GPD*-Hsp42 were co-transformed in the [*PSI*$^{+}$] strain and quantified. The combination of Hsp42 and Hsp31 did not increase the curing rate (ns=not significant). Data and images shown are representative of at least three independent biological experiments for all panels.

3.3.6 Effect of [*PSI*$^+$] curing in the *hsp31Δ* strain is not due to loss of Hsp104 thermotolerance function.

A possible mechanism for the decrease in [*PSI*$^+$] prion curing by Hsp104 in the *hsp31Δ* background is decreased expression or activity of Hsp104. To measure the functional competence of Hsp104 we tested the thermotolerance activity of Hsp104 in exponentially growing cells. We induced Hsp104 expression in both strains by incubating the culture at 37 °C for 30 minute and then heat shocked at 50 °C. The survival of cells after heat shock is dependent on Hsp104 induction, and we observed the rate of survival in *hsp31Δ* was comparable to the isogenic WT [*PSI*$^+$] strain (Figure 3.5A). Moreover, the basal thermotolerance without induction of Hsp104 was not affected by deletion of Hsp31 (Figure 3.5A). In addition, we observed a slightly elevated level of Hsp104 in the *hsp31Δ* strain compared to WT, hence the expression of Hsp104 is not compromised (Figure 3.5B). Thus, reduction in [*PSI*$^+$] prion curing in the *hsp31Δ* strain is not due to general impairment of Hsp104 activity or expression.

3.3.7 Hsp104 physically interacts with Hsp31

The close collaboration between Hsp104 and Hsp31 prompted us to test the physical association between them. Co-immunoprecipitation followed by western blot analysis in yeast lysates demonstrated that Hsp31 interacts with Hsp104. Immunoprecipitation was performed using *HSP31-9myc* genomically tagged at the endogenous locus and overexpressing Hsp104 either under the *GPD* or the *GAL* promoter. First, Hsp31-9myc was pulled down using anti-myc antibody conjugated to agarose beads from exponentially growing cell lysates. Western blots confirmed the successful pull down of *Hsp31-9myc* (Figure 3.5C; middle panel). The upper panel demonstrates the successful

pull-down of Hsp104 in both *GPD-HSP104* and *GAL-HSP104* expressing lysates but not in the empty vector control (Figure 3.5C). Similar results were obtained with an alternative co-immunoprecipitation approach in which polyclonal anti-Hsp104 antibody and protein G dynabeads were used to pull down Hsp104 followed by western blot analysis with anti-myc antibody to detect Hsp31. This approach confirmed the interactions and also demonstrated that Hsp31 is pulled down with strains having endogenous levels of Hsp104 (Figure 3.5C; bottom panel empty vector lane). These results demonstrate that Hsp31 is part of same complex with Hsp104 using two different immunoprecipitation protocols and the Hsp31-Hsp104 interaction is detectable under physiological expression levels.

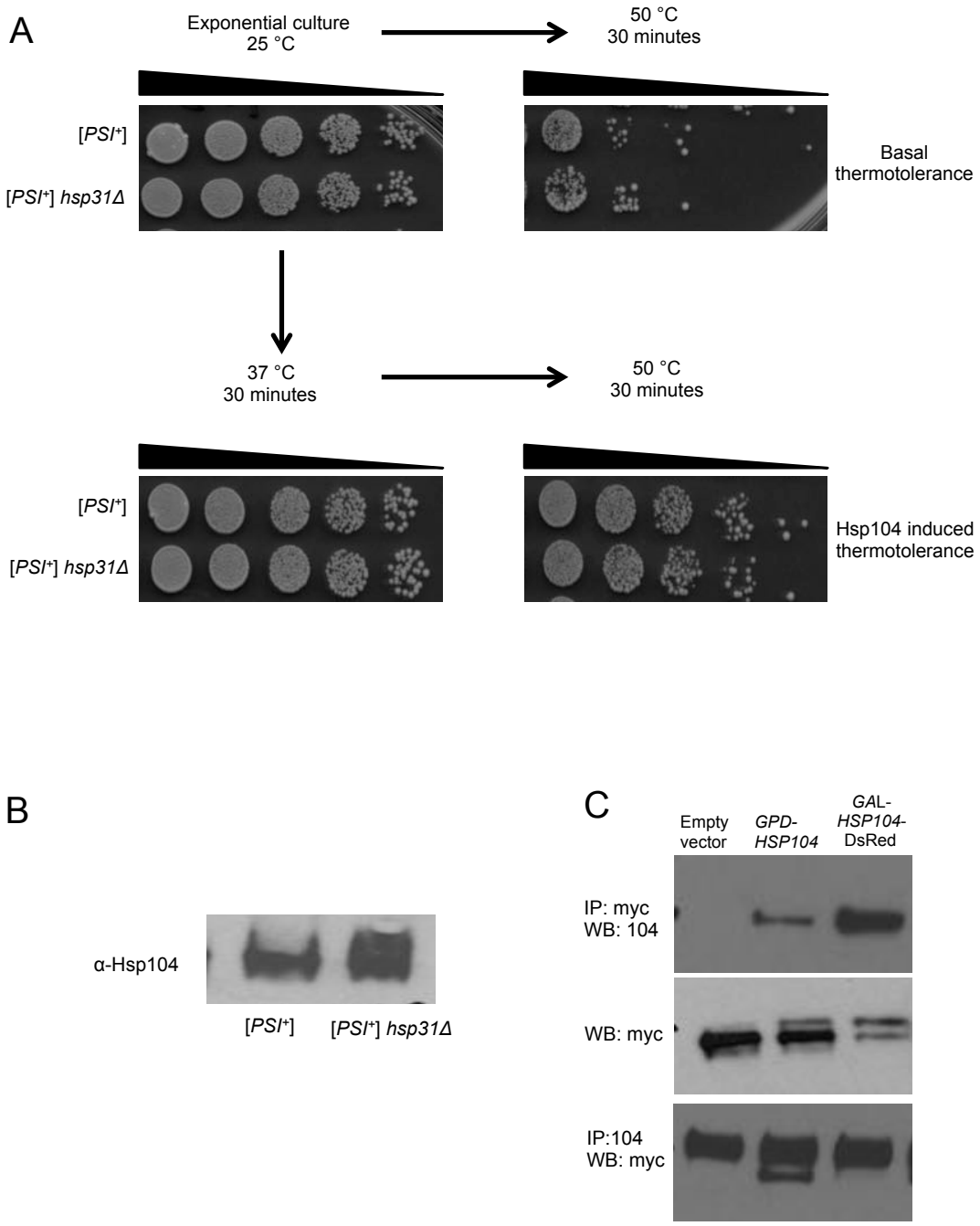

Figure 3.5. Hsp31 interacts with Hsp104 and deletion of HSP31 does not alter Hsp104's thermotolerance response.

(A) HSP31 deletion does not impair Hsp104's function in thermotolerance. Exponentially growing cells of the [*PSI*$^{+}$] *hsp31Δ* and [*PSI*$^{+}$] strain was drawn from the culture and decimal serial dilutions were plated onto YPD plates and incubated for 2 days at 30 °C in

each case. Both strains showed a comparable basal tolerance (top right image) and induced tolerance after pretreatment at 37 °C (bottom right image) for 30 min to a 50 °C heat shock treatment. Left images are non-treated cultures that serve as control. **(B)** Endogenous level of Hsp104 was determined in exponentially growing cultures of [*PSI*$^{+}$] *hsp31Δ* and [*PSI*$^{+}$] strains in YPD media using Hsp104 specific antibody. **(C)** Immunoprecipitation of Hsp31 from HSP31-9myc strain with overexpression of Hsp104 either under *GPD* or *GAL* promoter, using anti-myc antibody followed by immunoblotting with anti-Hsp104 antibody. Empty vector served as a control. Middle panel shows the successful pull down of Hsp31-9myc in all strains using anti-myc antibody. The lower panel Hsp104 was immunoprecipitated using anti-Hsp104 antibody followed by immunoblotting with anti-myc antibody.

3.3.8 Hsp31 together with Hsp104 antagonizes prion dependent toxicity of excess Sup35.

Overexpression of full length Sup35 or its PrD exhibits toxicity in the [*PSI*$^+$] strain (244,246). The toxicity of excess Sup35 in [*PSI*$^+$] or [*PSI*$^+$] *hsp31Δ* strain was investigated. Deletion of *HSP31* has no effect on Sup35 toxicity (Figure 3.6) in contrast to our previous report of increased toxicity when α-syn is expressed in the *hsp31Δ* strain background (158). However, elevated levels of Hsp31 expressed from the *GPD* promoter rescued [*PSI*$^+$] cells from Sup35 toxicity in both WT and deleted strains. As expected, Hsp104 reduce the toxicity of Sup35 to greater extent than Hsp31. Strikingly, Hsp31 together with Hsp104 strongly reduced the toxicity of Sup35 in the [*PSI*$^+$] strain (Figure 3.6). We also observed the rescue effect of sole expression of Hsp31 or Hsp104 and when expressed together in the [*PSI*$^+$] *hsp31Δ* strain. The level of rescue was not as dramatic as in the WT strains suggesting that the expression of endogenous Hsp31 has a role in reducing toxicity in conjunction with heterologous expression of Hsp31 or Hsp104. The role of endogenous Hsp31 is not clear but could be a direct effect of chaperone activity or because autophagy can be impaired in *hsp31Δ* strains (294) which may lead to increased proteotoxicity of Sup35.

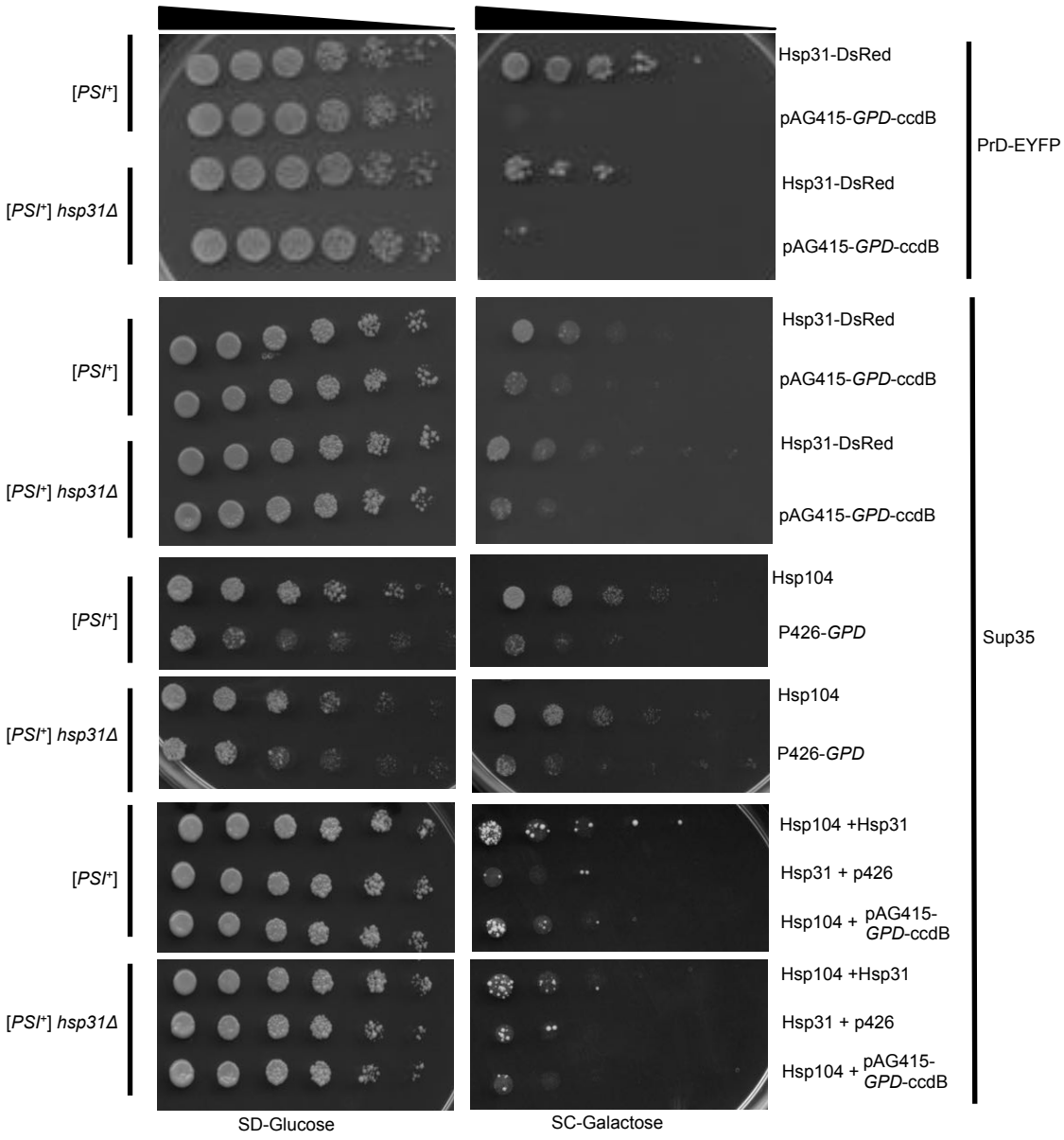

Figure 3.6. Hsp31 and Hsp104 reduce Sup35 prion toxicity.

Hsp31, Hsp104 or the indicated combination of both along with *GAL*-PrD-Sup35-EYFP or full length Sup35 were overexpressed in [*PSI*$^{+}$] and [*PSI*$^{+}$] *hsp31Δ* strains. Decimal serial dilutions were plated onto selection plates with 2% glucose that serve as control or 2% galactose to induce the expression. Plates were incubated at 30 °C for 3 days before producing the images. Hsp31 or Hsp104 rescued toxicity of *GAL*-PrD-Sup35-EYFP or full length Sup35 in these strains. Combination of Hsp31 and Hsp104 greatly reduce the toxicity compared to when they are individually expressed.

3.3.9 Hsp31 and Hsp104 modulate Sup35 aggregation in [*PSI*$^+$] cells

Collaboration of Hsp31 with Hsp104 to reduce Sup35 induced prion toxicity prompted us to investigate whether this activity correlates with protein disaggregation activity of Hsp104. To assess the state of Sup35 in [*PSI*$^+$] cells harboring Hsp31 and Hsp104, we performed sedimentation analysis to determine the ratio of Sup35 in the soluble versus aggregate forms. The individual expression of Hsp104 or Hsp31 resulted in a very strong signal in the insoluble pellet fraction. However, the combination of Hsp104 and Hsp31 markedly reduced Sup35 aggregation found in the pellet fraction and increased the amount of Sup35 found in the soluble fraction (Figure 3.7A). Soluble Sup35 was very susceptible to proteolysis during processing of the samples as evident by the lower molecular weight species, which is consistent with earlier reports (187,341). These results demonstrate that sole overexpression of Hsp31 does not appear to intervene in the established prion cycle present in a [*PSI*$^+$] strain but can inhibit aggregate formation and prionogenesis in a [*psi*$^-$] strain (Figure 3.1). However, the results also show that Hsp31 can cooperate with Hsp104 to reduce Sup35 toxicity and simultaneously increase Sup35 solubility.

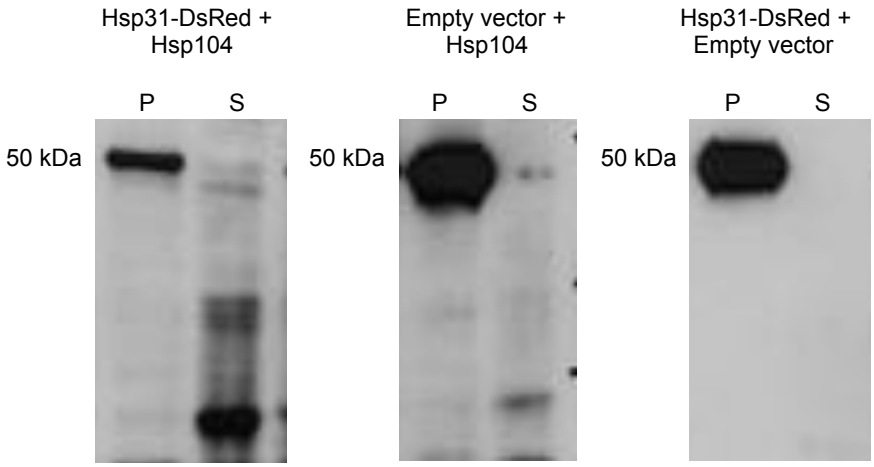

Figure 3.7. Hsp31 acts early in the prionogenesis process.

Hsp31 together with Hsp104 decrease the aggregation of Sup35 formed by overexpression of *GAL*-PrD-Sup35-EYFP. Crude lysates of cells expressing Hsp31, Hsp104 or both together were subjected to sedimentation analysis. Lysates were ultracentrifuged into P (pellet) and S (soluble) fractions and analyzed by immunoblotting using GFP-specific antibody.

3.4 Material and Methods

3.4.1 Yeast strains and plasmids

The [*psi⁻, PIN*$^{+}$] and [*PSI*$^{+}$] strains were used throughout the study for prion induction, curing and toxicity assays. The W303 *HSP31-9myc* strain was used for pull down assays. Details of the plasmid, strains and primers used in this study are provided in the tables (Table 3.1-3.3). Deletion of *HSP31* in [*PSI*$^{+}$] strain was obtained by transforming a PCR product containing the nourseothricin N- acetyl-transferase (*NAT*) gene flanked by *HSP31* homology regions. The primers consisted of 20 nucleotides for amplifying the *NAT* gene from pFA6a-*NAT*NT2 (Euroscarf), and 50 nucleotides immediately preceding the *HSP31* start codon or after the stop codon. The amplified product was integrated into [*PSI*$^{+}$] and [*psi⁻, PIN*$^{+}$] strain. Successful integration and deletion was confirmed by diagnostic PCR.

Table 3.1 List of yeast strains used in the study.

Strain	Genotype	Source/reference
[*PSI*$^+$] 74D-694	*MATa ade 1-14, his3, leu2, trp1, ura3* [*PSI*$^+$ *PIN*$^+$]	J-C. Rochet
W303-1A	*MATa can1-100 his3-11, 15 leu2-3, 112 trp1-1 ura3-1 ade2-1*	R. Rothstein
[*PSI*$^+$]-*hsp31Δ*	*W303-1A hsp31Δ::NATMX*	This study
W303-*HSP31-9myc*	*W303-1A HSP31-9myc::KANMX*	This study
[*psi*$^-$] 74D-694	74D-694 *MATa ade 1-14, his3, leu2, trp1, ura3* [*psi*$^-$ *PIN*$^+$]	J-C. Rochet

Table 3.2 List of plasmids used in the study

Plasmids	**Type of plasmid**	**Source/reference**
pAG415*GPD-HSP31*-dsRed	Yeast, CEN	This study
pAG415ccdB-dsRed	Yeast, CEN	Alberti et al.(318)
pAG424*GAL*-PrD-Sup35-EYFP	Yeast, 2 μ	Alberti et al.(180,318)
pLA1-Sup35	Yeast	J. Shorter(53)
p426-*GPD*	Yeast	J. Shorter(53)
p426-*GPD*-Hsp42	Yeast	J. Shorter(53)
p426-*GPD*-Hsp104	Yeast	J. Shorter(53)
p2HG-*GPD*-Hsp104	Yeast	J-C.Rochet
p2HG-*GPD*	Yeast	J-C.Rochet
pAG425-*GAL*-ccdB-DsRed	Yeast, 2 μ	Addgene
pAG425-*GAL*-Hsp104-DsRed	Yeast, 2 μ	This study

Table 3.3 List of primers used in the study

Gene/description	Forward	Reverse
hsp31Δ	AAGTACTTCCCACTGGC TAATTACACAGATAAAA CTCAAACAAATTTATAA TGACATGGAGGCCCAGA ATACCC	CTTACATCTATATAGTAGTACA AAGGAAATTCTAATTATCAAC CTTTGGCTCACAGTATAGCGAC CAGCATTCAC
9myc tagging of *HSP31*	TCTGCGCACTCCACTGC CGTAAGATCCATCGACG CTTTAAAAAACCGTACG CTGCAGGTCGAC	TCCTTACATCTATATAGTAGTA CAAAGGAAATTCTAATTATCA ACCTTTGGCTCAATCGATGAAT TCGAGCTCG
***HSP31* cloning**	AAACTCGAGATGGCCCC AAAAAAAGTTTTACTCG C	TTTGCTAGCTCAGTTTTTTAAA GCGTCGATGGATCTTAC
***HSP31* 9myc tag diagnostic**	ACAGAGAATTAACGTTA CTCATTCC	ATATTTGGATATTGGGGAAAC ACAT
***hsp31Δ* diagnostic**	TTCGTGGTCGTCTCGTA CTC	GCAGGGCATGCTCATGTAGA

3.4.2 Yeast growth conditions

We used isogenic [*psi*$^-$] and [*PSI*$^+$] derivatives of 74D-694 [*MAT**a***, *his3*, *leu2*, *trp1*, *ura3*; suppressible marker *ade1-14.* Cells were grown at 30 °C on synthetic dextrose medium (SD; 0.7% yeast nitrogen base, 2% glucose) with appropriate amino acid dropout mixture for selection and maintenance of the particular plasmid. Synthetic complete (SC) medium contains 2% raffinose in place of glucose and 2% galactose for induction of genes under the *GAL* promoter. ¼ YPD solid medium used in the plating assays contains 0.5% yeast extract, 2% peptone, and 2% glucose. Cultures were always maintained in actively growing conditions and OD_{600} was used to measure the growth rate.

3.4.3 SDD-AGE

The [*psi*$^-$] cells were co-transformed with pAG424-*GAL*-PrD-Sup35-EYFP and pAG415-*GPD*-HSP31-DsRed plasmids. Cultures were grown in SD media overnight and induced in SC 2% raffinose + 2% galactose media for 24 h. Prion aggregates were analyzed using SDD-AGE as described previously(158). Briefly, cells were harvested by centrifugation and spheroplasts were generated and lysed in 4 x SDS sample buffer at room temperature for 15 min before loading onto a 1.8 % agarose gel followed by transfer to nitrocellulose membrane. The membrane was immune-blotted using anti-GFP antibody (Roche; 11814460001) and anti-DsRed antibody (Santa Cruz Biotechnology; Sc-33353).

3.4.4 Fluorescence Microscopy and flow-cytometry

The [*psi*$^-$] strain was co-transformed with pAG424-*GAL*-PrD-Sup35-EYFP and pAG415-*GPD*-HSP31-DsRed. Successful transformation was selected and re-streaked on SD (-tryptophan -leucine) agar plates. Cells were grown overnight at 30 °C in SD (-tryptophan -leucine) medium and PrD-Sup35 expression was induced for 24 h in SC (-tryptophan -

leucine) medium with 2% raffinose and 2% galactose. Cells were examined under fluorescence microscopy using a Nikon A1 confocal microscope with a Nikon Plan apochromat 60 X (NA 1.4) oil immersion objective to acquire fluorescence and DIC images and were analyzed using Image J. The identical cultures used in microscopy were also subjected to flow cytometry. After induction cells were collected and washed with PBS, filtered and analyzed for EYFP fluorescence intensity using the Beckman Coulter FC500 flow cytometer with the FL-1 channel. A total of 10,000 events were acquired for each sample and data was analyzed using FlowJo software to calculate median fluorescence intensity.

3.4.5 Sup35 prion curing

Curing of [*PSI*$^{+}$] was performed by transforming the strain with plasmids, p2HG-*GPD*-Hsp104, pAG425-*GAL*-Hsp104, pAG415-*GPD*-*HSP31*-DsRed, p426-*GPD*-Hsp42 and their corresponding empty vectors. For double transformation both plasmids were co-transformed and selected on double dropout media simultaneously. Transferred cells were grown in the SD medium at 30 °C for overnight growth and plated on ¼ YPD plates which were incubated for three days at 30 °C and shifted for another day at 4 °C for colony color development. To score for curing, colonies with red color were counted as [*psi*$^{-}$]. Cultures carrying plasmid with the *GAL* promoter were grown in SC medium before plating on ¼ YPD.

3.4.6 Sup35 prion induction

For the induction experiment, at least three independent transformants with pAG424-*GAL*-PrD-Sup35-EYFP and pAG415-*GPD*-*HSP31*-DsRed plasmid were grown at 30 °C in SD medium overnight, centrifuges and washed three times with water, and shifted to

SC medium to induce prion formation. Aliquots were withdrawn at 6, 12 and 48 h and diluted to a density of 50,000 cells per 100 µl for plating onto ¼ YPD plate. The plates were then incubated for three days at 30 °C and another day at 4 °C for color development. Percentage of [*PSI*$^+$] induction was measured as the number of white ([*PSI*$^+$] colonies) colonies divided by the total number of colonies.

3.4.7 Prion toxicity assay

The [*PSI*$^+$] strain was transformed with pAL1 Sup35 and plasmids expressing Hsp31, Hsp42 and or Hsp104 along with their corresponding empty vector. After selection on SD plates, cells were grown into 5 ml of SD liquid media with 2 % glucose at 30 °C overnight. Cells were harvested and washed three times with water and a five fold serial dilution was performed with a starting OD_{600} of 0.8. Diluted samples of 5 µl were spotted onto SD and SC plates with the appropriate dropout selection. Plates were incubated at 30 °C for 3 days and imaged with a scanner.

3.4.8 Pull down assay

The *HSP31-9myc* tagged strain was transformed with plasmids pAG425-*GAL*-Hsp104 or p426-*GPD*-Hsp104. Cells lysates were prepared in a buffer (50 mM Tris–HCl, 1 mM EDTA, 5 mM DTT, 10% (v/v) glycerol, 0.5 M NaCl, at pH 7.5) with freshly added protease inhibitor cocktail (Roche). Anti-myc antibody-conjugated agarose beads were used to pull down Hsp31 protein by incubating the beads with the lysate at 4 °C for 1 h. After the pull down, beads were washed three times with PBS-T and bound protein was eluted by boiling the sample in SDS loading buffer before separating the proteins on SDS-PAGE and western blotting using Hsp104 antibody (Abcam; ab69549). Immunoprecipitation was also preformed in reverse by immobilizing Hsp104 antibody on

protein G dynabeads (Life Technology) and incubating the total cell lysate with this complex for 1 h. In this case, western blotting was performed using anti-myc antibody (Sigma; M4439).

3.4.9 Thermotolerance assay

WT [*PSI*$^+$] and [*PSI*$^+$] *hsp31Δ* strains were grown in YPD medium starting from OD_{600} of 0.2 until they reach exponential growth phase after 6 h. Equal number of cells from each strain were incubated at 37 °C to induce Hsp104 expression and then heat shocked at 50 °C for 20 min. Aliquots were placed on ice before and after heat shock. A portion of cultures were heat shocked at 50 °C without Hsp104 induction at 37 °C. Samples were collected and five-fold dilutions were spotted on YPD medium.

3.4.10 Sedimentation assay

[*PSI*$^+$] strains harboring Hsp31, Hsp104 and appropriate co-expression vector plasmids were grown for 12 h and centrifuged to collect cells. Cells were washed in water and lysed at 4 °C by bead beating in lysis buffer (50 mM Tris HCl pH 7.5, 50 mM NaCl, 2 mM EDTA and 5% Glycerol plus freshly added protease inhibitor cocktail(158)). Equal volume of cold RIPA buffer (50 mM Tris HCl pH 7.0, 150 mM NaCl, 1% Triton X-100, 0.5% deoxycholate and 0.1 % SDS) was added to the lysate and the mixture was vortexed for 10 s. Lysate was centrifuged at 800 rpm for 2 min at 4 °C in a Eppendorf microcentrifuge. Lysate supernatant was subjected to ultracentrifugation at 80,000 rpm in a TLA-120.2 rotor for 30 min using an Optima Max-XD Ultracentrifuge (Beckman Coulter). Supernatant was collected and pellet was re-suspended in equal volume of lysis and RIPA buffer. Supernatant and pellet fractions were subjected to SDS-PAGE and immunoblotted using GFP antibody (Roche).

3.5 Discussion

Previous studies have demonstrated Hsp31 is a multitasking protein involved in several cellular pathways ranging from functioning as a glutathione independent methylglyoxalase to stress responder that acts as a molecular chaperone. In this study, we have established the inhibitory role of Hsp31 in Sup35 prion formation and its collaboration with Hsp104 to prevent prion aggregation and toxicity in yeast. In the [*PSI*$^+$] prion strain, soluble Sup35 protein is depleted into insoluble prion aggregates, hence, it is no longer functional resulting in nonsense suppression. The stronger [*PSI*$^+$] prion phenotype is associated with larger amounts of protein aggregates. Overexpression of Sup35 PrD-EYFP in a [*psi*$^-$] strain efficiently induces *de novo* [*PSI*$^+$] prion formation and resulting aggregates, which appear as a peripheral ring associated with the vacuoles. The first step in *de novo* prion induction is the formation of a single prion seed, also known as a "propagon". These seeds sequester the soluble Sup35 and grow at both ends into larger aggregates that appeared as rings or dots under microscopy. Moreover, it has been suggested that not all cells with fluorescent aggregates will transform into [*PSI*$^+$] prions, rather about 50% of the cells with fluorescent foci will die and some of the aggregate-containing cells may not possess amyloids (342). Overexpression of Hsp31 in a [*psi*$^-$] strain inhibits Sup35 aggregate formation and this was confirmed by flow cytometry and SDD-AGE. These results validate the previous observation that Hsp31 reduces Sup35 aggregates in the W303 strain (158). In addition, the inhibition of Sup35 aggregation by Hsp31 could result in the inhibition of prion formation, because the [*PIN*$^+$] element required for prion induction is present in this strain. In fact, we observed that overexpression of Hsp31 results in a significant reduction in prion induction from Sup35-

PrD overexpression. This only take place efficiently when Sup35-PrD was overexpressed for a transient period of time and upon longer expression of Sup35-PrD, Hsp31 was unable to reduce prion induction. Importantly, Hsp31 alone is unable to cure the [*PSI*$^{+}$] prion indicating that it has no disaggregase activity. We postulate that the inability of curing but the concomitant ability to prevent the formation of *de novo* Sup35 SDS-resistant aggregates suggests that Hsp31 acts early in the process of prion oligomerization but once larger oligomers are formed it is not further active in preventing prion propagation (Figure 3.8).

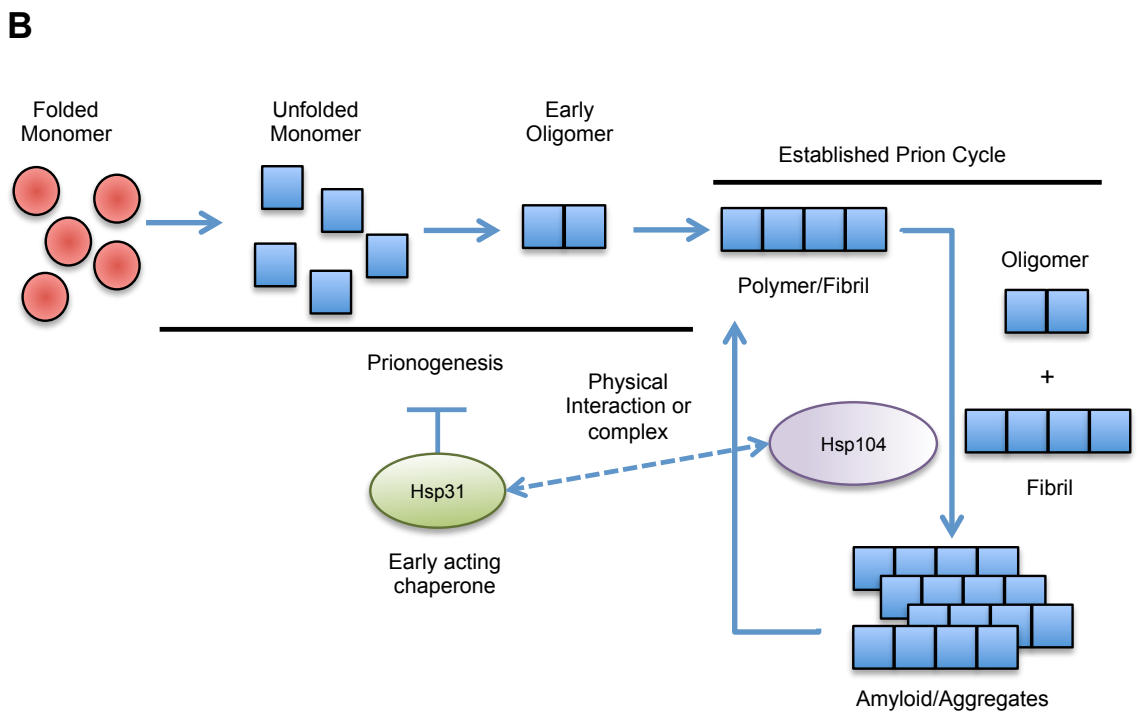

Figure 3.8 Hsp31 acts early in the prionogenesis process.

Model depicting the intervention of Hsp31 during the prionogenesis process but lack of involvement in an established chaperone cycle. Hsp31 and Hsp104 physically interact but it remains to be determined if this interaction is involved in a handoff of substrates.

Hsp31 may not participate in modulating an established prion cycle by itself but does appear to have a role in conjunction with Hsp104 because in a strain lacking Hsp31, the rate of [*PSI*$^+$] curing was reduced with Hsp104 overexpression. In addition, we showed Hsp31 overexpression promotes the elimination of [*PSI*$^+$] by Hsp104. In fact, another small HSP Hsp26 was shown to potentiate protein disaggregation by Hsp104. Interestingly, Hsp26 is only active as a disaggregase when it clusters together with the protein substrate and not after protein aggregation. A factor in considering the mechanism of action is that Hsp31 and the human ortholog, DJ-1, have protein deglycase activity (265,292). Prion glycation can occur spontaneously (343) and glycation can promote the stability of protein aggregates by covalent crosslinking(344) suggesting the activity of a deglycase may abrogate prion propogation. Deciphering the contribution of the enzyme activity versus chaperone function of Hsp31 would be revealing of the biological role of this multi-functional enzyme. We have previously shown that chaperone activity can be independent of the enzyme activity because overexpression of an enzymatically inactive Hsp31 mutant prevents the toxicity of α-syn in yeast. While there is enough evidence to propose Hsp31 acts early in the process of [*PSI*$^+$] prion oligomerization process, future investigation of Hsp31 binding to the Sup35 monomer or other early oligomer and the role of deglycation in inhibiting prion induction would be further revealing of the mechanism of action.

We eliminated several possible indirect mechanisms for the cooperation of Hsp31 with Hsp104 including the possibility that disruption of Hsp31 might compromise Hsp104 expression and thermotolerance function (Figure 3.5). Taking into account that deletion of Hsp31 down regulates the mRNA level of Ssa3, a possible effect of Hsp31 deletion on

[*PSI*$^{+}$] prion curing by Hsp104 could be due to imbalances between Hsp104 and Hsp70 chaperone as these are required for efficient prion curing. However, this cannot be the case when Hsp31 is co-expressed with Hsp104, as overexpression of Hsp31 does not alter the level of Hsp70 protein (158).

We also showed that Hsp31 together with Hsp104 significantly reduced Sup35 prion toxicity. These results indicate that Hsp31 cooperates with Hsp104 to potentiate Sup35 prion disaggregation and thereby prevent toxicity. Intriguingly, previous studies have shown such cooperation between sHSPs and ATP dependent chaperones as Hsp104 and Hsp70 (234,241,243). We also observed a significant reduction of Sup35 toxicity by Hsp31 alone. A number of possible explanations could account for these results such as, Hsp31 might prevent sequestration of soluble Sup35 into already present larger aggregates and therefore inhibit toxicity. We have previously demonstrated that Hsp31 can reduce oxidative stress in cells (158) and this may be the reason for the rescue of toxicity.

Intriguingly, we also found that Hsp31 physically interacts with Hsp104. Hsp104 is known to interact with Ydj1, and co-chaperones of Hsp90; Sti1 and Cpr7 (40,225). Interestingly, Sti1 and Cpr7 are not required for Sup35 prion propagation but deletion of either of these reduced the Sup35 prion curing by Hsp104. Hsp31 has been documented to interact with the yeast Hsp90, Hsp82 (345), based on affinity-mass spectrometry hence the interaction may involve a bridging chaperone such as Hsp90. However, our data is the first demonstration of Hsp31's interaction with Hsp104 and could mean these chaperones may pass substrates to each other. Although the molecular details of the

interaction are unknown, the involvement of Hsp31 in the prion modulation process and the apparent close functional cooperation with Hsp104 is an important step in understanding the biological roles of this multi-tasking protein.

CHAPTER 4. CONCLUSION AND FUTURE DIRECTIONS

4.1 Summary

Numerous human pathologies are associated with protein misfolding and aggregation including several neurodegenerative diseases such as AD, PD and prion diseases. For each such disease a different misfolded protein is responsible for neurodegeneration at different regions of the brain that leads to differential clinical effects. Although there is extensive understanding of these molecular mechanisms, there are still numerous unanswered questions. Several studies show the protective role of HSPs in misfolding processes that function as chaperones in modulating protein aggregation and their involvement in neurodegenerative diseases. In this thesis, we used yeast as a model system to gain insight into the role of Hsp31 as a molecular chaperone and characterized its function in PD and prion modulation in yeast.

4.2 What makes Hsp31 a multifunctional chaperone protein? What is the role of the C138 residue in catalytic triad of Hsp31?

An emerging view is that Hsp31 and its associated superfamily members each have divergent multitasking functions that have the common theme of responding and managing various types of cellular stress. Hsp31 is involved in multiple cellular functions including oxidative stress sensing, chaperone and detoxifying enzyme activities such as functions as methylglyoxalase and deglycation. In chapter 2, we have shown that

protective role of Hsp31's chaperone activity can operate independent of detoxifying enzyme activities in preventing the early stages of protein aggregate formation and associated cellular toxicities. The catalytic triad present in the DJ-1 superfamily members is the most common feature, mutation of which can lead to functional variation and destabilization of dimerization.

In this thesis we showed that Hsp31 is capable of acting as a chaperone without involvement of its enzymatic activity. Hsp31 possesses a conserved cysteine residue C138 that is present in different species (272). Previously, it was shown that mutation in C138 abrogates its enzymatic activity. However, in this thesis, we provide strong evidence that mutation of C138 has no effect on the chaperone activity of Hsp31. Future studies should be performed to further delineate the role of C138 in Hsp31. In DJ-1, the oxidative state of C106 is involved in redox sensing, and the mutation of it destabilizes the DJ-1 functions. Under oxidative stress condition DJ-1 homo-dimer destabilizes and therefore loss its protective effect (346,347). Similarly, Hsp31 exists predominantly as a homo-dimer in solution as shown previously (271,272), and it would be interesting to determine what is the role of dimerization state in the chaperone activity of Hsp31? It remains to be determined, what are the chaperone active sites, if C138 has a limited role in chaperone function? Furthermore, in chapter 3 we provide significant evidence that Hsp31 is involved in the modulation of prion aggregation, however, we never tested the effect of C138 mutation in these experiments. Studying these questions will provide a further mechanistic insight into the role of Hsp31 as a chaperone protein.

4.3 What is the link between Hsp31 deglycase activity and aggregation activity?

It is now well established that Hsp31 is a molecular chaperone that intervene in the aggregation of a broad range of protein substrates. Our studies provide strong evidence to delineating that Hsp31 intervenes early in the process of protein aggregation to prevent larger aggregate or oligomer formation. Future studies will need to focus on dissection of the mechanistic details of how Hsp31 prevents the formation of aggregates. Recent studies showed that enzymatic activity of Hsp31 is capable to deglycate the damaged proteins. One hypothesis is that Hsp31 binds to damaged or glycated substrate protein to deglycate them and therefore prevent the formation of aggregates caused by glycation of the monomeric proteins. It will be important to study that if Hsp31 binds to glycated monomeric protein and therefore prevent further aggregation of protein. It is not clear if MGO or glycated proteins are the prime substrate for Hsp31 or if both are important hence, determination of the *in vitro* enzymatic activities of Hsp31 on these two different substrates is important to determine. Further *in vivo* studies that explore the effect of Hsp31 on glycated proteins will be needed to provided insight into the mode of action and reveal the natural substrate(s) of Hsp31 with respect to its methylyglyoxalase/deglycase activities.

4.4 Determine the role and nature of the Hsp31 and Hsp104 interaction? What are the roles of Hsp82/Hsp70 and other co-chaperones in conjunction with Hsp31?

In chapter 3 we showed that Hsp31 cooperates with Hsp104 to prevent Sup35 prion aggregation. Future studies will focus on the nature of interaction between Hsp31 and Hsp104. Although, we have shown that Hsp31 can pull down endogenous levels of Hsp104, it is not known if this interaction is direct based on the co-immunoprecipitation.

In order to determine if the interaction is direct, *in vitro* binding assays using recombinant proteins would answer this question. If these two chaperones interact directly, we can further explore the interaction sites or regions important for such an interaction. Information on how the DJ-1/Hsp31 protein family interacts with other chaperones or co-factors is severely lacking. Furthermore, identification of direct interaction sites would allow a dissection and assessment of the role of this interaction on the overall activity of Hsp104 or Hsp31? Based on affinity-mass spectrometry, it has been documented previously, that Hsp31 interacts with the yeast Hsp90, Hsp82. It is also known that Hsp104 interacts with co-chaperones of Hsp90 hence, the interaction between Hsp104 and Hsp31 may require a bridging chaperone as Hsp90 or its co-chaperones; Sti1 and Cpr7. Alternatively, Hsp31 maybe a co-chaperone of Hsp90 or Hsp104 and may deliver substrates to these other chaperones as part of an overall multi-step chaperone cycle.

4.5 Functional diversity or overlap among Hsp31 paralogs in yeast.

The Hsp31 mini-family is composed of four paralogs; *HSP31* (*YDR533C*), *HSP32* (*YMR322C*), *HSP33* (*YOR391C*), and *HSP34* (*YPL280W*). Genes of the Hsp31 mini family are located at the subtelomeric region of the genome in *Saccharomyces cerevisiae*. *HSP31* is considered the parental gene with *HSP32*, *HSP33* and *HSP34* originating from it during gene duplication events. Among all the members of this mini-family, Hsp31 is most divergent and shares approximately 70% homology with the other members of the family those possess more than 90% homology between them. All the members of Hsp31 family contain the same Cys-His-Glu catalytic triad including the *E. coli* ortholog. Previously, it was shown that mutation in the catalytic triad largely abolishes glyoxalase activity but this catalytic triad is not required for chaperone activity of Hsp31. These

results indicate that the anti-aggregation activity of Hsp31 is not under the influence of its enzymatic activity rather, it has a direct chaperone activity against misfolded proteins. Intriguingly, all the paralogs of the Hsp31 minifamily possess comparable activity against α-syn aggregation and toxicity when they are overexpressed from the *GAL* promoter. However, unlike Hsp31, the other paralogs possess very little methylglyoxalase activity and are unable to protect the cells from glyoxal toxicity (260,348). These results support the notion that anti-aggregation activity of Hsp31 mini-family is independent of its enzymatic activity. Furthermore, all the members of the Hsp31 family contain the same catalytic triad required for methylglyoxalse activity but so far only Hsp31 is determined as the most active enzyme *in vitro* and *in vivo.* Despite the presence of the catalytic triad Hsp34 is found to be a very weak methylglyoxalase, which indicates that other regions in the protein sequence are also important for enzymatic activity. Hsp31 and Hsp34's divergent activity has only been shown for MGO, and the different paralogs could have differential activity depending on the substrate type. In future research, it will be important to determine the functional diversity between paralogs of Hsp31 in term of its methylglyoxalase and other enzymatic activities. As, the lack of methylglyoxalase activity in one of the paralogs is evidence that the paralogs are diverging but additional studies dissecting the roles within this paralog group are needed to further uncover these diverging functions. It is also important to note that other biomolecules such as nucleic acids are also susceptible to oxidative damage and could also be substrates for the Hsp31 protein family.

In contrast, the chaperone activity of Hsp31 and its paralog are comparable (106). Also, the chaperone activity of Hsp31, Hsp32 and Hsp33 against a cytoplasmic aggregation-

prone protein is independent of their role in oxidative stress response and the vacuolar degradation pathway (262). It would be interesting to study the functional overlap of these family members. The Hsp31 protein family is broadly spread across fungal species with varying levels of paralog duplications and additional evidence of divergence including differences in localization in the *Schizosaccharomyces pombe* Hsp31 family members (272).

4.6 Conclusion

In conclusion, study presented here significantly contributed to understand the molecular role of Hsp31 as a chaperone in protein misfolding diseases. Hsp31 promotes cell survival under different stress conditions by participating in multiple cellular pathways. Although, currently we know that Hsp31 is a multifunctional stress responder chaperone proteins that have homologs in almost every organisms, the exact molecular mechanism of Hsp31 remains enigmatic. Further studying the mode of action of Hsp31 provides a promising model to understand the cytoprotective functions of DJ-1 that can be a potential target for neurodegenerative disease as PD.

REFERENCES

REFERENCES

1. Ruggiano, A., Foresti, O., and Carvalho, P. (2014) Quality control: ER-associated degradation: protein quality control and beyond. *J Cell Biol* **204**, 869-879
2. Zattas, D., and Hochstrasser, M. (2015) Ubiquitin-dependent protein degradation at the yeast endoplasmic reticulum and nuclear envelope. *Crit Rev Biochem Mol Biol* **50**, 1-17
3. Wickner, S., Maurizi, M. R., and Gottesman, S. (1999) Posttranslational quality control: folding, refolding, and degrading proteins. *Science* **286**, 1888-1893
4. Boban, M., and Foisner, R. (2016) Degradation-mediated protein quality control at the inner nuclear membrane. *Nucleus*, 0
5. Rusmini, P., Crippa, V., Cristofani, R., Rinaldi, C., Cicardi, M. E., Galbiati, M., Carra, S., Malik, B., Greensmith, L., and Poletti, A. (2015) The Role of the Protein Quality Control System in SBMA. *J Mol Neurosci*
6. Mukherjee, R., and Chakrabarti, O. (2016) Ubiquitin-mediated regulation of the E3 ligase GP78 by MGRN1 in trans affects mitochondrial homeostasis. *J Cell Sci* **129**, 757-773
7. Webster, B. M., and Lusk, C. P. (2016) Border Safety: Quality Control at the Nuclear Envelope. *Trends Cell Biol* **26**, 29-39
8. Halperin, L., Jung, J., and Michalak, M. (2014) The many functions of the endoplasmic reticulum chaperones and folding enzymes. *IUBMB Life* **66**, 318-326
9. Kurland, C. G. (1992) Translational accuracy and the fitness of bacteria. *Annu Rev Genet* **26**, 29-50
10. Hurtley, S. M., and Helenius, A. (1989) Protein oligomerization in the endoplasmic reticulum. *Annu Rev Cell Biol* **5**, 277-307
11. Ibba, M., and Söll, D. (1999) Quality control mechanisms during translation. *Science* **286**, 1893-1897
12. Lindahl, T., and Wood, R. D. (1999) Quality control by DNA repair. *Science* **286**, 1897-1905
13. Hyttinen, J. M., Amadio, M., Viiri, J., Pascale, A., Salminen, A., and Kaarniranta, K. (2014) Clearance of misfolded and aggregated proteins by aggrephagy and implications for aggregation diseases. *Ageing Res Rev* **18C**, 16-28
14. Shah, S. Z., Zhao, D., Khan, S. H., and Yang, L. (2015) Unfolded Protein Response Pathways in Neurodegenerative Diseases. *J Mol Neurosci* **57**, 529-537
15. Amor, A. J., Castanzo, D. T., Delany, S. P., Selechnik, D. M., van Ooy, A., and Cameron, D. M. (2015) The ribosome-associated complex antagonizes prion formation in yeast. *Prion* **9**, 144-164

16. Harrison, R. S., Sharpe, P. C., Singh, Y., and Fairlie, D. P. (2007) Amyloid peptides and proteins in review. *Rev Physiol Biochem Pharmacol* **159**, 1-77
17. Franssens, V., Boelen, E., Anandhakumar, J., Vanhelmont, T., Büttner, S., and Winderickx, J. (2010) Yeast unfolds the road map toward alpha-synuclein-induced cell death. *Cell Death Differ* **17**, 746-753
18. Wang, M., and Kaufman, R. J. (2016) Protein misfolding in the endoplasmic reticulum as a conduit to human disease. *Nature* **529**, 326-335
19. Hammarström, P. (2009) Protein folding, misfolding and disease. *FEBS Lett* **583**, 2579-2580
20. Cardinale, A., Chiesa, R., and Sierks, M. (2014) Protein misfolding and neurodegenerative diseases. *Int J Cell Biol* **2014**, 217371
21. Ellisdon, A. M., and Bottomley, S. P. (2004) The role of protein misfolding in the pathogenesis of human diseases. *IUBMB Life* **56**, 119-123
22. Penke, B., Bogár, F., and Fülöp, L. (2016) Protein Folding and Misfolding, Endoplasmic Reticulum Stress in Neurodegenerative Diseases: in Trace of Novel Drug Targets. *Curr Protein Pept Sci* **17**, 169-182
23. Singh, J., and Udgaonkar, J. B. (2015) Molecular Mechanism of the Misfolding and Oligomerization of the Prion Protein: Current Understanding and Its Implications. *Biochemistry* **54**, 4431-4442
24. Englander, S. W., Mayne, L., and Krishna, M. M. (2007) Protein folding and misfolding: mechanism and principles. *Q Rev Biophys* **40**, 287-326
25. Borgia, A., Kemplen, K. R., Borgia, M. B., Soranno, A., Shammas, S., Wunderlich, B., Nettels, D., Best, R. B., Clarke, J., and Schuler, B. (2015) Transient misfolding dominates multidomain protein folding. *Nat Commun* **6**, 8861
26. Kim, Y. E., Hipp, M. S., Bracher, A., Hayer-Hartl, M., and Hartl, F. U. (2013) Molecular chaperone functions in protein folding and proteostasis. *Annu Rev Biochem* **82**, 323-355
27. Hubbard, T. J., and Sander, C. (1991) The role of heat-shock and chaperone proteins in protein folding: possible molecular mechanisms. *Protein Eng* **4**, 711-717
28. Gong, Y., Kakihara, Y., Krogan, N., Greenblatt, J., Emili, A., Zhang, Z., and Houry, W. A. (2009) An atlas of chaperone-protein interactions in Saccharomyces cerevisiae: implications to protein folding pathways in the cell. *Mol Syst Biol* **5**, 275
29. Burel, C., Mezger, V., Pinto, M., Rallu, M., Trigon, S., and Morange, M. (1992) Mammalian heat shock protein families. Expression and functions. *Experientia* **48**, 629-634
30. Ellis, R. J., van der Vies, S. M., and Hemmingsen, S. M. (1989) The molecular chaperone concept. *Biochem Soc Symp* **55**, 145-153
31. Horwich, A. L., and Willison, K. R. (1993) Protein folding in the cell: functions of two families of molecular chaperone, hsp 60 and TF55-TCP1. *Philos Trans R Soc Lond B Biol Sci* **339**, 313-325; discussion 325-316
32. Kelley, W. L., and Georgopoulos, C. (1992) Chaperones and protein folding. *Curr Opin Cell Biol* **4**, 984-991

33. Young, J. C. (2010) Mechanisms of the Hsp70 chaperone system. *Biochem Cell Biol* **88**, 291-300
34. Pratt, W. B., Morishima, Y., Gestwicki, J. E., Lieberman, A. P., and Osawa, Y. (2014) A model in which heat shock protein 90 targets protein-folding clefts: rationale for a new approach to neuroprotective treatment of protein folding diseases. *Exp Biol Med (Maywood)* **239**, 1405-1413
35. Miura, T., Minegishi, H., Usami, R., and Abe, F. (2006) Systematic analysis of HSP gene expression and effects on cell growth and survival at high hydrostatic pressure in Saccharomyces cerevisiae. *Extremophiles* **10**, 279-284
36. Cyr, D. M., and Ramos, C. H. (2015) Specification of Hsp70 function by Type I and Type II Hsp40. *Subcell Biochem* **78**, 91-102
37. Duncan, E. J., Cheetham, M. E., Chapple, J. P., and van der Spuy, J. (2015) The role of HSP70 and its co-chaperones in protein misfolding, aggregation and disease. *Subcell Biochem* **78**, 243-273
38. Mogk, A., Kummer, E., and Bukau, B. (2015) Cooperation of Hsp70 and Hsp100 chaperone machines in protein disaggregation. *Front Mol Biosci* **2**, 22
39. Reidy, M., Sharma, R., Shastry, S., Roberts, B. L., Albino-Flores, I., Wickner, S., and Masison, D. C. (2014) Hsp40s specify functions of Hsp104 and Hsp90 protein chaperone machines. *PLoS Genet* **10**, e1004720
40. Reidy, M., and Masison, D. C. (2010) Sti1 regulation of Hsp70 and Hsp90 is critical for curing of Saccharomyces cerevisiae [PSI+] prions by Hsp104. *Mol Cell Biol* **30**, 3542-3552
41. Walter, S., and Buchner, J. (2002) Molecular Chaperones—Cellular Machines for Protein Folding. *Angewandte Chemie International Edition* **41**, 1098-1113
42. Ritossa, F. (1962) A new puffing pattern induced by temperature shock and DNP in drosophila. *Experientia* **18**, 571-573
43. Rotossa, F. (1996) Discovery of the heat shock response. *Cell stress Chaperones* **1**, 97-98
44. Bakthisaran, R., Tangirala, R., and Rao, C. M. (2015) Small heat shock proteins: Role in cellular functions and pathology. *Biochim Biophys Acta* **1854**, 291-319
45. Mokry, D. Z., Abrahão, J., and Ramos, C. H. (2015) Disaggregases, molecular chaperones that resolubilize protein aggregates. *An Acad Bras Cienc* **87**, 1273-1292
46. Schlesinger, M. J. (1990) Heat shock proteins. *Journal of Biological Chemistry* **265**, 12111-12114
47. Clark, J. I., and Muchowski, P. J. (2000) Small heat-shock proteins and their potential role in human disease. *Current Opinion in Structural Biology* **10**, 52-59
48. Eyles, S. J., and Gierasch, L. M. (2010) Nature's molecular sponges: Small heat shock proteins grow into their chaperone roles. *Proceedings of the National Academy of Sciences* **107**, 2727-2728
49. Jakob, U., Gaestel, M., Engel, K., and Buchner, J. (1993) Small heat shock proteins are molecular chaperones. *Journal of Biological Chemistry* **268**, 1517-1520

50. Wehmeyer, N., and Vierling, E. (2000) The expression of small heat shock proteins in seeds responds to discrete developmental signals and suggests a general protective role in desiccation tolerance. *Plant Physiol* **122**, 1099-1108
51. Zeng, L., Tan, J., Lu, T., Lei, Q., Chen, C., and Hu, Z. (2015) Small heat shock proteins and the endoplasmic reticulum: potential attractive therapeutic targets? *Curr Mol Med* **15**, 38-46
52. Sun, Y., and MacRae, T. H. (2005) The small heat shock proteins and their role in human disease. *FEBS Journal* **272**, 2613-2627
53. Duennwald, M. L., Echeverria, A., and Shorter, J. (2012) Small heat shock proteins potentiate amyloid dissolution by protein disaggregases from yeast and humans. *PLoS Biol* **10**, e1001346
54. Kovacs, G. G. (2016) Molecular Pathological Classification of Neurodegenerative Diseases: Turning towards Precision Medicine. *Int J Mol Sci* **17**
55. Carr, F. (2016) Neurodegenerative disease: Forming fragments. *Nat Rev Neurosci* **17**, 74-75
56. Agid, Y. (1993) [Mechanism of cell death in neurodegenerative disorders: apropos of Parkinson disease]. *C R Seances Soc Biol Fil* **187**, 37-46
57. Hamill, R. W., Caine, E., Eskin, T., Lapham, L., Shoulson, I., and McNeill, T. H. (1988) Neurodegenerative disorders and aging. Alzheimer's disease and Parkinson's disease--common ground. *Ann N Y Acad Sci* **515**, 411-420
58. Ceballos, I., Javoy-Agid, F., Delacourte, A., Defossez, A., Nicole, A., and Sinet, P. M. (1990) Parkinson's disease and Alzheimer's disease: neurodegenerative disorders due to brain antioxidant system deficiency? *Adv Exp Med Biol* **264**, 493-498
59. Crunkhorn, S. (2016) Neurodegenerative disease: Immunotherapy opportunity emerges for Alzheimer disease. *Nat Rev Drug Discov*
60. Iqbal, K., Liu, F., and Gong, C. X. (2016) Tau and neurodegenerative disease: the story so far. *Nat Rev Neurol* **12**, 15-27
61. Rojas, J. C., and Boxer, A. L. (2016) Neurodegenerative disease in 2015: Targeting tauopathies for therapeutic translation. *Nat Rev Neurol* **12**, 74-76
62. Dias, V., Junn, E., and Mouradian, M. M. (2013) The role of oxidative stress in Parkinson's disease. *J Parkinsons Dis* **3**, 461-491
63. Jellinger, K. A. (2010) Basic mechanisms of neurodegeneration: a critical update. *Journal of Cellular and Molecular Medicine* **14**, 457-487
64. Mandemakers, W., Morais, V. A., and De Strooper, B. (2007) A cell biological perspective on mitochondrial dysfunction in Parkinson disease and other neurodegenerative diseases. *J Cell Sci* **120**, 1707-1716
65. Albers, D. S., and Beal, M. F. (2000) Mitochondrial dysfunction and oxidative stress in aging and neurodegenerative disease. *J Neural Transm Suppl* **59**, 133-154
66. Butterfield, D. A., Palmieri, E. M., and Castegna, A. (2016) Clinical implications from proteomic studies in neurodegenerative diseases: lessons from mitochondrial proteins. *Expert Rev Proteomics*
67. Matsuda, N., and Tanaka, K. (2011) [Neurodegenerative disorder as "mitochondrial dysfunction disease"]. *Rinsho Shinkeigaku* **51**, 988

68. Carvalho, A. N., Firuzi, O., Gama, M. J., van Horssen, J., and Saso, L. (2016) Oxidative stress and antioxidants in neurological diseases: is there still hope? *Curr Drug Targets*
69. Langkilde, A. E., Morris, K. L., Serpell, L. C., Svergun, D. I., and Vestergaard, B. (2015) The architecture of amyloid-like peptide fibrils revealed by X-ray scattering, diffraction and electron microscopy. *Acta Crystallogr D Biol Crystallogr* **71**, 882-895
70. Conway, K. A., Harper, J. D., and Lansbury, P. T. (2000) Fibrils Formed in Vitro from α-Synuclein and Two Mutant Forms Linked to Parkinson's Disease are Typical Amyloid†. *Biochemistry* **39**, 2552-2563
71. Sunde, M., and Blake, C. C. (1998) From the globular to the fibrous state: protein structure and structural conversion in amyloid formation. *Q Rev Biophys* **31**, 1-39
72. Benzinger, T. L., Gregory, D. M., Burkoth, T. S., Miller-Auer, H., Lynn, D. G., Botto, R. E., and Meredith, S. C. (2000) Two-dimensional structure of beta-amyloid(10-35) fibrils. *Biochemistry* **39**, 3491-3499
73. Ross, C. A., Poirier, M. A., Wanker, E. E., and Amzel, M. (2003) Polyglutamine fibrillogenesis: the pathway unfolds. *Proc Natl Acad Sci U S A* **100**, 1-3
74. Behl, C., Davis, J. B., Lesley, R., and Schubert, D. (1994) Hydrogen peroxide mediates amyloid β protein toxicity. *Cell* **77**, 817-827
75. Meisl, G., Kirkegaard, J. B., Arosio, P., Michaels, T. C., Vendruscolo, M., Dobson, C. M., Linse, S., and Knowles, T. P. (2016) Molecular mechanisms of protein aggregation from global fitting of kinetic models. *Nat Protoc* **11**, 252-272
76. Villemagne, V. L. (2016) Amyloid imaging: Past, Present and Future Perspectives. *Ageing Res Rev*
77. Ross, C. A., and Poirier, M. A. (2004) Protein aggregation and neurodegenerative disease. *Nat Med* **10 Suppl**, S10-17
78. Sacchettini, J. C., and Kelly, J. W. (2002) Therapeutic strategies for human amyloid diseases. *Nat Rev Drug Discov* **1**, 267-275
79. Chen, S., Berthelier, V., Hamilton, J. B., O'Nuallain, B., and Wetzel, R. (2002) Amyloid-like features of polyglutamine aggregates and their assembly kinetics. *Biochemistry* **41**, 7391-7399
80. Pike, C. J., Walencewicz, A. J., Glabe, C. G., and Cotman, C. W. (1991) Aggregation-related toxicity of synthetic beta-amyloid protein in hippocampal cultures. *Eur J Pharmacol* **207**, 367-368
81. Hoyer, S. (1994) Neurodegeneration, Alzheimer's disease, and beta-amyloid toxicity. *Life Sci* **55**, 1977-1983
82. Stefani, M., and Dobson, C. M. (2003) Protein aggregation and aggregate toxicity: new insights into protein folding, misfolding diseases and biological evolution. *J Mol Med (Berl)* **81**, 678-699
83. Bossy-Wetzel, E., Schwarzenbacher, R., and Lipton, S. A. (2004) Molecular pathways to neurodegeneration. *Nat Med* **10 Suppl**, S2-9
84. Sundal, C., Fujioka, S., Uitti, R. J., and Wszolek, Z. K. (2012) Autosomal dominant Parkinson's disease. *Parkinsonism & Related Disorders* **18, Supplement 1**, S7-S10

85. Meissner, W. G., Frasier, M., Gasser, T., Goetz, C. G., Lozano, A., Piccini, P., Obeso, J. A., Rascol, O., Schapira, A., Voon, V., Weiner, D. M., Tison, F., and Bezard, E. (2011) Priorities in Parkinson's disease research. *Nat Rev Drug Discov* **10**, 377-393
86. Parkinson, J. (2002) An essay on the shaking palsy. 1817. *J Neuropsychiatry Clin Neurosci* **14**, 223-236; discussion 222
87. Schnabel, J. (2010) Secrets of the shaking palsy. *Nature* **466**, S2-S5
88. Dorsey, E. R., Constantinescu, R., Thompson, J. P., Biglan, K. M., Holloway, R. G., Kieburtz, K., Marshall, F. J., Ravina, B. M., Schifitto, G., Siderowf, A., and Tanner, C. M. (2007) Projected number of people with Parkinson disease in the most populous nations, 2005 through 2030. *Neurology* **68**, 384-386
89. Casey, G. (2013) Parkinson's disease: a long and difficult journey. *Nurs N Z* **19**, 20-24
90. Mohan, A., Mather, K. A., Thalamuthu, A., Baune, B. T., and Sachdev, P. S. (2016) Gene expression in the aging human brain: an overview. *Curr Opin Psychiatry* **29**, 159-167
91. Sherer, T. B., Chowdhury, S., Peabody, K., and Brooks, D. W. (2012) Overcoming obstacles in Parkinson's disease. *Mov Disord* **27**, 1606-1611
92. Feng, Y., Jankovic, J., and Wu, Y. C. (2015) Epigenetic mechanisms in Parkinson's disease. *J Neurol Sci* **349**, 3-9
93. Giovannini, P., Piccolo, I., Genitrini, S., Soliveri, P., Girotti, F., Geminiani, G., Scigliano, G., and Caraceni, T. (1991) Early-onset Parkinson's disease. *Mov Disord* **6**, 36-42
94. Savica, R., Grossardt, B. R., Bower, J. H., Ahlskog, J. E., and Rocca, W. A. (2013) Risk factors for Parkinson's disease may differ in men and women: an exploratory study. *Horm Behav* **63**, 308-314
95. Ueki, A., and Otsuka, M. (2004) Life style risks of Parkinson's disease: association between decreased water intake and constipation. *J Neurol* **251 Suppl 7**, vII18-23
96. Palacios, N., Gao, X., McCullough, M. L., Jacobs, E. J., Patel, A. V., Mayo, T., Schwarzschild, M. A., and Ascherio, A. (2011) Obesity, diabetes, and risk of Parkinson's disease. *Mov Disord* **26**, 2253-2259
97. Checkoway, H., Powers, K., Smith-Weller, T., Franklin, G. M., Longstreth, W. T., and Swanson, P. D. (2002) Parkinson's disease risks associated with cigarette smoking, alcohol consumption, and caffeine intake. *Am J Epidemiol* **155**, 732-738
98. Bailleul, P. A., Newnam, G. P., Steenbergen, J. N., and Chernoff, Y. O. (1999) Genetic study of interactions between the cytoskeletal assembly protein sla1 and prion-forming domain of the release factor Sup35 (eRF3) in Saccharomyces cerevisiae. *Genetics* **153**, 81-94
99. Chartier-Harlin, M.-C., Kachergus, J., Roumier, C., Mouroux, V., Douay, X., Lincoln, S., Levecque, C., Larvor, L., Andrieux, J., Hulihan, M., Waucquier, N., Defebvre, L., Amouyel, P., Farrer, M., and Destée, A. (2004) Alpha-synuclein locus duplication as a cause of familial Parkinson's disease. *The Lancet* **364**, 1167-1169

100. Cookson, M. (2009) alpha-Synuclein and neuronal cell death. *Molecular Neurodegeneration* **4**, 9
101. McLean, P. J., Kawamata, H., Ribich, S., and Hyman, B. T. (2000) Membrane association and protein conformation of alpha-synuclein in intact neurons. Effect of Parkinson's disease-linked mutations. *J Biol Chem* **275**, 8812-8816
102. Taguchi, K., Watanabe, Y., Tsujimura, A., Tatebe, H., Miyata, S., Tokuda, T., Mizuno, T., and Tanaka, M. (2014) Differential expression of alpha-synuclein in hippocampal neurons. *PLoS One* **9**, e89327
103. Cookson, M., and Brug, M. (2008) Cell systems and the toxic mechanism(s) of alpha-synuclein. *Exp Neurol* **209**, 5 - 11
104. Cooper, A., Gitler, A., Cashikar, A., Haynes, C., Hill, K., Bhullar, B., Liu, K., Xu, K., Strathearn, K., Liu, F., Cao, S., Caldwell, K., Caldwell, G., Marsischky, G., Kolodner, R., Labaer, J., Rochet, J., Bonini, N., and Lindquist, S. (2006) Alpha-synuclein blocks ER-Golgi traffic and Rab1 rescues neuron loss in Parkinson's models. *Science* **313**, 324 - 328
105. Hsu, L., Sagara, Y., Arroyo, A., Rockenstein, E., Sisk, A., Mallory, M., Wong, J., Takenouchi, T., Hashimoto, M., and Masliah, E. (2000) alpha-synuclein promotes mitochondrial deficit and oxidative stress. *Am J Pathol* **157**, 401 - 410
106. Zondler, L., Miller-Fleming, L., Repici, M., Gonçalves, S., Tenreiro, S., Rosado-Ramos, R., Betzer, C., Straatman, K. R., Jensen, P. H., Giorgini, F., and Outeiro, T. F. (2014) DJ-1 interactions with α-synuclein attenuate aggregation and cellular toxicity in models of Parkinson's disease. *Cell Death Dis* **5**, e1350
107. Atik, A., Stewart, T., and Zhang, J. (2016) Alpha-synuclein as a biomarker for Parkinson's disease. *Brain Pathol*
108. Scherfler, C., Göbel, G., Müller, C., Nocker, M., Wenning, G. K., Schocke, M., Poewe, W., and Seppi, K. (2016) Diagnostic potential of automated subcortical volume segmentation in atypical parkinsonism. *Neurology*
109. Postuma, R. B., Gagnon, J. F., and Montplaisir, J. (2010) Clinical prediction of Parkinson's disease: planning for the age of neuroprotection. *J Neurol Neurosurg Psychiatry* **81**, 1008-1013
110. Burkhard, P. (2015) [Parkinson disease diagnosis: not so easy...]. *Rev Med Suisse* **11**, 304-305
111. Martí, M. J., and Tolosa, E. (2013) Parkinson disease: New guidelines for diagnosis of Parkinson disease. *Nat Rev Neurol* **9**, 190-191
112. Levin, J., Kurz, A., Arzberger, T., Giese, A., and Höglinger, G. U. (2016) The Differential Diagnosis and Treatment of Atypical Parkinsonism. *Dtsch Arztebl Int* **113**, 61-69
113. Rajput, A. H., and Rajput, A. (2014) Accuracy of Parkinson disease diagnosis unchanged in 2 decades. *Neurology* **83**, 386-387
114. Miller, D. B., and O'Callaghan, J. P. (2015) Biomarkers of Parkinson's disease: present and future. *Metabolism* **64**, S40-46
115. Mattison, H. A., Stewart, T., and Zhang, J. (2012) Applying bioinformatics to proteomics: Is machine learning the answer to biomarker discovery for PD and MSA? *Movement Disorders* **27**, 1595-1597

116. Hall, S., Surova, Y., Öhrfelt, A., Zetterberg, H., Lindqvist, D., and Hansson, O. (2015) CSF biomarkers and clinical progression of Parkinson disease. *Neurology* **84**, 57-63
117. Perlmutter, J. S., and Norris, S. A. (2014) Neuroimaging biomarkers for Parkinson disease: facts and fantasy. *Ann Neurol* **76**, 769-783
118. Foulds, P. G., Mitchell, J. D., Parker, A., Turner, R., Green, G., Diggle, P., Hasegawa, M., Taylor, M., Mann, D., and Allsop, D. (2011) Phosphorylated α-synuclein can be detected in blood plasma and is potentially a useful biomarker for Parkinson's disease. *The FASEB Journal* **25**, 4127-4137
119. Bonifati, V., Rizzu, P., van Baren, M. J., Schaap, O., Breedveld, G. J., Krieger, E., Dekker, M. C., Squitieri, F., Ibanez, P., Joosse, M., van Dongen, J. W., Vanacore, N., van Swieten, J. C., Brice, A., Meco, G., van Duijn, C. M., Oostra, B. A., and Heutink, P. (2003) Mutations in the DJ-1 gene associated with autosomal recessive early-onset parkinsonism. *Science* **299**, 256-259
120. Davis, J. W., Grandinetti, A., Waslien, C. I., Ross, G. W., White, L. R., and Morens, D. M. (1996) Observations on serum uric acid levels and the risk of idiopathic Parkinson's disease. *Am J Epidemiol* **144**, 480-484
121. de Lau, L. M., Koudstaal, P. J., Hofman, A., and Breteler, M. M. (2005) Serum uric acid levels and the risk of Parkinson disease. *Ann Neurol* **58**, 797-800
122. Chen-Plotkin, A. S., Hu, W. T., Siderowf, A., Weintraub, D., Goldmann Gross, R., Hurtig, H. I., Xie, S. X., Arnold, S. E., Grossman, M., Clark, C. M., Shaw, L. M., McCluskey, L., Elman, L., Van Deerlin, V. M., Lee, V. M., Soares, H., and Trojanowski, J. Q. (2011) Plasma epidermal growth factor levels predict cognitive decline in Parkinson disease. *Ann Neurol* **69**, 655-663
123. Qiang, J. K., Wong, Y. C., Siderowf, A., Hurtig, H. I., Xie, S. X., Lee, V. M., Trojanowski, J. Q., Yearout, D., B Leverenz, J., Montine, T. J., Stern, M., Mendick, S., Jennings, D., Zabetian, C., Marek, K., and Chen-Plotkin, A. S. (2013) Plasma apolipoprotein A1 as a biomarker for Parkinson disease. *Ann Neurol* **74**, 119-127
124. Hatano, T., Saiki, S., Okuzumi, A., Mohney, R. P., and Hattori, N. (2016) Identification of novel biomarkers for Parkinson's disease by metabolomic technologies. *J Neurol Neurosurg Psychiatry* **87**, 295-301
125. Alongi, P., Iaccarino, L., and Perani, D. (2014) PET Neuroimaging: Insights on Dystonia and Tourette Syndrome and Potential Applications. *Front Neurol* **5**, 183
126. Dekker, M. C. J., Eshuis, S. A., Maguire, R. P., Veenma-van der Duijn, L., Pruim, J., Snijders, P. J. L. M., Oostra, B. A., van Duijn, C. M., and Leenders, K. L. (2004) PET neuroimaging and mutations in the DJ-1 gene. *Journal of Neural Transmission* **111**, 1575-1581
127. Zou, J., Weng, R. H., Chen, Z. Y., Wei, X. B., Wang, R., Chen, D., Xia, Y., and Wang, Q. (2016) Position Emission Tomography/Single-Photon Emission Tomography Neuroimaging for Detection of Premotor Parkinson's Disease. *CNS Neurosci Ther* **22**, 167-177
128. Pagano, G., Ferrara, N., Brooks, D. J., and Pavese, N. (2016) Age at onset and Parkinson disease phenotype. *Neurology*

129. Schrag, A., and Quinn, N. (2000) Dyskinesias and motor fluctuations in Parkinson's disease. A community-based study. *Brain* **123 (Pt 11)**, 2297-2305
130. Raffo De Ferrari, A., Lagravinese, G., Pelosin, E., Pardini, M., Serrati, C., Abbruzzese, G., and Avanzino, L. (2015) Freezing of gait and affective theory of mind in Parkinson disease. *Parkinsonism Relat Disord* **21**, 509-513
131. Belin, J., Houéto, J. L., Constans, T., Hommet, C., de Toffol, B., and Mondon, K. (2015) [Geriatric particularities of Parkinson's disease: Clinical and therapeutic aspects]. *Rev Neurol (Paris)* **171**, 841-852
132. Petrova, M., Mehrabian-Spasova, S., Aarsland, D., Raycheva, M., and Traykov, L. (2015) Clinical and Neuropsychological Differences between Mild Parkinson's Disease Dementia and Dementia with Lewy Bodies. *Dement Geriatr Cogn Dis Extra* **5**, 212-220
133. Luquin, M. R., Scipioni, O., Vaamonde, J., Gershanik, O., and Obeso, J. A. (1992) Levodopa-induced dyskinesias in Parkinson's disease: clinical and pharmacological classification. *Mov Disord* **7**, 117-124
134. Zis, P., Rizos, A., Martinez-Martin, P., Pal, S., Silverdale, M., Sharma, J. C., Sauerbier, A., and Chaudhuri, K. R. (2014) Non-motor symptoms profile and burden in drug naïve versus long-term Parkinson's disease patients. *J Parkinsons Dis* **4**, 541-547
135. Lim, S. Y., and Lang, A. E. (2010) The nonmotor symptoms of Parkinson's disease--an overview. *Mov Disord* **25 Suppl 1**, S123-130
136. Poewe, W., and Mahlknecht, P. (2009) The clinical progression of Parkinson's disease. *Parkinsonism Relat Disord* **15 Suppl 4**, S28-32
137. Comella, C. L. (2007) Sleep disorders in Parkinson's disease: an overview. *Mov Disord* **22 Suppl 17**, S367-373
138. Löhle, M., Storch, A., and Reichmann, H. (2009) Beyond tremor and rigidity: non-motor features of Parkinson's disease. *J Neural Transm (Vienna)* **116**, 1483-1492
139. Lotia, M., and Jankovic, J. (2016) New and Emerging Medical Therapies in Parkinson's Disease. *Expert Opin Pharmacother*
140. Orme, R. P., Middleditch, C., Waite, L., and Fricker, R. A. (2016) The Role of Vitamin D3 in the Development and Neuroprotection of Midbrain Dopamine Neurons. *Vitam Horm* **100**, 273-297
141. Olsen, J. H., Tangerud, K., Wermuth, L., Frederiksen, K., and Friis, S. (2007) Treatment with levodopa and risk for malignant melanoma. *Mov Disord* **22**, 1252-1257
142. Fahn, S. (2015) The medical treatment of Parkinson disease from James Parkinson to George Cotzias. *Mov Disord* **30**, 4-18
143. Chase, A. (2015) Parkinson disease: treatment needs vary between Parkinson disease subtypes. *Nat Rev Neurol* **11**, 123
144. Ossig, C., and Reichmann, H. (2015) Treatment strategies in early and advanced Parkinson disease. *Neurol Clin* **33**, 19-37
145. Connolly, B. S., and Lang, A. E. (2014) Pharmacological treatment of Parkinson disease: a review. *JAMA* **311**, 1670-1683

146. Takeda, A. (2013) [Treatment & management guidelines 2011 for Parkinson disease]. *Rinsho Shinkeigaku* **53**, 1346-1347
147. Duker, A. P., and Espay, A. J. (2013) Surgical treatment of Parkinson disease: past, present, and future. *Neurol Clin* **31**, 799-808
148. Witt, S. N., and Flower, T. R. (2006) alpha-Synuclein, oxidative stress and apoptosis from the perspective of a yeast model of Parkinson's disease. *FEMS Yeast Res* **6**, 1107-1116
149. Popova, B., Kleinknecht, A., and Braus, G. H. (2015) Posttranslational Modifications and Clearing of α-Synuclein Aggregates in Yeast. *Biomolecules* **5**, 617-634
150. Bocharova, N., Chave-Cox, R., Sokolov, S., Knorre, D., and Severin, F. (2009) Protein aggregation and neurodegeneration: clues from a yeast model of Huntington's disease. *Biochemistry (Mosc)* **74**, 231-234
151. Flower, T. R., Chesnokova, L. S., Froelich, C. A., Dixon, C., and Witt, S. N. (2005) Heat shock prevents alpha-synuclein-induced apoptosis in a yeast model of Parkinson's disease. *J Mol Biol* **351**, 1081-1100
152. Miller-Fleming, L., Giorgini, F., and Outeiro, T. F. (2008) Yeast as a model for studying human neurodegenerative disorders. *Biotechnology Journal* **3**, 325-338
153. Moosavi, B., Mousavi, B., and Macreadie, I. G. (2015) Yeast Model of Amyloid-β and Tau Aggregation in Alzheimer's Disease. *J Alzheimers Dis* **47**, 9-16
154. Pereira, C., Costa, V., Martins, L. M., and Saraiva, L. (2015) A yeast model of the Parkinson's disease-associated protein Parkin. *Exp Cell Res* **333**, 73-79
155. Smith, M. G., and Snyder, M. (2006) Yeast as a model for human disease. *Curr Protoc Hum Genet* **Chapter 15**, Unit 15.16
156. Wells, L., and Fridovich-Keil, J. L. (1996) The yeast, Saccharomyces cerevisiae, as a model system for the study of human genetic disease. *SAAS Bull Biochem Biotechnol* **9**, 83-88
157. Verduyckt, M., Vignaud, H., Bynens, T., Van den Brande, J., Franssens, V., Cullin, C., and Winderickx, J. (2016) Yeast as a Model for Alzheimer's Disease: Latest Studies and Advanced Strategies. *Methods Mol Biol* **1303**, 197-215
158. Tsai, C. J., Aslam, K., Drendel, H. M., Asiago, J. M., Goode, K. M., Paul, L. N., Rochet, J. C., and Hazbun, T. R. (2015) Hsp31 Is a Stress Response Chaperone That Intervenes in the Protein Misfolding Process. *J Biol Chem* **290**, 24816-24834
159. Chase, A. (2014) Prion disease: New assays might facilitate the diagnosis of Creutzfeldt-Jakob disease in living patients. *Nat Rev Neurol* **10**, 545
160. Appleby, B. S., Rincon-Beardsley, T. D., Appleby, K. K., Crain, B. J., and Wallin, M. T. (2014) Initial diagnoses of patients ultimately diagnosed with prion disease. *J Alzheimers Dis* **42**, 833-839
161. Hofmann, J., Wolf, H., Grassmann, A., Arndt, V., Graham, J., and Vorberg, I. (2012) Creutzfeldt-Jakob disease and mad cows: lessons learnt from yeast cells. *Swiss Med Wkly* **142**, 0
162. Crozet, C., Beranger, F., and Lehmann, S. (2008) Cellular pathogenesis in prion diseases. *Vet Res* **39**, 44
163. McDonald, A. J., and Millhauser, G. L. (2014) PrP overdrive: does inhibition of α-cleavage contribute to PrP(C) toxicity and prion disease? *Prion* **8**

164. Kovacs, G. G., and Budka, H. (2008) Prion diseases: from protein to cell pathology. *Am J Pathol* **172**, 555-565
165. Kovács, G. G., Voigtländer, T., Gelpi, E., and Budka, H. (2004) Rationale for diagnosing human prion disease. *World J Biol Psychiatry* **5**, 83-91
166. Bacchetti, P. (2003) Age and variant Creutzfeldt-Jakob disease. *Emerg Infect Dis* **9**, 1611-1612
167. Basu, A. (2003) New variant Creutzfeldt-Jakob disease: a controversial but potential blood transfusion risk. *Nepal Med Coll J* **5**, 51-52
168. Fontenot, A. B. (2003) The fundamentals of variant Creutzfeldt-Jakob disease. *J Neurosci Nurs* **35**, 327-331
169. Saá, P., Yakovleva, O., de Castro, J., Vasilyeva, I., De Paoli, S. H., Simak, J., and Cervenakova, L. (2014) First demonstration of transmissible spongiform encephalopathy-associated prion protein (PrPTSE) in extracellular vesicles from plasma of mice infected with mouse-adapted variant Creutzfeldt-Jakob disease by in vitro amplification. *J Biol Chem* **289**, 29247-29260
170. Will, R. G. (2003) The biology and epidemiology of variant Creutzfeldt-Jakob disease. *Bull Mem Acad R Med Belg* **158**, 250-256; discussion 256-257
171. Sato, T. (2003) [Infectious prion disease: CJD with dura mater transplantation]. *Rinsho Shinkeigaku* **43**, 870-872
172. Ironside, J. W. (1998) Prion diseases in man. *J Pathol* **186**, 227-234
173. Johnson, R. T., and Gibbs, C. J. (1998) Creutzfeldt-Jakob disease and related transmissible spongiform encephalopathies. *N Engl J Med* **339**, 1994-2004
174. Zomosa-Signoret, V., Arnaud, J. D., Fontes, P., Alvarez-Martinez, M. T., and Liautard, J. P. (2008) Physiological role of the cellular prion protein. *Vet Res* **39**, 9
175. Sanders, D. W., Kaufman, S. K., Holmes, B. B., and Diamond, M. I. (2016) Prions and Protein Assemblies that Convey Biological Information in Health and Disease. *Neuron* **89**, 433-448
176. Weissmann, C., and Flechsig, E. (2003) PrP knock-out and PrP transgenic mice in prion research. *Br Med Bull* **66**, 43-60
177. Legname, G., Baskakov, I. V., Nguyen, H. O., Riesner, D., Cohen, F. E., DeArmond, S. J., and Prusiner, S. B. (2004) Synthetic mammalian prions. *Science* **305**, 673-676
178. Aguzzi, A., Nuvolone, M., and Zhu, C. (2013) The immunobiology of prion diseases. *Nat Rev Immunol* **13**, 888-902
179. Lee, I. Y., Westaway, D., Smit, A. F., Wang, K., Seto, J., Chen, L., Acharya, C., Ankener, M., Baskin, D., Cooper, C., Yao, H., Prusiner, S. B., and Hood, L. E. (1998) Complete genomic sequence and analysis of the prion protein gene region from three mammalian species. *Genome Res* **8**, 1022-1037
180. Alberti, S., Halfmann, R., King, O., Kapila, A., and Lindquist, S. (2009) A systematic survey identifies prions and illuminates sequence features of prionogenic proteins. *Cell* **137**, 146-158
181. Derkatch, I. L., Bradley, M. E., Zhou, P., Chernoff, Y. O., and Liebman, S. W. (1997) Genetic and environmental factors affecting the de novo appearance of the [PSI+] prion in Saccharomyces cerevisiae. *Genetics* **147**, 507-519

182. Liebman, S. W., and Chernoff, Y. O. (2012) Prions in yeast. *Genetics* **191**, 1041-1072
183. Kushnirov, V. V., and Ter-Avanesyan, M. D. (1998) Structure and replication of yeast prions. *Cell* **94**, 13-16
184. Doronina, V. A., Staniforth, G. L., Speldewinde, S. H., Tuite, M. F., and Grant, C. M. (2015) Oxidative stress conditions increase the frequency of de novo formation of the yeast [PSI+] prion. *Mol Microbiol* **96**, 163-174
185. Manogaran, A. L., Fajardo, V. M., Reid, R. J., Rothstein, R., and Liebman, S. W. (2010) Most, but not all, yeast strains in the deletion library contain the [PIN(+)] prion. *Yeast* **27**, 159-166
186. Wickner, R. B. (1994) [URE3] as an altered URE2 protein: evidence for a prion analog in Saccharomyces cerevisiae. *Science* **264**, 566-569
187. Paushkin, S. V., Kushnirov, V. V., Smirnov, V. N., and Ter-Avanesyan, M. D. (1996) Propagation of the yeast prion-like [psi+] determinant is mediated by oligomerization of the SUP35-encoded polypeptide chain release factor. *EMBO J* **15**, 3127-3134
188. Wickner, R. B., Taylor, K. L., Edskes, H. K., Maddelein, M. L., Moriyama, H., and Roberts, B. T. (2000) Prions of yeast as heritable amyloidoses. *J Struct Biol* **130**, 310-322
189. Chernoff, Y. O., Galkin, A. P., Lewitin, E., Chernova, T. A., Newnam, G. P., and Belenkiy, S. M. (2000) Evolutionary conservation of prion-forming abilities of the yeast Sup35 protein. *Mol Microbiol* **35**, 865-876
190. Glover, J. R., Kowal, A. S., Schirmer, E. C., Patino, M. M., Liu, J. J., and Lindquist, S. (1997) Self-seeded fibers formed by Sup35, the protein determinant of [PSI+], a heritable prion-like factor of S. cerevisiae. *Cell* **89**, 811-819
191. Zhou, P., Derkatch, I. L., and Liebman, S. W. (2001) The relationship between visible intracellular aggregates that appear after overexpression of Sup35 and the yeast prion-like elements [PSI(+)] and [PIN(+)]. *Mol Microbiol* **39**, 37-46
192. Edskes, H. K., Gray, V. T., and Wickner, R. B. (1999) The [URE3] prion is an aggregated form of Ure2p that can be cured by overexpression of Ure2p fragments. *Proc Natl Acad Sci U S A* **96**, 1498-1503
193. Fernandez-Bellot, E., Guillemet, E., and Cullin, C. (2000) The yeast prion [URE3] can be greatly induced by a functional mutated URE2 allele. *EMBO J* **19**, 3215-3222
194. Brachmann, A., Baxa, U., and Wickner, R. B. (2005) Prion generation in vitro: amyloid of Ure2p is infectious. *EMBO J* **24**, 3082-3092
195. Brachmann, A., Toombs, J. A., and Ross, E. D. (2006) Reporter assay systems for [URE3] detection and analysis. *Methods* **39**, 35-42
196. Pieri, L., Bucciantini, M., Nosi, D., Formigli, L., Savistchenko, J., Melki, R., and Stefani, M. (2006) The yeast prion Ure2p native-like assemblies are toxic to mammalian cells regardless of their aggregation state. *J Biol Chem* **281**, 15337-15344

197. Shelkovnikova, T. A., Kulikova, A. A., Tsvetkov, P. O., Peters, O., Bachurin, S. O., Buchman, V. L., and Ninkina, N. N. (2012) Proteinopathies, neurodegenerative disorders with protein aggregation-based pathology. *Molecular Biology* **46**, 362-374
198. Kalastavadi, T., and True, H. L. (2010) Analysis of the [RNQ+] prion reveals stability of amyloid fibers as the key determinant of yeast prion variant propagation. *J Biol Chem* **285**, 20748-20755
199. Bateman, D. A., and Wickner, R. B. (2013) The [PSI+] prion exists as a dynamic cloud of variants. *PLoS Genet* **9**, e1003257
200. Wickner, R. B., Edskes, H. K., Shewmaker, F., Kryndushkin, D., and Nemecek, J. (2009) Prion variants, species barriers, generation and propagation. *J Biol* **8**, 47
201. Bradley, M. E., and Liebman, S. W. (2003) Destabilizing interactions among [PSI(+)] and [PIN(+)] yeast prion variants. *Genetics* **165**, 1675-1685
202. Sharma, J., and Liebman, S. W. (2012) [PSI(+)] prion variant establishment in yeast. *Mol Microbiol* **86**, 866-881
203. Ross, E. D., Minton, A., and Wickner, R. B. (2005) Prion domains: sequences, structures and interactions. *Nat Cell Biol* **7**, 1039-1044
204. Inge-Vechtomov, S. G., Zhouravleva, G. A., and Chernoff, Y. O. (2007) Biological roles of prion domains. *Prion* **1**, 228-235
205. Liu, J. J., Sondheimer, N., and Lindquist, S. L. (2002) Changes in the middle region of Sup35 profoundly alter the nature of epigenetic inheritance for the yeast prion [PSI+]. *Proc Natl Acad Sci U S A* **99 Suppl 4**, 16446-16453
206. Crow, E. T., Du, Z., and Li, L. (2011) A small, glutamine-free domain propagates the [SWI(+)] prion in budding yeast. *Mol Cell Biol* **31**, 3436-3444
207. Halfmann, R., Alberti, S., Krishnan, R., Lyle, N., O'Donnell, C. W., King, O. D., Berger, B., Pappu, R. V., and Lindquist, S. (2011) Opposing effects of glutamine and asparagine govern prion formation by intrinsically disordered proteins. *Mol Cell* **43**, 72-84
208. Bradley, M. E., Edskes, H. K., Hong, J. Y., Wickner, R. B., and Liebman, S. W. (2002) Interactions among prions and prion "strains" in yeast. *Proc Natl Acad Sci U S A* **99 Suppl 4**, 16392-16399
209. Derkatch, I. L., Bradley, M. E., Masse, S. V., Zadorsky, S. P., Polozkov, G. V., Inge-Vechtomov, S. G., and Liebman, S. W. (2000) Dependence and independence of [PSI(+)] and [PIN(+)]: a two-prion system in yeast? *EMBO J* **19**, 1942-1952
210. Krishnan, R., and Lindquist, S. L. (2005) Structural insights into a yeast prion illuminate nucleation and strain diversity. *Nature* **435**, 765-772
211. Derkatch, I. L., Chernoff, Y. O., Kushnirov, V. V., Inge-Vechtomov, S. G., and Liebman, S. W. (1996) Genesis and variability of [PSI] prion factors in Saccharomyces cerevisiae. *Genetics* **144**, 1375-1386
212. Lancaster, A. K., Bardill, J. P., True, H. L., and Masel, J. (2010) The spontaneous appearance rate of the yeast prion [PSI+] and its implications for the evolution of the evolvability properties of the [PSI+] system. *Genetics* **184**, 393-400

213. Tyedmers, J., Treusch, S., Dong, J., McCaffery, J. M., Bevis, B., and Lindquist, S. (2010) Prion induction involves an ancient system for the sequestration of aggregated proteins and heritable changes in prion fragmentation. *Proc Natl Acad Sci U S A* **107**, 8633-8638
214. Tyedmers, J., Madariaga, M. L., and Lindquist, S. (2008) Prion switching in response to environmental stress. *PLoS Biol* **6**, e294
215. Ganusova, E. E., Ozolins, L. N., Bhagat, S., Newnam, G. P., Wegrzyn, R. D., Sherman, M. Y., and Chernoff, Y. O. (2006) Modulation of prion formation, aggregation, and toxicity by the actin cytoskeleton in yeast. *Mol Cell Biol* **26**, 617-629
216. Bailleul-Winslett, P. A., Newnam, G. P., Wegrzyn, R. D., and Chernoff, Y. O. (2000) An antiprion effect of the anticytoskeletal drug latrunculin A in yeast. *Gene Expr* **9**, 145-156
217. Chernova, T. A., Romanyuk, A. V., Karpova, T. S., Shanks, J. R., Ali, M., Moffatt, N., Howie, R. L., O'Dell, A., McNally, J. G., Liebman, S. W., Chernoff, Y. O., and Wilkinson, K. D. (2011) Prion induction by the short-lived, stress-induced protein Lsb2 is regulated by ubiquitination and association with the actin cytoskeleton. *Mol Cell* **43**, 242-252
218. Feliciano, D., and Di Pietro, S. M. (2012) SLAC, a complex between Sla1 and Las17, regulates actin polymerization during clathrin-mediated endocytosis. *Mol Biol Cell* **23**, 4256-4272
219. Moosavi, B., Mousavi, B., and Yang, G. F. (2016) Actin, Membrane Trafficking and the Control of Prion Induction, Propagation and Transmission in Yeast. *Traffic* **17**, 5-20
220. Cummings, C. J., Mancini, M. A., Antalffy, B., DeFranco, D. B., Orr, H. T., and Zoghbi, H. Y. (1998) Chaperone suppression of aggregation and altered subcellular proteasome localization imply protein misfolding in SCA1. *Nat Genet* **19**, 148-154
221. Yang, Z., Stone, D. E., and Liebman, S. W. (2014) Prion-promoted phosphorylation of heterologous amyloid is coupled with ubiquitin-proteasome system inhibition and toxicity. *Mol Microbiol* **93**, 1043-1056
222. Chernoff, Y. O., Lindquist, S. L., Ono, B., Inge-Vechtomov, S. G., and Liebman, S. W. (1995) Role of the chaperone protein Hsp104 in propagation of the yeast prion-like factor [psi+]. *Science* **268**, 880-884
223. Park, Y. N., Zhao, X., Yim, Y. I., Todor, H., Ellerbrock, R., Reidy, M., Eisenberg, E., Masison, D. C., and Greene, L. E. (2014) Hsp104 overexpression cures Saccharomyces cerevisiae [PSI+] by causing dissolution of the prion seeds. *Eukaryot Cell* **13**, 635-647
224. Masison, D. C., Kirkland, P. A., and Sharma, D. (2009) Influence of Hsp70s and their regulators on yeast prion propagation. *Prion* **3**, 65-73
225. Shorter, J., and Lindquist, S. (2008) Hsp104, Hsp70 and Hsp40 interplay regulates formation, growth and elimination of Sup35 prions. *EMBO J* **27**, 2712-2724
226. Doyle, S. M., and Wickner, S. (2009) Hsp104 and ClpB: protein disaggregating machines. *Trends in biochemical sciences* **34**, 40-48

227. Romanova, N. V., and Chernoff, Y. O. (2009) Hsp104 and prion propagation. *Protein Pept Lett* **16**, 598-605
228. Sweeny, E. A., and Shorter, J. (2015) Mechanistic and Structural Insights into the Prion-Disaggregase Activity of Hsp104. *J Mol Biol*
229. Wegrzyn, R. D., Bapat, K., Newnam, G. P., Zink, A. D., and Chernoff, Y. O. (2001) Mechanism of prion loss after Hsp104 inactivation in yeast. *Mol Cell Biol* **21**, 4656-4669
230. Sweeny, E. A., Jackrel, M. E., Go, M. S., Sochor, M. A., Razzo, B. M., DeSantis, M. E., Gupta, K., and Shorter, J. (2015) The Hsp104 N-terminal domain enables disaggregase plasticity and potentiation. *Mol Cell* **57**, 836-849
231. Borchsenius, A. S., Müller, S., Newnam, G. P., Inge-Vechtomov, S. G., and Chernoff, Y. O. (2006) Prion variant maintained only at high levels of the Hsp104 disaggregase. *Curr Genet* **49**, 21-29
232. Bösl, B., Grimminger, V., and Walter, S. (2006) The molecular chaperone Hsp104--a molecular machine for protein disaggregation. *J Struct Biol* **156**, 139-148
233. Park, Y. N., Morales, D., Rubinson, E. H., Masison, D., Eisenberg, E., and Greene, L. E. (2012) Differences in the curing of [PSI+] prion by various methods of Hsp104 inactivation. *PLoS One* **7**, e37692
234. Haslbeck, M., Miess, A., Stromer, T., Walter, S., and Buchner, J. (2005) Disassembling protein aggregates in the yeast cytosol. The cooperation of Hsp26 with Ssa1 and Hsp104. *J Biol Chem* **280**, 23861-23868
235. Moran, C., Kinsella, G. K., Zhang, Z. R., Perrett, S., and Jones, G. W. (2013) Mutational analysis of Sse1 (Hsp110) suggests an integral role for this chaperone in yeast prion propagation in vivo. *G3 (Bethesda)* **3**, 1409-1418
236. Chernoff, Y. O., Newnam, G. P., Kumar, J., Allen, K., and Zink, A. D. (1999) Evidence for a protein mutator in yeast: role of the Hsp70-related chaperone ssb in formation, stability, and toxicity of the [PSI] prion. *Mol Cell Biol* **19**, 8103-8112
237. Chernoff, Y. O., and Kiktev, D. A. (2016) Dual role of ribosome-associated chaperones in prion formation and propagation. *Curr Genet*
238. Allen, K. D., Wegrzyn, R. D., Chernova, T. A., Müller, S., Newnam, G. P., Winslett, P. A., Wittich, K. B., Wilkinson, K. D., and Chernoff, Y. O. (2005) Hsp70 chaperones as modulators of prion life cycle: novel effects of Ssa and Ssb on the Saccharomyces cerevisiae prion [PSI+]. *Genetics* **169**, 1227-1242
239. Schwimmer, C., and Masison, D. C. (2002) Antagonistic interactions between yeast [PSI(+)] and [URE3] prions and curing of [URE3] by Hsp70 protein chaperone Ssa1p but not by Ssa2p. *Mol Cell Biol* **22**, 3590-3598
240. Specht, S., Miller, S. B., Mogk, A., and Bukau, B. (2011) Hsp42 is required for sequestration of protein aggregates into deposition sites in Saccharomyces cerevisiae. *J Cell Biol* **195**, 617-629

241. Walter, G. M., Smith, M. C., Wisén, S., Basrur, V., Elenitoba-Johnson, K. S., Duennwald, M. L., Kumar, A., and Gestwicki, J. E. (2011) Ordered assembly of heat shock proteins, Hsp26, Hsp70, Hsp90, and Hsp104, on expanded polyglutamine fragments revealed by chemical probes. *J Biol Chem* **286**, 40486-40493
242. Haslbeck, M., Braun, N., Stromer, T., Richter, B., Model, N., Weinkauf, S., and Buchner, J. (2004) Hsp42 is the general small heat shock protein in the cytosol of Saccharomyces cerevisiae. *EMBO J* **23**, 638-649
243. Cashikar, A. G., Duennwald, M., and Lindquist, S. L. (2005) A chaperone pathway in protein disaggregation. Hsp26 alters the nature of protein aggregates to facilitate reactivation by Hsp104. *J Biol Chem* **280**, 23869-23875
244. Pezza, J. A., Villali, J., Sindi, S. S., and Serio, T. R. (2014) Amyloid-associated activity contributes to the severity and toxicity of a prion phenotype. *Nat Commun* **5**, 4384
245. Zhao, X., Park, Y. N., Todor, H., Moomau, C., Masison, D., Eisenberg, E., and Greene, L. E. (2012) Sequestration of Sup35 by aggregates of huntingtin fragments causes toxicity of [PSI+] yeast. *J Biol Chem* **287**, 23346-23355
246. Vishveshwara, N., Bradley, M. E., and Liebman, S. W. (2009) Sequestration of essential proteins causes prion associated toxicity in yeast. *Mol Microbiol* **73**, 1101-1114
247. Vishveshwara, N., and Liebman, S. W. (2009) Heterologous cross-seeding mimics cross-species prion conversion in a yeast model. *BMC Biol* **7**, 26
248. Eaglestone, S. S., Cox, B. S., and Tuite, M. F. (1999) Translation termination efficiency can be regulated in Saccharomyces cerevisiae by environmental stress through a prion-mediated mechanism. *EMBO J* **18**, 1974-1981
249. Jung, G., Jones, G., Wegrzyn, R. D., and Masison, D. C. (2000) A role for cytosolic hsp70 in yeast [PSI(+)] prion propagation and [PSI(+)] as a cellular stress. *Genetics* **156**, 559-570
250. McGlinchey, R. P., Kryndushkin, D., and Wickner, R. B. (2011) Suicidal [PSI+] is a lethal yeast prion. *Proc Natl Acad Sci U S A* **108**, 5337-5341
251. Gokhale, K. C., Newnam, G. P., Sherman, M. Y., and Chernoff, Y. O. (2005) Modulation of prion-dependent polyglutamine aggregation and toxicity by chaperone proteins in the yeast model. *J Biol Chem* **280**, 22809-22818
252. Gong, H., Romanova, N. V., Allen, K. D., Chandramowlishwaran, P., Gokhale, K., Newnam, G. P., Mieczkowski, P., Sherman, M. Y., and Chernoff, Y. O. (2012) Polyglutamine toxicity is controlled by prion composition and gene dosage in yeast. *PLoS Genet* **8**, e1002634
253. Wilson, M., Collins, J., Hod, Y., Ringe, D., and Petsko, G. (2003) The 1.1-A resolution crystal structure of DJ-1, the protein mutated in autosomal recessive early onset Parkinson's disease. *Proc Natl Acad Sci U S A* **100**, 9256 - 9261
254. Guo, P.-C., Zhou, Y.-Y., Ma, X.-X., and Li, W.-F. (2010) Structure of Hsp33/YOR391Cp from the yeast Saccharomyces cerevisiae. *Acta Crystallographica Section F* **66**, 1557-1561

255. Quigley, P., Korotkov, K., Baneyx, F., and Hol, W. (2003) The 1.6-A crystal structure of the class of chaperones represented by Escherichia coli Hsp31 reveals a putative catalytic triad. *Proc Natl Acad Sci U S A* **100**, 3137 - 3142
256. Marc Graille, Sophie Quevillon-Cheruel, Nicolas Leulliot, Cong-Zhao Zhou, Ines Li de La Sierra Gallay, Lilian Jacquamet, Jean-Luc Ferrer, Dominique Liger, Anne Poupon, Janin, J., and Tilbeurgh, H. v. (2004) Crystal Structure of the YDR533c S. cerevisiae Protein, a Class II Member of the Hsp31 Family. *Structure* **12**, 839-847
257. Tao, X., and Tong, L. (2003) Crystal Structure of Human DJ-1, a Protein Associated with Early Onset Parkinson's Disease. *Journal of Biological Chemistry* **278**, 31372-31379
258. Wilson, M. A., Ringe, D., and Petsko, G. A. (2005) The Atomic Resolution Crystal Structure of the YajL (ThiJ) Protein from Escherichia coli: A Close Prokaryotic Homologue of the Parkinsonism-associated Protein DJ-1. *Journal of Molecular Biology* **353**, 678-691
259. Bandyopadhyay, S., and Cookson, M. (2004) Evolutionary and functional relationships within the DJ1 superfamily. *BMC Evolutionary Biology* **4**, 6
260. Bankapalli, K., Saladi, S., Awadia, S. S., Goswami, A. V., Samaddar, M., and D'Silva, P. (2015) Robust Glyoxalase activity of Hsp31, a ThiJ/DJ-1/PfpI Family Member Protein, Is Critical for Oxidative Stress Resistance in Saccharomyces cerevisiae. *J Biol Chem* **290**, 26491-26507
261. Hasim, S., Hussin, N. A., Alomar, F., Bidasee, K. R., Nickerson, K. W., and Wilson, M. A. (2014) A glutathione-independent glyoxalase of the DJ-1 superfamily plays an important role in managing metabolically generated methylglyoxal in Candida albicans. *J Biol Chem* **289**, 1662-1674
262. Amm, I., Norell, D., and Wolf, D. H. (2015) Absence of the Yeast Hsp31 Chaperones of the DJ-1 Superfamily Perturbs Cytoplasmic Protein Quality Control in Late Growth Phase. *PLoS One* **10**, e0140363
263. Malki, A., Caldas, T., Abdallah, J., Kern, R., Eckey, V., Kim, S. J., Cha, S.-S., Mori, H., and Richarme, G. (2005) Peptidase Activity of the Escherichia coli Hsp31 Chaperone. *Journal of Biological Chemistry* **280**, 14420-14426
264. Zhao, Q., Su, Y., Wang, Z., Chen, C., Wu, T., and Huang, Y. (2014) Identification of glutathione (GSH)-independent glyoxalase III from Schizosaccharomyces pombe. *BMC Evol Biol* **14**, 86
265. Mihoub, M., Abdallah, J., Gontero, B., Dairou, J., and Richarme, G. (2015) The DJ-1 superfamily member Hsp31 repairs proteins from glycation by methylglyoxal and glyoxal. *Biochem Biophys Res Commun* **463**, 1305-1310
266. Subedi, K. P., Choi, D., Kim, I., Min, B., and Park, C. (2011) Hsp31 of Escherichia coli K-12 is glyoxalase III. *Mol Microbiol* **81**, 926-936
267. Abou-Sleiman, P. M., Healy, D. G., Quinn, N., Lees, A. J., and Wood, N. W. (2003) The role of pathogenic DJ-1 mutations in Parkinson's disease. *Annals of Neurology* **54**, 283-286

268. Aleyasin, H., Rousseaux, M. W. C., Phillips, M., Kim, R. H., Bland, R. J., Callaghan, S., Slack, R. S., During, M. J., Mak, T. W., and Park, D. S. (2007) The Parkinson's disease gene DJ-1 is also a key regulator of stroke-induced damage. *Proceedings of the National Academy of Sciences* **104**, 18748-18753
269. Ariga, H., Takahashi-Niki, K., Kato, I., Maita, H., Niki, T., and Iguchi-Ariga, S. M. (2013) Neuroprotective function of DJ-1 in Parkinson's disease. *Oxid Med Cell Longev* **2013**, 683920
270. Nagakubo, D., Taira, T., Kitaura, H., Ikeda, M., Tamai, K., Iguchi-Ariga, S. M., and Ariga, H. (1997) DJ-1, a novel oncogene which transforms mouse NIH3T3 cells in cooperation with ras. *Biochem Biophys Res Commun* **231**, 509-513
271. Mark A. Wilson, C. V. S. A., Jennifer L. Collins, Dagmar Ringe, and Gregory A. Petsko. (2004) The 1.8-Å resolution crystal structure of YDR533Cp from Saccharomyces cerevisiae: A member of the DJ-1/ThiJ/PfpI superfamily. *Proc Natl Acad Sci U S A.* **101**, 1531-1536
272. Graille, M., Quevillon-Cheruel, S., Leulliot, N., Zhou, C. Z., Li de la Sierra Gallay, I., Jacquamet, L., Ferrer, J. L., Liger, D., Poupon, A., Janin, J., and van Tilbeurgh, H. (2004) Crystal structure of the YDR533c S. cerevisiae protein, a class II member of the Hsp31 family. *Structure* **12**, 839-847
273. Du, X., Choi, I. G., Kim, R., Wang, W., Jancarik, J., Yokota, H., and Kim, S. H. (2000) Crystal structure of an intracellular protease from Pyrococcus horikoshii at 2-A resolution. *Proc Natl Acad Sci U S A* **97**, 14079-14084
274. Abdallah, J., Caldas, T., Kthiri, F., Kern, R., and Richarme, G. (2007) YhbO protects cells against multiple stresses. *J Bacteriol* **189**, 9140-9144
275. Ariga, H. (2015) Common mechanisms of onset of cancer and neurodegenerative diseases. *Biol Pharm Bull* **38**, 795-808
276. Liu, H., Wang, M., Li, M., Wang, D., Rao, Q., Wang, Y., Xu, Z., and Wang, J. (2008) Expression and role of DJ-1 in leukemia. *Biochem Biophys Res Commun* **375**, 477-483
277. He, X., Zheng, Z., Li, J., Ben, Q., Liu, J., Zhang, J., Ji, J., Yu, B., Chen, X., Su, L., Zhou, L., Liu, B., and Yuan, Y. (2012) DJ-1 promotes invasion and metastasis of pancreatic cancer cells by activating SRC/ERK/uPA. *Carcinogenesis* **33**, 555-562
278. Arnouk, H., Merkley, M. A., Podolsky, R. H., Stöppler, H., Santos, C., Alvarez, M., Mariategui, J., Ferris, D., Lee, J. R., and Dynan, W. S. (2009) Characterization of Molecular Markers Indicative of Cervical Cancer Progression. *Proteomics Clin Appl* **3**, 516-527
279. Chen, Y., Kang, M., Lu, W., Guo, Q., Zhang, B., Xie, Q., and Wu, Y. (2012) DJ-1, a novel biomarker and a selected target gene for overcoming chemoresistance in pancreatic cancer. *J Cancer Res Clin Oncol* **138**, 1463-1474
280. Le Naour, F., Misek, D. E., Krause, M. C., Deneux, L., Giordano, T. J., Scholl, S., and Hanash, S. M. (2001) Proteomics-based identification of RS/DJ-1 as a novel circulating tumor antigen in breast cancer. *Clin Cancer Res* **7**, 3328-3335
281. Kahle, P. J., Waak, J., and Gasser, T. (2009) DJ-1 and prevention of oxidative stress in Parkinson's disease and other age-related disorders. *Free Radical Biology and Medicine* **47**, 1354-1361

282. Bandopadhyay, R., Kingsbury, A. E., Cookson, M. R., Reid, A. R., Evans, I. M., Hope, A. D., Pittman, A. M., Lashley, T., Canet-Aviles, R., Miller, D. W., McLendon, C., Strand, C., Leonard, A. J., Abou-Sleiman, P. M., Healy, D. G., Ariga, H., Wood, N. W., de Silva, R., Revesz, T., Hardy, J. A., and Lees, A. J. (2004) The expression of DJ-1 (PARK7) in normal human CNS and idiopathic Parkinson's disease. *Brain* **127**, 420-430
283. Hague, S., Rogaeva, E., Hernandez, D., Gulick, C., Singleton, A., Hanson, M., Johnson, J., Weiser, R., Gallardo, M., Ravina, B., Gwinn-Hardy, K., Crawley, A., St George-Hyslop, P., Lang, A., Heutink, P., Bonifati, V., and Hardy, J. (2003) Early-onset Parkinson's disease caused by a compound heterozygous DJ-1 mutation. *Ann Neurol* **54**, 271 - 274
284. Lev N, R. D., Ickowicz D, Melamed E, Offen D. (2006) Role of DJ-1 in Parkinson's disease. *J Mol Neurosci* **29**, 215-225
285. Lucas, J. I., and MarÃ-n, I. (2007) A New Evolutionary Paradigm for the Parkinson Disease Gene DJ-1. *Molecular Biology and Evolution* **24**, 551-561
286. Zhao, J., Yu, S., Zheng, Y., Yang, H., and Zhang, J. (2016) Oxidative Modification and Its Implications for the Neurodegeneration of Parkinson's Disease. *Mol Neurobiol*
287. Ito, G., Ariga, H., Nakagawa, Y., and Iwatsubo, T. (2006) Roles of distinct cysteine residues in S-nitrosylation and dimerization of DJ-1. *Biochemical and Biophysical Research Communications* **339**, 667-672
288. Hulleman, J. D., Chemistry, P. U. M., and Pharmacology, M. (2007) *Regulation of DJ-1 Structure and Function: Implications for Parkinson's Disease*, Purdue University
289. (2012) Effect of Single Amino Acid Substitution on Oxidative Modifications of the Parkinson's Disease-Related Protein, DJ-1.
290. Lee, J. Y., Song, J., Kwon, K., Jang, S., Kim, C., Baek, K., Kim, J., and Park, C. (2012) Human DJ-1 and its homologs are novel glyoxalases. *Hum Mol Genet* **21**, 3215-3225
291. Toyoda, Y., Erkut, C., Pan-Montojo, F., Boland, S., Stewart, M. P., Müller, D. J., Wurst, W., Hyman, A. A., and Kurzchalia, T. V. (2014) Products of the Parkinson's disease-related glyoxalase DJ-1, D-lactate and glycolate, support mitochondrial membrane potential and neuronal survival. *Biol Open* **3**, 777-784
292. Richarme, G., Mihoub, M., Dairou, J., Bui, L. C., Leger, T., and Lamouri, A. (2015) Parkinsonism-associated protein DJ-1/Park7 is a major protein deglycase that repairs methylglyoxal- and glyoxal-glycated cysteine, arginine, and lysine residues. *J Biol Chem* **290**, 1885-1897
293. Cuevas, S., Yang, Y., Konkalmatt, P., Asico, L. D., Feranil, J., Jones, J., Villar, V. A., Armando, I., and Jose, P. A. (2015) Role of nuclear factor erythroid 2-related factor 2 in the oxidative stress-dependent hypertension associated with the depletion of DJ-1. *Hypertension* **65**, 1251-1257

294. Miller-Fleming, L., Antas, P., Pais, T. F., Smalley, J. L., Giorgini, F., and Outeiro, T. F. (2014) Yeast DJ-1 superfamily members are required for diauxic-shift reprogramming and cell survival in stationary phase. *Proc Natl Acad Sci U S A* **111**, 7012-7017
295. Adrianna Skonecznaa, Miciałkiewiczb, A., and Skoneczny, M. (2007) Saccharomyces cerevisiae Hsp31p, a stress response protein conferring protection against reactive oxygen species. *Free Radical Biology and Medicine* **42**, 1409-1420
296. Wilson, M. A. (2014) Metabolic role for yeast DJ-1 superfamily proteins. *Proc Natl Acad Sci U S A* **111**, 6858-6859
297. Madian, A. G., Hindupur, J., Hulleman, J. D., Diaz-Maldonado, N., Mishra, V. R., Guigard, E., Kay, C. M., Rochet, J. C., and Regnier, F. E. (2012) Effect of single amino acid substitution on oxidative modifications of the Parkinson's disease-related protein, DJ-1. *Mol Cell Proteomics* **11**, M111.010892
298. Hulleman, J. D., Mirzaei, H., Guigard, E., Taylor, K. L., Ray, S. S., Kay, C. M., Regnier, F. E., and Rochet, J.-C. (2007) Destabilization of DJ-1 by Familial Substitution and Oxidative Modifications: an Implications for Parkinson's Disease's. *Biochemistry* **46**, 5776-5789
299. Sajjad, M. U., Green, E. W., Miller-Fleming, L., Hands, S., Herrera, F., Campesan, S., Khoshnan, A., Outeiro, T. F., Giorgini, F., and Wyttenbach, A. (2014) DJ-1 modulates aggregation and pathogenesis in models of Huntington's disease. *Hum Mol Genet* **23**, 755-766
300. Krzewska, J., Tanaka, M., Burston, S. G., and Melki, R. (2007) Biochemical and functional analysis of the assembly of full-length Sup35p and its prion-forming domain. *J Biol Chem* **282**, 1679-1686
301. Flower, T., Chesnokova, L., Froelich, C., Dixon, C., and Witt, S. (2005) Heat shock prevents alpha-synuclein-induced apoptosis in a yeast model of Parkinson's disease. *J Mol Biol* **351**, 1081 - 1100
302. Grant, C. M. (2015) Sup35 methionine oxidation is a trigger for de novo [PSI(+)] prion formation. *Prion* **9**, 257-265
303. Skoneczna, A., Miciałkiewicz, A., and Skoneczny, M. (2007) Saccharomyces cerevisiae Hsp31p, a stress response protein conferring protection against reactive oxygen species. *Free Radic Biol Med* **42**, 1409-1420
304. Batelli S, A. D., Rametta R, Polito L, Prato F, Pesaresi M, Negro A, Forloni G. (2008) DJ-1 modulates alpha-synuclein aggregation state in a cellular model of oxidative stress: relevance for Parkinson's disease and involvement of HSP70. *PLoS ONE* **2**, e1884
305. Mujacic, M., Bader, M. W., and Baneyx, F. (2004) Escherichia coli Hsp31 functions as a holding chaperone that cooperates with the DnaK-DnaJ-GrpE system in the management of protein misfolding under severe stress conditions. *Mol Microbiol* **51**, 849-859
306. Angeloni, C., Zambonin, L., and Hrelia, S. (2014) Role of methylglyoxal in Alzheimer's disease. *Biomed Res Int* **2014**, 238485

307. Vistoli, G., De Maddis, D., Cipak, A., Zarkovic, N., Carini, M., and Aldini, G. (2013) Advanced glycoxidation and lipoxidation end products (AGEs and ALEs): an overview of their mechanisms of formation. *Free Radic Res* **47 Suppl 1**, 3-27
308. Shaikh, S., and Nicholson, L. F. (2008) Advanced glycation end products induce in vitro cross-linking of alpha-synuclein and accelerate the process of intracellular inclusion body formation. *J Neurosci Res* **86**, 2071-2082
309. Kvam, E., Nannenga, B. L., Wang, M. S., Jia, Z., Sierks, M. R., and Messer, A. (2009) Conformational targeting of fibrillar polyglutamine proteins in live cells escalates aggregation and cytotoxicity. *PLoS One* **4**, e5727
310. Nixon, R. A. (2013) The role of autophagy in neurodegenerative disease. *Nat Med* **19**, 983-997
311. Qi, L., and Zhang, X. D. (2014) Role of chaperone-mediated autophagy in degrading Huntington's disease-associated huntingtin protein. *Acta Biochim Biophys Sin (Shanghai)* **46**, 83-91
312. Au, A. K., Bayir, H., Kochanek, P. M., and Clark, R. S. (2010) Evaluation of autophagy using mouse models of brain injury. *Biochim Biophys Acta* **1802**, 918-923
313. Juhász, G., Erdi, B., Sass, M., and Neufeld, T. P. (2007) Atg7-dependent autophagy promotes neuronal health, stress tolerance, and longevity but is dispensable for metamorphosis in Drosophila. *Genes Dev* **21**, 3061-3066
314. Petroi, D., Popova, B., Taheri-Talesh, N., Irniger, S., Shahpasandzadeh, H., Zweckstetter, M., Outeiro, T. F., and Braus, G. H. (2012) Aggregate clearance of α-synuclein in Saccharomyces cerevisiae depends more on autophagosome and vacuole function than on the proteasome. *J Biol Chem* **287**, 27567-27579
315. David C. Amberg, U. M. U., Syracuse, Daniel J. Burke, U. o. V. M. C., Charlottesville, and Strathern, J. N. (2005) Methods in Yeast Genetics: A Cold Spring Harbor Laboratory Course Manual, 2005 Edition.
316. Tardiff, D. F., Jui, N. T., Khurana, V., Tambe, M. A., Thompson, M. L., Chung, C. Y., Kamadurai, H. B., Kim, H. T., Lancaster, A. K., Caldwell, K. A., Caldwell, G. A., Rochet, J. C., Buchwald, S. L., and Lindquist, S. (2013) Yeast reveal a "druggable" Rsp5/Nedd4 network that ameliorates α-synuclein toxicity in neurons. *Science* **342**, 979-983
317. Chung, C. Y., Khurana, V., Auluck, P. K., Tardiff, D. F., Mazzulli, J. R., Soldner, F., Baru, V., Lou, Y., Freyzon, Y., Cho, S., Mungenast, A. E., Muffat, J., Mitalipova, M., Pluth, M. D., Jui, N. T., Schüle, B., Lippard, S. J., Tsai, L. H., Krainc, D., Buchwald, S. L., Jaenisch, R., and Lindquist, S. (2013) Identification and rescue of α-synuclein toxicity in Parkinson patient-derived neurons. *Science* **342**, 983-987
318. Alberti, S., Gitler, A. D., and Lindquist, S. (2007) A suite of Gateway® cloning vectors for high-throughput genetic analysis in Saccharomyces cerevisiae. *Yeast* **24**, 913-919

319. Gelperin, D. M., White, M. A., Wilkinson, M. L., Kon, Y., Kung, L. A., Wise, K. J., Lopez-Hoyo, N., Jiang, L., Piccirillo, S., Yu, H., Gerstein, M., Dumont, M. E., Phizicky, E. M., Snyder, M., and Grayhack, E. J. (2005) Biochemical and genetic analysis of the yeast proteome with a movable ORF collection. *Genes & Development* **19**, 2816-2826
320. Wenig, P., and Odermatt, J. (2010) OpenChrom: a cross-platform open source software for the mass spectrometric analysis of chromatographic data. *BMC Bioinformatics* **11**, 405
321. Halfmann, R., and Lindquist, S. (2008) Screening for amyloid aggregation by Semi-Denaturing Detergent-Agarose Gel Electrophoresis. *J Vis Exp*
322. Galdieri L, M. S., Yu S, Vancura A. (2010) Transcriptional regulation in yeast during diauxic shift and stationary phase. *OMICS* **14**, 629-638
323. Morano, K. A., Grant, C. M., and Moye-Rowley, W. S. (2012) The response to heat shock and oxidative stress in Saccharomyces cerevisiae. *Genetics* **190**, 1157-1195
324. Chen, D., Toone, W. M., Mata, J., Lyne, R., Burns, G., Kivinen, K., Brazma, A., Jones, N., and Bähler, J. (2003) Global transcriptional responses of fission yeast to environmental stress. *Mol Biol Cell* **14**, 214-229
325. Gitler, A. D., Bevis, B. J., Shorter, J., Strathearn, K. E., Hamamichi, S., Su, L. J., Caldwell, K. A., Caldwell, G. A., Rochet, J. C., McCaffery, J. M., Barlowe, C., and Lindquist, S. (2008) The Parkinson's disease protein alpha-synuclein disrupts cellular Rab homeostasis. *Proc Natl Acad Sci U S A* **105**, 145-150
326. Hulleman, J. D., Mirzaei, H., Guigard, E., Taylor, K. L., Ray, S. S., Kay, C. M., Regnier, F. E., and Rochet, J. C. (2007) Destabilization of DJ-1 by familial substitution and oxidative modifications: implications for Parkinson's disease. *Biochemistry* **46**, 5776-5789
327. Tenreiro, S., Reimão-Pinto, M. M., Antas, P., Rino, J., Wawrzycka, D., Macedo, D., Rosado-Ramos, R., Amen, T., Waiss, M., Magalhães, F., Gomes, A., Santos, C. N., Kaganovich, D., and Outeiro, T. F. (2014) Phosphorylation modulates clearance of alpha-synuclein inclusions in a yeast model of Parkinson's disease. *PLoS Genet* **10**, e1004302
328. Chen, J., Li, L., and Chin, L. S. (2010) Parkinson disease protein DJ-1 converts from a zymogen to a protease by carboxyl-terminal cleavage. *Hum Mol Genet* **19**, 2395-2408
329. Koide-Yoshida, S., Niki, T., Ueda, M., Himeno, S., Taira, T., Iguchi-Ariga, S. M., Ando, Y., and Ariga, H. (2007) DJ-1 degrades transthyretin and an inactive form of DJ-1 is secreted in familial amyloidotic polyneuropathy. *Int J Mol Med* **19**, 885-893
330. van der Brug, M. P., Blackinton, J., Chandran, J., Hao, L. Y., Lal, A., Mazan-Mamczarz, K., Martindale, J., Xie, C., Ahmad, R., Thomas, K. J., Beilina, A., Gibbs, J. R., Ding, J., Myers, A. J., Zhan, M., Cai, H., Bonini, N. M., Gorospe, M., and Cookson, M. R. (2008) RNA binding activity of the recessive parkinsonism protein DJ-1 supports involvement in multiple cellular pathways. *Proc Natl Acad Sci U S A* **105**, 10244-10249

331. Wickner, R. B., Edskes, H. K., Bateman, D. A., Kelly, A. C., Gorkovskiy, A., Dayani, Y., and Zhou, A. (2014) Amyloid diseases of yeast: prions are proteins acting as genes. *Essays Biochem* **56**, 193-205
332. Portillo, A., Hashemi, M., Zhang, Y., Breydo, L., Uversky, V. N., and Lyubchenko, Y. L. (2015) Role of monomer arrangement in the amyloid self-assembly. *Biochim Biophys Acta* **1854**, 218-228
333. Mankar, S., Anoop, A., Sen, S., and Maji, S. K. (2011) Nanomaterials: amyloids reflect their brighter side. *Nano Rev* **2**
334. Helsen, C. W., and Glover, J. R. (2012) A new perspective on Hsp104-mediated propagation and curing of the yeast prion [PSI (+)]. *Prion* **6**, 234-239
335. Newnam, G. P., Birchmore, J. L., and Chernoff, Y. O. (2011) Destabilization and recovery of a yeast prion after mild heat shock. *J Mol Biol* **408**, 432-448
336. Reidy, M., and Masison, D. C. (2011) Modulation and elimination of yeast prions by protein chaperones and co-chaperones. *Prion* **5**, 245-249
337. Sporn, Z. A., and Hines, J. K. (2015) Hsp40 function in yeast prion propagation: Amyloid diversity necessitates chaperone functional complexity. *Prion* **9**, 80-89
338. Haslbeck, M., Walke, S., Stromer, T., Ehrnsperger, M., White, H. E., Chen, S., Saibil, H. R., and Buchner, J. (1999) Hsp26: a temperature-regulated chaperone. *EMBO J* **18**, 6744-6751
339. Aslam, K., and Hazbun, T. R. (2016) Hsp31, a member of the DJ-1 superfamily, is a multitasking stress responder with chaperone activity. *Prion*
340. Wickner, R. B., Bezsonov, E., and Bateman, D. A. (2014) Normal levels of the antiprion proteins Btn2 and Cur1 cure most newly formed [URE3] prion variants. *Proc Natl Acad Sci U S A* **111**, E2711-2720
341. Kochneva-Pervukhova, N. V., Alexandrov, A. I., and Ter-Avanesyan, M. D. (2012) Amyloid-mediated sequestration of essential proteins contributes to mutant huntingtin toxicity in yeast. *PLoS One* **7**, e29832
342. Arslan, F., Hong, J. Y., Kanneganti, V., Park, S. K., and Liebman, S. W. (2015) Heterologous aggregates promote de novo prion appearance via more than one mechanism. *PLoS Genet* **11**, e1004814
343. Panza, G., Dumpitak, C., and Birkmann, E. (2010) Influence of the maillard reaction to prion protein aggregation. *Rejuvenation research* **13**, 220-223
344. Vicente Miranda, H., and Outeiro, T. F. (2010) The sour side of neurodegenerative disorders: the effects of protein glycation. *The Journal of pathology* **221**, 13-25
345. Zhao, R., Davey, M., Hsu, Y. C., Kaplanek, P., Tong, A., Parsons, A. B., Krogan, N., Cagney, G., Mai, D., Greenblatt, J., Boone, C., Emili, A., and Houry, W. A. (2005) Navigating the chaperone network: an integrative map of physical and genetic interactions mediated by the hsp90 chaperone. *Cell* **120**, 715-727
346. Wilson, M. A. (2011) The role of cysteine oxidation in DJ-1 function and dysfunction. *Antioxid Redox Signal* **15**, 111-122
347. Björkblom, B., Maple-Grødem, J., Puno, M. R., Odell, M., Larsen, J. P., and Møller, S. G. (2014) Reactive oxygen species-mediated DJ-1 monomerization modulates intracellular trafficking involving karyopherin β2. *Mol Cell Biol* **34**, 3024-3040

348. Aslam, K., and Hazbun, T. R. (2016) Hsp31, a member of the DJ-1 superfamily, is a multitasking stress responder with chaperone activity. *Prion*.

APPENDICES

APPENDICES

Appendix A Overexpression of Hsp31 under native promoter in yeast

Proteins under different plasmid system exhibit differential expression and therefore influence their activities. Most of the studies performed in this thesis are by expressing Hsp31 under *GPD* promoter using pAG415-*GPD*-Hsp31-DsRed. This plasmid expressed a steady state level of Hsp31 in different yeast strains. Next we ask if Hsp31 under its native promoter can also overexpress the similar level of Hsp31 in different yeast strains. We cloned Hsp31 native promoter into pESC-Leu plasmid by replacing the *GAL* promoter. This is a 2 μ plasmid that contains myc tag attached to the Hsp31. We transformed this plasmid into W303 and BY4741 yeast strains. Successful transformants were selected and cells were allowed to grow into SD-Leu liquid media O/N. Next day, yeast cell lysate were prepared and subjected to western blots for analysis of protein expression. Hsp31 was detected by blotting the membrane with myc antibody (Sigma). For positive control, we used pESC-Leu original plasmid under *GAL* promoter expressing Hsp31-myc (Figure A1). We find this plasmid is expressing steady state level of Hsp31 in both strains therefore it provides a useful tool to obtain Hsp31 expression under native condition.

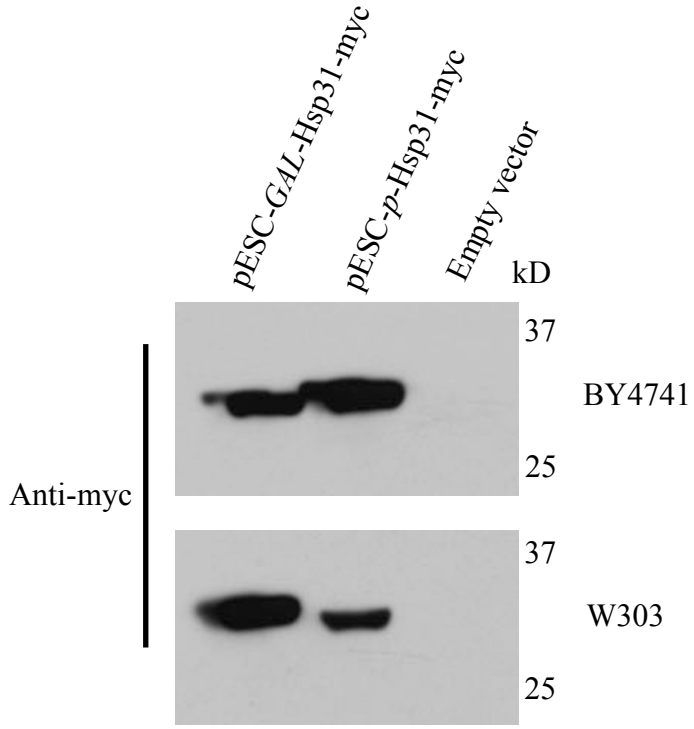

Figure A1. Hsp31 expression under native promoter.

W303 and BY4741 yeast cell lysate harboring pESC-Leu-*p*-Hsp31-myc were prepared and subjected to western blots for analysis of protein expression. Hsp31 was detected by blotting the membrane with myc antibody (Sigma). For positive control, we used pESC-Leu original plasmid under *GAL* promoter expressing Hsp31-myc.

Appendix B Hsp31 pull down for partner proteins

In order to further elucidate the mechanism of Hsp31 in preventing aggregation and to narrow down its other possible role first it is important to determine the cellular substrates of Hsp31 that we predict are either oxidatively damaged proteins or chaperones or both. We proposed to take the approach to use a strain with endogenously tag Hsp31 with 9myc. We used this strain to affinity purify Hsp31 using agarose beads. Clear lysate obtained from this strain was incubated with anti-myc agarose beads overnight at 4°C with shaking. Successful pull down was confirmed by running a SDS-PAGE gel and staining with Sypro Ruby stain followed by western blot using specific anti-myc antibody (Figure B1). To increase the possibility of identifying Hsp31 client interactions we digested the protein pull down on beads directly and subjected to mass spec analysis (Table A1). Proteins that were present in a control sample (non-tagged strain lysate) or with fewer peptide or spectral counts were removed and the final list is displayed in Table 1. Hsp31 was the most predominantly identified protein and Hsp31 paralogs (Hsp32 and Hsp33) were also identified. Potential co-chaperones were also observed including several Hsp70 isoforms and Hsp104. We performed further verification of some of these interactions by using various pull down experiments but results remains inconclusive except for interaction between Hsp31 and Hsp104 that is described in Chapter 3. For rest of the potential client proteins we performed pull down assay by transforming client protein under MORF plasmid system into Hsp31-9myc tagged yeast strain. First we performed the immunoprecipitation of Hsp31 by using myc tagged agarose beads and subjected to western blot using anti HA antibody. Most of the clients proteins showed positive signal that could be the reason of non specific binding of the

protein to agarose beads as these constructs are tagged with protein A along with HA (Figure B2). In fact, we confirmed that possibility by using the WT stains without 9myc tagged Hsp31 was still able to bind with the proteins (Figure B3). Due to high affinity of protein-A binding with agarose beads we could not processed these experiments further. Next, we proposed to use another technique by using purified GST-Hsp31 protein and incubating it with lysate generated from cells (Hsp31-9myc) expressing client proteins under MORF system. After incubation, samples were subjected to SDS-PAGE and blotted with either GST or myc antibody. This experiment shows clear positive interaction between Hsp31 and Hsp32 that was used as positive control. All other client proteins came back negative (Figure B4). Based on these experiments none of the tested client proteins directly interact with Hsp31 however, it is needed to confirm by using other plasmid system such as Tap tagged. We also suspect that some of Hsp31interactions with client proteins are transient in nature and different experimental conditions are necessary to detect such interactions. Further verification of these interactions and their role in the function of hsp31 will be pursued in future.

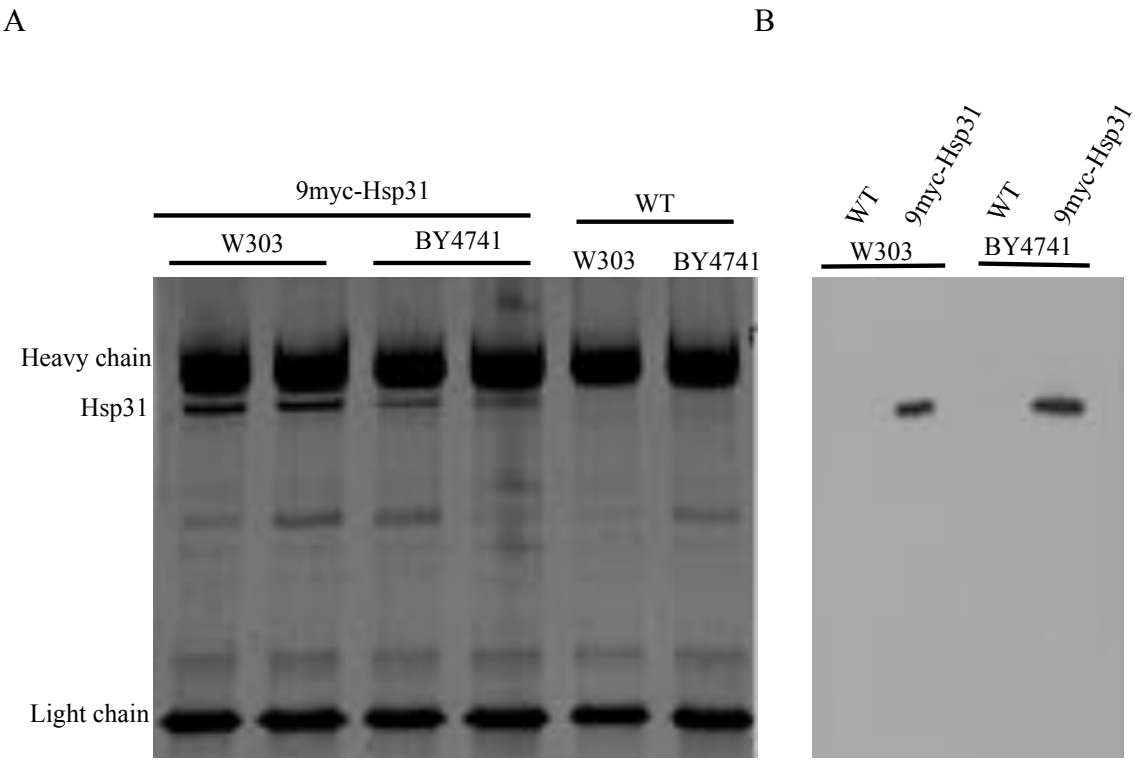

Figure B1. Pull down of Hsp31 using 9myc-Hsp31 strains to analyze protein interaction.

(A) Lysates were prepared from 9myc tagged Hsp31 and WT strains followed by pull down using protein G-agarose beads and anti myc antibody. Samples were run on SDS-PAGE followed by staining with SYPRO-Ruby. **(B)** Immunobloting of pull down samples from WT and 9myc-Hsp31 tagged strains were probed with anti-myc antibody

Table B1 Hsp31 partner proteins identified by combination of Pull down using agarose beads and affinity mass spec analysis.

Protein Name	Protein Accession #	Peptide count	Spectral count	MW KDa
Hsp31	gi|45270564	18	600	25
Enolase II, a phosphopyruvate hydratase	gi|323337363	14	37	46
***Stress-seventy subfamily B protein**	gi|151944335	14	35	66
Fatty Acid Synthetase	gi|323302648	15	15	22
***Chaperone ATPase HSP104**	gi|6323002	9	11	102
≠Mitochondrial porin	gi|151944477	9	13	31
DNA Polymerase	gi|323348993	8	10	124
***Hsp33**	gi|323350061	7	25	25
Voltage-dependent anion-selective channel	gi|173166	7	11	_
***A Complex Of Sse1p And Hsp70**	gi|190613718	6	8	77
ExtraCellular Mutant ECM (DNA dependent ATPase)	gi|6321024	6	14	127
Ribosomal 60S subunit protein L27B	gi|323337248	5	8	155
Subunit of Elongator complex	gi|323308952	5	19	89

Table B1 continued

Mdl2p, Mitochondrial inner membrane transporter	**gi|259149887**	**5**	**13**	**85**
GAPDH, isozyme 1 (Tdh1)	gi|323308411	5	4	35
Mitochondrial outer membrane (OM45)	gi|172066	4	6	44
Mitoch phosphatidate cytidylyltransferase (Tam41)	gi|323309019	4	6	44
***Hsp70 (Ssa1p) nucleotide exchange factor**	gi|323305941	4	4	69
Glyceraldehyde-3-phosphate dehydrogenase	gi|151943468	4	4	35
***Hsp32**	gi|323345814	3	18	25
ubiquinol--cytochrome-c reductase subunit 2	gi|6325449	3	3	40
***Heat-shock protein [S. cerevisiae YJM789]**	gi|151945807	3	14	_
Vacuolar Protein Sorting 4	gi|158430364	2	26	48
Transcription initiation Factor IIB	gi|323305366	1	145	72
Mitochondrial 37S ribosomal protein RSM22	gi|6322694	1	67	72

* Heat Shock Protein

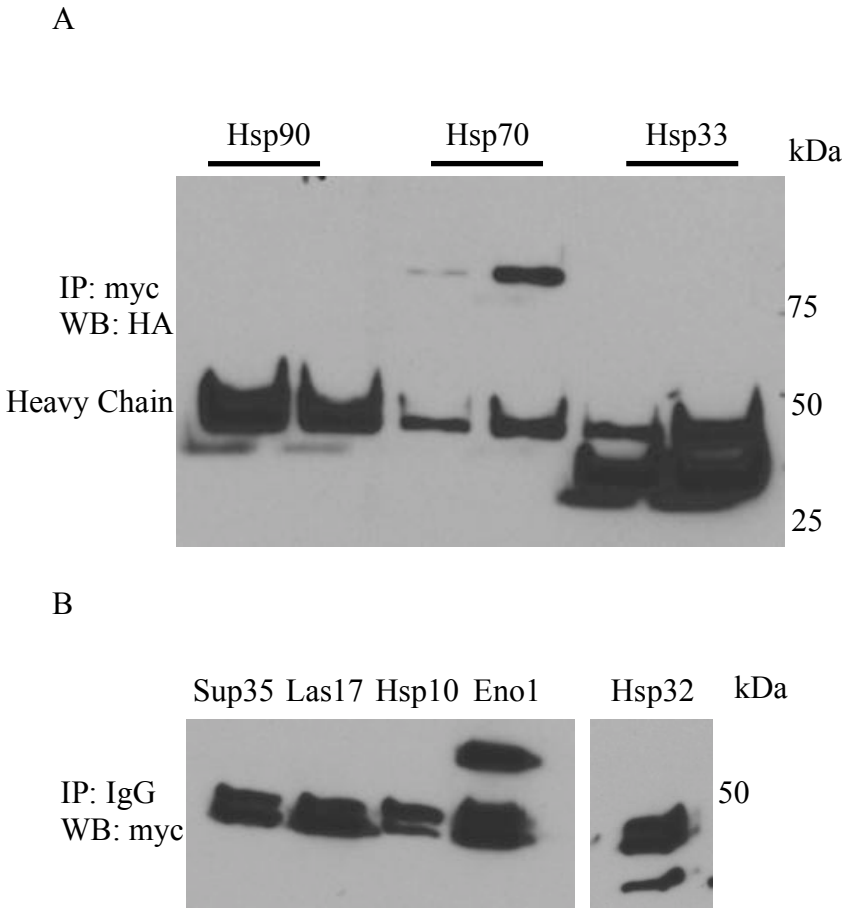

Figure B2. Pull down of Hsp31 using *HSP31*-9myc strain

(A) Immunoprecipitation (IP) of Hsp31 from *HSP31*-9myc genomically tagged strain with overexpression of Hsp90, Hsp70 and Hsp33 under MORF plasmid expression system. IP was performed using myc conjugated agarose beads followed by WB using HA antibody. (B) IP of MORF Sup35, Las17, Hsp10, Eno1 and Hsp32 that are transferred and overexpressed in Hsp31-9myc genomically tagged strain. IgG sepharose beads was use to pull down protein-A tagged attached to these proteins. Samples were separated on 10% SDS-PAGE gel and immunoblotted using myc antibody.

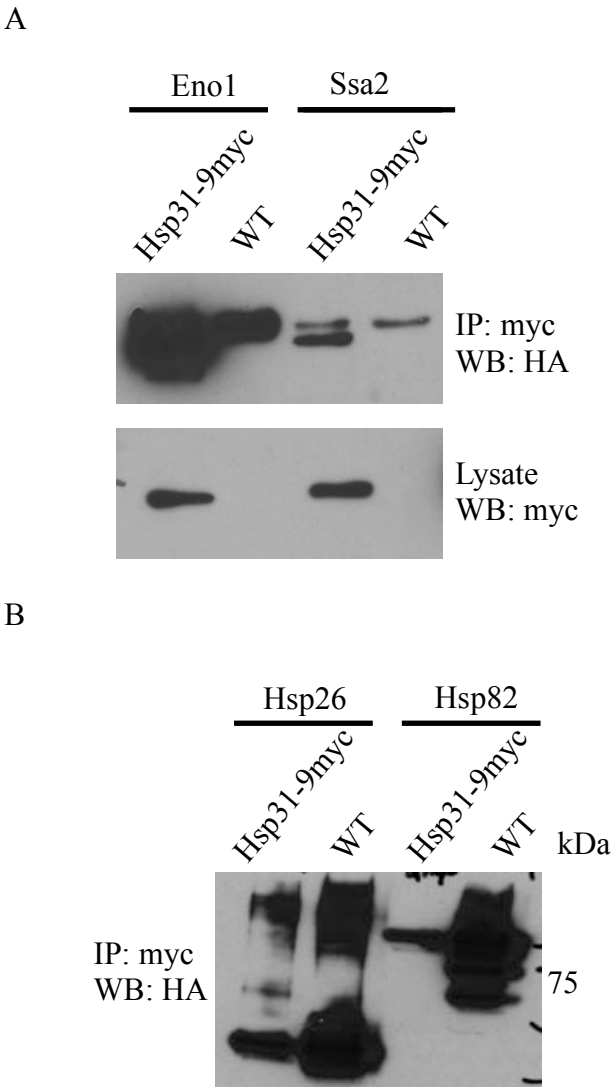

Figure B3. Hsp31 pull down using WT and *HSP31*-9myc strain.

(A) Immunoprecipitation (IP) of Hsp31 from *HSP31*-9myc genomically tagged strain harboring MORF plasmid expressing Ssa2 or Eno1. WT strain was included as negative control. IP was performed using myc conjugated agarose beads followed by WB using HA antibody. (B) Immunoprecipitation (IP) of Hsp31 from Hsp31-9myc genomically tagged strain harboring MORF plasmid expressing Hsp26 or Hsp82. WT strain was included as negative control. IP was performed using myc conjugated agarose beads. Samples were subjected to WB and immunoblotted using HA antibody.

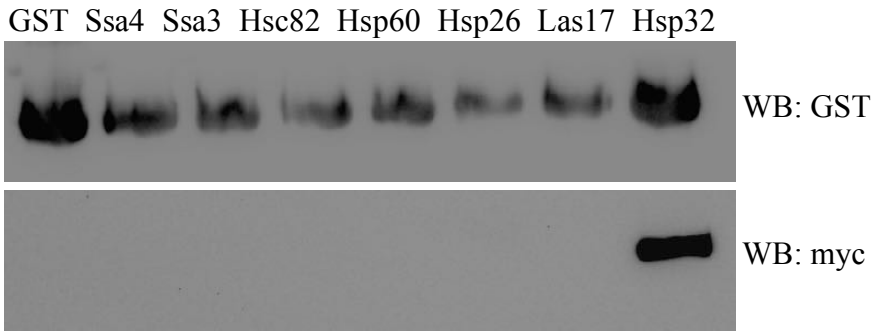

Figure B4. Immunoprecipitation of purified GST-Hsp31 with lysate.

Hsp31-GST was purified from *E coli* and incubated with the yeast lysate generated from cells with genomically tagged 9myc-Hsp31 and expressing MORF Ssa4, Ssa3, Hsc82, Hsp60, Hsp26, Las17 and Hsp32 for 2 hrs. Samples were separated on 10% SDS-PAGE and immunoblotted using either GST (upper panel) or myc antibody (lower panel). Only positive control Hsp32 was pull-down.

VITA

VITA

Kiran Aslam was born in Bahawalpur, Pakistan, the daughter of Muhammad Aslam and Mukhtiar Bibi. After completing her high school degree she entered the Islamia University of Bahawalpur, in Bahawalpur and received the degree of Bachelor of Pharmacy in August 2005. She earned a fellowship to attend the graduate school at one of the prestigious research institute of the country, HEJ research institute of Chemistry and Molecular Medicine located inside the Karachi University in Karachi. She received Master in Philosophy degree from the Department of Pharmacology in Neuropharmacology in 2009. During her stay at the Karachi University she participated in several national and international conferences. She achieved several accolades including the best poster award, travel award from Japan Neuroscience Society and International Brain Research Organization (IBRO) award to attend workshop in Bangkok. Thailand. In 2010 she won IBRO studentship based on her proposed project to get trained at the University College London (UCL) in London, UK. She joined the lab of Prof. Jim Owen at division of medicine at Royal Free Campus in London, UK.

Later in 2010, she secured Fulbright fellowship offered by the United States of Education Foundation in Pakistan and the International Institute of Education in USA to attend a graduate school for PhD in the USA. She enrolled in the Department of Medicinal Chemistry and Molecular Pharmacology at Purdue University. She joined the lab of Dr.

Tony Hazbun and started working on project to understand the molecular mechanism of protein misfolding that is hallmark of many neurodegenerative diseases. The focus of the project was to understand the molecular role of Hsp31 protein, a yeast homolog of human DJ-1 that is involved in PD. During her time here she participated, presented and published her work in many international conferences. She also published her work in the Journal of Biological Chemistry and the Prion journal. She also received the Koo and Paget travel award to attend the Keystone Symposium “Common mechanism of Neurodegeneration” in June 2016.

PUBLICATIONS

PUBLICATIONS

- Chia-Jui Tsai*, **Kiran Aslam***, Holli M Drendel, Josephat M Asiago, Kourtney M Goode, Lake N Paul, Jean-Christophe Rochet, Tony R Hazbun Hsp31 is a Stress-Response Chaperone that Intervenes in the Protein Misfolding Process. *The Journal of biological chemistry*, 290(41):24816-34, 2015

  *First Co-author

- **Kiran Aslam**, Tony Hazbun Hsp31, a member of the DJ-1 superfamily, is a multitasking stress responder with chaperone activity. *Prion* Apr 2016

- **Kiran Aslam,** Chia-Jui Tsai, Tony Hazbun. Small heat shock protein Hsp31 cooperates with Hsp104 to modulate the Sup35 prion aggregation. Prion Submitted March 2016.